TOXIC EFFECTS OF TITANIUM DIOXIDE NANOPARTICLES AND MULTI-WALLED CARBON NANOTUBES *IN VITRO* AND *IN VIVO*

PATINYA SUKWONG

A THESIS SUBMITTED IN PARTIAL FULFILLMENT
OF THE REQUIREMENTS FOR
THE DEGREE OF DOCTOR OF PHILOSOPHY (TOXICOLOGY)
FACULTY OF GRADUATE STUDIES
MAHIDOL UNIVERSITY
2015

Thesis
entitled

TOXIC EFFECTS OF TITANIUM DIOXIDE NANOPARTICLES AND MULTI-WALLED CARBON NANOTUBES *IN VITRO* AND *IN VIVO*

…….
Mr. Patinya Sukwong
Candidate

…….
Mrs. Dakrong Pissuwan,
Ph.D.Science (Nanobiotechnology)
Major advisor

…….
Assoc. Prof. Krongtong Yoovathaworn,
Ph.D. (Pharmacology)
Co-advisor

…….
Prof. Pawinee Piyachaturawat,
Ph.D. (Physiology)
Co-advisor

…….
Asst. Prof. Arthit Chairoungdua,
Ph.D. (Molecular Biology)
Co-advisor

…….
Asst. Prof. Auemphorn Mutchimwong,
Ph.D. (Air Quality Assessment)
Acting Dean
Faculty of Graduate Studies
Mahidol University

…….
Prof. Skorn Mongkolsuk, Ph.D.
Program Director
Doctor of Philosophy Program in Toxicology
Faculty of Science, Mahidol University

Thesis
entitled

TOXIC EFFECTS OF TITANIUM DIOXIDE NANOPARTICLES AND MULTI-WALLED CARBON NANOTUBES *IN VITRO* AND *IN VIVO*

was submitted to the Faculty of Graduate Studies, Mahidol University
for the degree of Doctor of Philosophy (Toxicology)
on
March 26, 2015

……
Mr. Patinya Sukwong
Candidate

……
Prof. Takuro Niidome, PhD.
Chair

……
Mrs. Dakrong Pissuwan,
Ph.D.Science (Nanobiotechnology)
Member

……
Assoc. Prof. Krongtong Yoovathaworn,
Ph.D. (Pharmacology)
Member

……
Prof. Pawinee Piyachaturawat,
Ph.D. (Physiology)
Member

……
Asst. Prof. Arthit Chairoungdua,
Ph.D. (Molecular Biology)
Member

……
Asst. Prof. Auemphorn Mutchimwong,
Ph.D. (Air Quality Assessment)
Acting Dean
Faculty of Graduate Studies
Mahidol University

……
Prof. Skorn Mongkolsuk, Ph.D.
Dean
Faculty of Science
Mahidol University

ACKNOWLEDGEMENTS

For the success of the thesis, I would like to express my sincere gratitude and deep appreciation to two of my major supervisors Assoc. Prof. Dr. Krongtong Yoovathaworn and Dr. Dakrong Pissuwan, for their support, encouragement, guidance and advice. Their insistence for perfection has instilled in me the drive to always strive for the better. Without two of them, this work could never be accomplished. I wish to express my appreciation to my co-advisors; Prof. Dr. Pawinee Piyachaturawat and Assist. Prof. Dr. Arthit Chairoungdua, for their valuable advice, useful discussion and encouragement throughout the duration of this work. My appreciation also extended to the external committee Prof. Dr. Takuro Niidome Graduate School of Science and Technology, Kumamoto University, Japan, for kindness and precious suggestion during thesis defense examination.

I gratefully acknowledge Assist. Prof. Dr. Toemsak Srikhirin, Department of Physics, Faculty of Science, Mahidol University, for providing TiO_2-NPs used in this thesis. I am equally grateful for Assoc. Prof. Dr. Sukumal Chongthammakun, Department of Anatomy, Faculty of Science, Mahidol University, for kindly providing C6 glioma cells used in this thesis.

I would like to thank Mr. Koravit Somkid and Miss Supunsa Kongseng, my best friends in Toxicology program, for their assistance on animal testing experiment and nanotoxicity testing. Considerable thank was for Miss Kanoknetr Suksen and everyone in their cell culture lab for their technical assistance and a warm atmosphere throughout my work.

I wish to acknowledge the research funding, academic and technical support from the Center of Excellence on Environmental Health and Toxicology, Postgraduate Education and Research Development Office (PERDO), Ministry of Education.

I would like to give a special thanks to all my friends and staff in the Toxicology Graduste Program, Faculty of Science, Mahidol University for their encouragement and wonderful friendship.

Finally, I would like to give all my heart to my parents, my brother and sister, and my wife for their loves, caring, consulting, understanding and many encouragements throughout my study. Without their supports, my success would never come true.

Patinya Sukwong

TOXIC EFFECTS OF TITANIUM DIOXIDE NANOPARTICLES AND MULTI-WALLED CARBON NANOTUBES *IN VITRO* AND *IN VIVO*

PATINYA SUKWONG 5037484 SCTX/D

Ph.D. (TOXICOLOGY)

THESIS ADVISORY COMMITTEE: DAKRONG PISSUWAN, Ph.D.,
KRONGTONG YOOVATHAWORN, Ph.D.,
PAWINEE PIYACHATURAWAT, Ph.D., ARTHIT CHAIROUNGDUA, Ph.D.

ABSTRACT

Nanomaterials are of interest in various applications. Titanium dioxide nanoparticles (TiO_2-NPs) and multi-walled carbon nanotubes (MWCNTs) are one of the versatile nanomaterials used in nanotechnology products such as sunscreen, cosmetics, electronic devices, paint, and sports gear. Therefore, workers and consumers are potentially exposed to TiO_2-NPs and MWCNTs. Since these particles have a small size at a nanoscale level they are capable of penetrating biological structures. An increase in the use of TiO_2-NPs and MWCNTs is therefore raising concerns on possibly adverse effects on human health. Due to this reason, the main purpose of this thesis is to investigate the toxic effect of TiO_2-NPs and MWCNTs *in vitro* and *in vivo*. The impact of TiO_2-NPs on the induction of toxicity in immune (RAW 264.7) and brain cancer (C6 glioma) cells is investigated in this thesis. Cell viability, DNA fragmentation, apoptosis cell death, and inflammatory response molecules were measured after treating RAW 264.7 and C6 glioma cells with various concentrations of TiO_2-NPs. The results in this thesis showed that TiO_2-NPs at concentrations $\geq$ 25 μg/ml could strongly induce toxicity in both cells. However, it was found that the RAW 264.7 cell is more sensitive to TiO_2-NPs than C6 cells.

Following *in vitro* investigation, *in vivo* toxicity of TiO_2-NPs and MWCNTs in mice was examined. Intranasal exposure of mice with TiO_2-NPs and MWCNTs for 6 and 24 h was performed. Inflammatory response molecules in bronchoalveolar lavage fluid were determined. The results showed that MWCNTs induced higher toxicity in treated mice than TiO_2-NPs at the same concentration and exposure time. In addition, another useful information of TiO_2-NP and MWCNT characterization is described in this thesis. The information on characterization of both nanoparticles could help explain how particles are associated with the induction of toxicity *in vitro* and *in vivo*. The overall results of this thesis provide useful information for using these nanomaterials effectively with health concerns.

KEY WORDS: NANOTOXICITY/ INFLAMMATORY RESPONSE/ PRO-INFLAMMATORY CYTOKINE/ TIO2-NPS/ MWCNTS

141 pages

ผลกระทบทางด้านความเป็นพิษของอนุภาคนาโนไทเทเนียม และท่อนาโนคาร์บอนแบบมีผนังหลายชั้น ในเซลล์และในสัตว์ทดลอง

TOXIC EFFECTS OF TITANIUM DIOXIDE NANOPARTICLES AND MULTI-WALLED CARBON NANOTUBES *IN VITRO* AND *IN VIVO*

ปฏิญญา สุขวงศ์ 5037484 SCTX/D

ปร.ด. (พิษวิทยา)

คณะกรรมการที่ปรึกษาวิทยานิพนธ์: ดาครอง พิศสุวรรณ, Ph.D., กรองทอง ยุวถาวร, Ph.D.,
ภาวิณี ปิยะจตุรวัฒน์, Ph.D., อาทิตย์ ไชยร้องเดื่อ, Ph.D.

บทคัดย่อ

วัสดุที่มีขนาดในระดับนาโน ถูกสนใจนำไปใช้สำหรับการประยุกต์ด้านต่างๆเป็นอย่างมาก อนุภาคนาโนไทเทเนียม และท่อนาโนคาร์บอนแบบมีผนังหลายชั้น เป็นหนึ่งในวัสดุขนาดระดับนาโนที่ถูกนำมาใช้ในผลิตภัณฑ์ที่มีการนำนาโนเทคโนโลยีเข้ามาใช้ เช่น ในครีมกันแดด เครื่องสำอาง อุปกรณ์อิเลคทรอนิค สี และอุปกรณ์กีฬา ด้วยเหตุนี้ คนงานที่ทำงานในโรงงานผลิต และผู้บริโภคมีโอกาสสูงที่จะได้รับสัมผัสกับวัสดุนาโนทั้งสองชนิดนี้ เนื่องจากวัสดุดังกล่าวมีขนาดเล็กในระดับนาโนเมตรจึงทำให้วัสดุประเภทนี้สามารถแทรกซึมเข้าสู่โครงสร้างทางชีววิทยาได้ เนื่องจากมีการใช้อนุภาคนาโนไทเทเนียม และท่อนาโนคาร์บอนแบบมีผนังหลายชั้นเพิ่มมากขึ้น ดังนั้นการคำนึงผลกระทบของอนุภาคนาโนทั้งสองชนิดต่อสุขภาพ และสิ่งแวดล้อมได้รับความสนใจมากขึ้น วิทยานิพนธ์เล่มนี้ได้ทำการศึกษาความเป็นพิษของ อนุภาคนาโนไทเทเนียม และท่อนาโนคาร์บอนแบบมีผนังหลายชั้น โดยดำเนินการทดสอบความเป็นพิษของอนุภานาโนในเซลล์เพาะเลี้ยง และในสัตว์ทดลอง วิทยานิพนธ์เล่มนี้ ได้ทำการศึกษาความเป็นพิษของอนุภาคนาโนไทเทเนียม ที่มีต่อเซลล์ในระบบภูมิคุ้มกันของร่างกาย (RAW 264.7) และเซลล์มะเร็งสมอง (C6) โดยทำการศึกษาถึงการมีชีวิตรอดของเซลล์ การเกิดการแตกหักของดีเอ็นเอ การตายของเซลล์แบบอะพอพโตซิส และการเกิดการอักเสบ ที่เกิดจากการสัมผัสกับอนุภาคนาโนไทเทเนียมที่ความเข้มข้นต่างๆ ผลจากการศึกษาพบว่า อนุภาคนาโนไทเทเนียมที่ความเข้มข้นมากกว่าหรือเท่ากับ 25 μg/ml สามารถชักนำให้เกิดความเป็นพิษแก่เซลล์ทั้งสองชนิด โดยที่เซลล์ RAW 264.7 มีความไวต่ออนุภาคนาโนไทเทเนียมมากกว่าเซลล์ C6

หลังจากการทดสอบในเซลล์ ได้ทำการศึกษาความเป็นพิษที่เกิดในสัตว์ทดลอง โดยทดสอบในหนูที่ถูกหยอดอนุภาคนาโนไทเทเนียม และท่อนาโนคาร์บอนแบบมีผนังหลายชั้นผ่านทางรูจมูกของหนู หลังจากที่หนูรับสัมผัสอนุภาคนาโนดังกล่าวเป็นเวลา 6 และ 24 ชั่วโมง ได้ทำการตรวจวัดสารที่เป็นดัชนีของการเกิดการอักเสบโดยวัดจากน้ำล้างหลอดลม และปอด ผลจากการทดลองพบว่า ท่อนาโนคาร์บอนแบบมีผนังหลายชั้น มีความเป็นพิษต่อหนู มากกว่าอนุภาคนาโนไทเทเนียม เมื่อทดสอบที่ความเข้มข้น และในระยะเวลาการสัมผัสที่เท่ากัน นอกจากนี้คุณสมบัติของอนุภาคนาโนทั้งสองชนิดได้ถูกอธิบายไว้ในวิทยานิพนธ์เล่มนี้ ผลการศึกษาที่ได้จากวิทยานิพนธ์ สามารถนำไปใช้เป็นข้อมูลประกอบการพิจารณา ในการนำอนุภาคนาโนไปใช้อย่างมีประสิทธิภาพ โดยมีการคำนึงถึงผลกระทบของอนุภาคนาโนต่อสุขภาพ

141 หน้า

CONTENTS

CONTENTS (cont.)

CONTENTS (cont.)

CONTENTS (cont.)

CONTENTS (cont.)

CONTENTS (cont.)

LIST OF TABLES

LIST OF FIGURES

LIST OF FIGURES (cont.)

LIST OF FIGURES (cont.)

LIST OF FIGURES (cont.)

LIST OF ABBREVIATIONS

H_2DCFDA	2’7’-dichlorofluorescin diacetate
8-OHdG	8-hydroxy-2'-deoxyguanosine
Al	Aluminium
AP	Alkaline phosphatase
AP-1	Activator protein 1
ATP	Adenosine triphosphate
APS	Ammonium persulfate
ANOVA	Analysis of variance
Apaf-1	Apoptotic activating-factor 1
AA	Arachidonic acid
AFM	Atomic force microscopy
bp	Base pair
Bcl-2	B-cell lymphoma 2
Bcl-X_L	B-cell lymphoma-extra large
Bax	Bcl-2-associated X protein
Bak	Bcl-2 homologous antagonist killer
Bcl-w	Bcl-2-like protein 2
B-actin	Beta-actin
β-catenin	Beta-catenin
BBB	Blood brain barrier
BSA	Bovine serum albumin
BAL	Broncho alveolar lavage
BALF	Broncho alveolar lavage fluid
CdS	Cadmium sulfide
CB	Carbon black
CO_2	Carbon dioxide
CNTs	Carbon nanotubes

LIST OF ABBREVIATIONS (cont.)

CAg	Carbon-coated silver
CAT	Catalase
CNS	Central nervous system
CCL3	Chemokine (C-C motif) ligand 3
CCL11	Chemokine (C-C motif) ligand 11
CXCL10	Chemokine (C-X-C motif) ligand 10
COPD	Chronic obstructive pulmonary disease
CRE	cAMP-response element
COX-2	Cyclooxygenase-2
NS-398	Cyclooxygenase-2 inhibitor
Cyto-c	Cytochrome c
H_2O_2	Hydrogenperoxide
°C	Degree Celsius
DW	Deionized water
DMSO	Dimethyl sulfoxide
DLS	Dynamic light scattering
DNA	Deoxyribonucleic acid
MTT	3-(4,5-Dimethylthiazol-2-yl)-2,5-diphenyltetrazoliumbromide
DCF	Dichlorofluorescein
DLS	Dynamic light scattering
DMEM	Dulbecco's Modified Eagle's Medium
EDX	Energy-dispersive X-ray spectroscopy
ELISA	Enzyme-linked immunosorbent assay
HK-2	Epithelial proximal cell lines
et al.	et alli (Latin), and other people
etc.	et ectera (Latin), other things
EDTA	Ethylene diamine tetra acetic acid

LIST OF ABBREVIATIONS (cont.)

ERKs	Extracellular-signal-regulated kinases
FBS	Fetal bovine serum
FITC	Fluorescein isothiocyanate
FTIR	Fourier transform infrared spectroscopy
C60	Fullerene-60
C60-NPs	Fullerene-60 nanoparticles
GBM	Glioblastomas cells
C6	Glioma cell lines
IP15	Glomerular mesangial cell lines
GSH	Glutathione
GSTM1	Glutathione-S-transferase M1
GPx	Glutathione peroxidase
GSK-3β	Glycogen synthase kinase 3 beta
Au	Gold
g	Gram
HO-1	Heme oxygenase-1
h	Hour
THP-1	Human acute monocytic leukemic cell line
HEK 239	Human Embryonic Kidney 293 cell lines
U87	Human primary glioblastoma cell lines
H_2O_2	Hydrogen peroxide
$^{\bullet}OH$	Hydroxyl radical
iNOS	Inducible nitric oxide synthase
IκB	Inhibitor of kappa B
IKK1 or IKK-α	Inhibitor of nuclear factor kappa-B kinase subunit alpha
IKK2 or IKK-β	Inhibitor of nuclear factor kappa-B kinase subunit beta
I.D.	Inner diameter
INS-GNPs	Insulin-targeted gold nanoparticles

LIST OF ABBREVIATIONS (cont.)

IL-1α	Interleukin-1 alpha
IL-1β	Interleukin-1 beta
IL-5	Interleukin-5
IL-6	Interleukin-6
IL-10	Interleukin-10
IL-13	Interleukin-13
IL-17A	Interleukin-17A
IL-33	Interleukin-33
IARC	International Agency for Research on Cancer
JNK	Jun amino-terminal kinases
kg	Kilogram
LDH	Lactate dehydrogenase
LPS	Lipopolysaccharides
LiCl	Lithium chloride
MgO	Magnesium oxide
MIP	Macrophage inhibitory protein
mRNA	Messenger RNA
MALDI-TOF	Matrix-assisted laser desorption/ionization time-of-flight mass spectrometry
MMP-12	Matrix metallopeptiidase 12 or macrophage metalloelastase
MMP13	Matrix metallopeptidase 13
µg	Microgram
µg/kgBW	Microgram per kilogram body weight
µg/ml	Microgram per milliliter
µg/cm^2	Microgram per square centimeter
µg/cm^3	Microgram per cubic centimeter
µl	Microliter

LIST OF ABBREVIATIONS (cont.)

µm	Micrometer
µM	Micromolar
mA	Milliamp
mg	Milligram
mg/kg	Milligram per kilogram
mg/ml	Milligram per milliliter
ml	Milliliter
mM	Millimolar
mV	Milli volt
min	Minute
MMP	Mitochondrial membrane potential
MAPKs	Mitogen-activated protein kinases
MAP3K	Mitogen-activated protein kinases kinase kinase
MKPs	MAPK phosphatases
MCP	Monocyte chemotactic protein
MEF	Mouse embryonic fibroblasts
RAW 264.7	Murine macrophage cells
BV2	Murine microglial cell line
MWCNTS	Multi-walled carbon nanotubes
nm	Nanometer
NPs	Nanoparticles
NADPH	Nicotinamide adenine dinucleotide phosphate
NO	Nitric oxide
NF-κB	Nuclear factor-kappa B
NIK	Nuclear factor-kappa B inducing kinase
NMR	Nuclear magnetic resonance
O.D.	Outside diameter
PMs	Particulate matters

LIST OF ABBREVIATIONS (cont.)

%	Percent
wt%	Percent by weight
PCI	Phenol/chloroform/isoamyl alcohol
PMSF	Phenylmethane sulfonyl fluoride
PBS	Phosphate-buffered saline
PBMCs	Peripheral blood mononuclear cell
PS	Phosphatidylserine
PDI	Polydispersity index
PI	Propidium iodide
PGI_2	Prostacyclin or prostaglandin I2
PG	Prostaglandin
PGD_2	Prostaglandin D2
PGE_2	Prostaglandin E2
$PGF_{2\alpha}$	Prostaglandin F2 alpha
PGH_2	Prostaglandin H2
NQO1	Quinone oxidoreductase
ROS	Reactive oxygen species
RT-PCR	Reverse transcription polymerase chain reaction
RNase A	Ribonuclease A
RNS	Reactive nitrogen species
rpm	Rounds Per Minute
SEM	Scanning electron microscopy
SiO_2	Silicon dioxide
SMs	Silicon microparticles
SNs	Silicon nanoparticles
Ag	Silver
Ag-NPs	Silver nanoparticles
SWCNTs	Single-walled carbon nanotubes

LIST OF ABBREVIATIONS (cont.)

SDS	Sodium dodecyl sulphate
SDS-PAGE	Sodium dodecyl sulphate polyacrylamide gel Electrophoresis
SE	Standard error of mean
SD	Standard deviation
$O_2^{\bullet-}$	Superoxide anion radical
SOD	Superoxide dismutases
TEMED	Tetramethylethylenediamine
G_0	The resting phase in cell cycle
G_1	The first growth period of the cell cycle
TXA_2	Thromboxane A2
TiO_2-NPs	Titanium dioxide nanoparticles
TLR2	Toll-like receptor 2
TLR4	Toll-like receptor 4
TGF-β	Transforming growth factor beta
TEM	Transmission electron microscope
TBST	Tris-buffered saline with Tween 20
TNF-α	Tumor necrosis factor alpha
TNFR	Tumor necrosis factor receptor
2θ	Two theta
UV	Ultra violet
w/v	Weight per volume
WHO	World Health Organization
XAFS	X-ray absorption fine structure spectrometry
XPS	X-ray photoelectron spectroscopy
XRD	X-rays powder diffraction
ζ potential	zeta potential
ZnO-NPs	Zinc oxide nanoparticles

CHAPTER I
INTRODUCTION

1.1 Background

Nanotechnology can be defined as engineered structures, systems and devices that have at least one dimension less than 100 nm (1, 2). An increasing number of applications using nanomaterials has been launched in the market as household products (such as cosmetics, food additives, etc.) and in various industries (such as catalysts and semiconductors (3-5)).

Titanium dioxide nanoparticles (TiO_2-NPs) have been recently used in several products (6-8), especially in cosmetics and packaging (9). Because of their unique properties (including transparency and photocatalytic property), TiO_2-NPs are attractive for biological, chemical, and industrial applications. Interesting properties of TiO_2-NPs allow them to be used as a protective material for solar ray protection (such as sunscreen lotion and light stabilization in wood coatings) (8, 10, 11). Moreover, TiO_2-NPs can be used in chemical degradation, anti-microbial activity, phosphopeptide enrichment from biological materials, and in medical purposes such as implants and tissue engineering (9).

Carbon-based nanoparticles such as fullerenes and carbon nanotubes are also widely used in everyday products. Due to their unique structures, great strength, long aspect ratio and good properties in thermal and electrical conductivity, they have been used in electronics, optics, materials science, and architecture. Generally, carbon nanotubes (CNTs) can be engineered into two forms, as a rolled up single layer (SWCNTs) or multiple layers (MWCNTs). These two forms have been used for medical purposes, including biomedical engineering, tissue engineering, drug delivery gene therapy and biosensors (12-14).

Due to the widespread use of these two nanomaterials, it is important to investigate their toxicity. A number of publications have recently reported the adverse effects of NPs *in vitro* and *in vivo*. Particle size and surface area of the nanomaterials

may lead to an increase in biological activity that can enhance any intrinsic toxicity (4). Biological effects, such as inflammation and genotoxicity, due to inhaled nanoparticles were reported (15, 16). The most important exposure route for airborne nanoparticles is inhalation (16, 17). After the nanoparticles enter the body through inhalation, they may translocate to secondary target organs (blood vasculature, heart, liver, spleen, kidneys, and brain) (11, 18). Thus, the toxicity of inhaled nanoparticles should be studied.

The toxicity effect of TiO_2-NPs on mammalian cells has been investigated in various studies (19-22). However, several studies have reported that TiO_2-NPs did not induce toxicity with *in vitro* testing (23-26). For example, Park *et al*. (22) reported that both nano- and micro-sized TiO_2 particles exhibited no significant toxicity in human alveolar epithelial cells (A549 cells). Recently, Wilhelmi *et al*. (26) reported the toxicity of TiO_2-NPs on macrophage cells (RAW 264.7). They found that small doses of TiO_2-NPs (1, 5, 10, 40, and 80 $\mu g/cm^2$) did not induce cell death; however, there was evidence of DNA fragmentation when measured by flow analysis after being treated with TiO_2-NPs at 80 $\mu g/cm^2$ for 24 h.

At the same time, several studies have reported that TiO_2-NPs potentially cause toxicity in mammalian cells. The possible mechanism of TiO_2-NPs to induce cell apoptosis through lysosome membrane destabilization and lipid peroxidation in the 16HBE14o-bronchial epithelial cell line was reported by Hussain *et al*. (19). It is important to note that both the size and crystal structure of TiO_2 can contribute to cell toxicity. Stolle *et al*. (27) reported that the rutile and anatase crystal structure of TiO_2-NPs led to the death of HEL-30 mouse keratinocyte cells. The effect of the size and surface area of TiO_2-NPs on cell toxicity was presented in many reports (10, 28, 29). Reactive oxygen species (ROS) generation and oxidative stress are also an important mechanism that can induce cell toxicity. The exposure of TiO_2-NPs to cells can generate ROS and oxidative stress. Several studies revealed that TiO_2-NPs strongly induce oxidative DNA damage in cultured cells (20, 29-32). The expression of apoptosis proteins such as p53, BAX, Cyto-c, Apaf-1, caspase-9 and caspase-3, was also enhanced by TiO_2-NPs. This later caused toxicity in cells (10, 33-35).

In the case of CNTs, it has been reported that they produce a different toxicity effect from TiO_2-NPs because of their fiber shape, length, and stability. The

toxicity effect of CNTs on cells is similar to that from asbestos fiber. The long tube of CNTs can cause incomplete phagocytosis of macrophages. This leads to huge ROS generation that can enlarge the inflammatory response in cells (36, 37). It is well known that oxidative stress mechanisms are involved with various oxidase enzymes (NADPH oxidase, myeloperoxidase, and horseradish peroxidase etc.). These enzymes are mostly found in phagocytic cells types (such as macrophages) (38-42). Therefore, the phagocytosis of CNTs by macrophages induces ROS production and inflammation. Besides oxidative stress mechanisms, it was reported that the CNTs can cause cell toxicity via non-oxidative stress pathways. As described by Shvedova *et al.* (37), cellular damage caused by CNTs may be represented by physical interference, for example, the disruption of the mitotic spindle caused by single-walled carbon nanotubes (SWCNTs) (43). Srivastava *et al.* (44) also reported that the extramitochondrial ROS induction was found in A549 cells treated with MWCNTs. The ROS was induced by the generation of cytochrome P450, which is the heme-thiolate proteins involved in oxidative metabolism. In addition, the cytotoxicity of MWCNTs in human macrophage cells was reported by Zhu *et al.* (45). They investigated the toxicity of purified and acid-purified MWCNTs (at concentrations of 5, 10, 25, and 50 μg/ml for 24 h) on U937. Their results indicated that at high concentrations (25 and 50μg/ml), acid-purified MWCNTs were significantly toxic to U937 cells.

Macrophages are the immune cells that play an important role in the clearance of inhaled particles and exogenous substances (46-48). Thus, the exposure of nanoparticles by inhalation may lead to a persistent activation of alveolar macrophages. This activation can induce inflammatory cytokines such as tumor necrosis factor alpha (TNF-α) and interleukin-1 beta (IL-1β), ROS, and reactive nitrogen species (RNS) production. The release of these biomolecular molecules can lead to chronic inflammation resulting in lung fibrosis formation and later on, cancer (16, 26, 49). Therefore, it is important to pay attention to the cytotoxic effect of nanomaterials entering the body through inhalation. The toxicity of a substance depends on many factors, for example, entry route, exposure time, number of exposures (single or multiple dose) and toxic substance form (50-52). Since NPs have special physical properties, the concentration of nanoparticles and the exposure time of

human contact should be strongly considered. The dose-dependent effect on the toxicity of various nanoparticles in cells was reported by Lai *et al*. (53). They studied the effect of TiO_2, ZnO, and MgO nanoparticles on human neural and human fibroblasts cells at different doses of NPs.

Various studies have investigated the effect of nanoparticles on immune cells. For example, Paino *et al*. (54) reported the cytotoxicity and DNA damage on PBMCs treated with low doses (0.01 and 1 μM respectively) of gold nanoparticles. TiO_2 and ZnO at concentrations from 1-100 μg/ml were not toxic to PBMCs (55). Chen *et al*. (56) reported the cytotoxicity of MWCNTs in RAW 264.7 cells. Their results revealed that the cytotoxicity of MWCNTs in these cells was a dose-dependent response. They also concluded that the cytotoxicity was correlated with the increase of oxidative stress. The investigation of toxicity effects in *in vivo* is also important. The *in vivo* study can provide more understanding of kinetics, effects, and mechanisms of nanoparticles in a living system compared with *in vitro* (57). *In vitro* and *in vivo* models are both used for testing of lung toxicity of airborne NPs, but *in vitro* assays as predictive screens for toxicity assessment of NPs in commerce are simpler, faster and more cost-effective than *in vivo* assays. Moreover, rodents (mice and rats) have similarities in their bodies with humans, are small in size, are easy to handle and may produce offspring in a short period of time. However, both *in vivo* and *in vitro* examinations have remarkable advantages and disadvantages. Therefore the combination of these assays may have benefits for the early detection of possible toxicological effects, and the new relationships between the primary outcomes can be revealed (58).

Brain is an important organ that maintains homeostasis of human body. The blood brain barrier (BBB) is a key factor to protect the brain from invading organisms or unwanted substances. The transportation of NPs through BBB possibly occurs via passive diffusion, active transport, and receptor-mediated transport mechanisms (59-61). Currently, there is an increasing need of a new model for effective drug delivery to the brain that can be useful for central nervous system disorder treatment (62). Additionally, a brain tumor is a disease in central nervous system that highly causes death in children (63, 64). Recently, nanotechnology has been applied to deliver therapeutic drugs into the brain via transporters or internalizing

receptors of BBB capillaries (61, 64, 65). Various studies have shown that NPs at size range between 5 to 7 nm are able to cross BBB (66-73), but the toxic mechanisms are still unclear. However, Wu *et al.* (74) reported that the SiO_2-NPs at the size of 15 nm were found in rat's brain after intranasal instillation. In recent study by Shilo *et al*. (75) also reported that insulin-conjugated gold nanoparticles (INS-GNPs) at the size of 20 nm had an ability to cross BBB via the special mechanism called receptor-mediated endocytosis. These evidences show that NPs at the sizes of 15-20 nm could also pass through BBB.

Due to above information, besides focusing on the nanotoxicity of NPs on immune cells, this thesis therefore focuses on investigating the effect of TiO_2-NPs on glioma cancer cells. The outcome from this study could lead to the possibility of using TiO_2-NPs for therapeutic cancer applications. In addition, its outcome may help indicate whether or not TiO_2-NPs can induce the growth of cancer cells. It is well known that glioma is a high chemo and radio resistant brain cancer (76). The C6 glioma cells have been widely used for a variety of studies in cancer research (77). These cells have also been widely used in experimental neuro-oncology to evaluate the therapeutic efficacy of a variety of modalities, including chemotherapy (78), antiangiogenic therapy (79), proteosome inhibitors (80), radiation therapy (81), and gene therapy (82). The application of TiO_2-NPs for treatment of brain tumors was reported by López *et al*. (83). C6 glioma cells have been used by inoculation with Wistar rats, where TiO_2-NPs that contained $Pt(NH_3)_4Cl_2$ were used to reduce tumor growth. Their results revealed that tumor growth was reduced by 56%. This indicates that a synergistic effect between the TiO_2-NPs carrier and the platinum drug could destroy glioma cells.

The translocation of nanoparticles can occur via inhalation, therefore, the investigation of the cytotoxic effect of TiO_2-NPs on glioma cells could help develop new technology for cancer destruction via inhalation.

In this thesis, I aim to investigate the toxicology of TiO_2-NPs in murine macrophage cells (RAW 264.7) and in rat glioma cells (C6). The investigation of the effects of TiO_2-NPs and MWCNTs in *in vivo* was also performed.

1.2 Objectives

Because of the very small size and special properties of material NPs, distribution and accumulation may occur in various organs after contaminating the body. More investigations of the effects of TiO_2-NPs on immune and cancer cells and MWCNTs on *in vivo* are required. Therefore the goals of this thesis are to investigate the cytotoxicity and inflammatory induction by TiO_2-NPs and MWCNTs in *in vitro* and *in vivo* respectively. RAW 264.7 cells were used as a model for *in vitro* study because these cells play a vital role in the immune system (47, 84, 85). Furthermore, C6 cells were also used as a model cancer cell for investigating the killing effect of TiO_2-NPs on the aggressive brain cancer.

In vivo study was carried out in mice. Even though *in vitro* investigation of NPs is simpler, faster and more cost effective than *in vivo*, *in vivo* study is also required for gaining more information on NPs effects on a living system.

The specific objectives of this study are shown as follows:

1) To determine the toxicity effects of TiO_2-NPs on RAW 264.7 and C6 cells.

2) To determine the effects of TiO_2-NPs on intracellular ROS production of a RAW 264.7 cells.

3) To evaluate the effects of TiO_2-NPs on pro-inflammatory cytokine productions of RAW 264.7 and C6 cells.

4) To study the effects of TiO_2-NPs and MWCNTs on *in vivo* systems by investigating proinflammatory cytokine productions released in broncho alveolar lavage fluid (BALF) after TiO_2-NPs and MWCNTs have been instilled intranasally into mice.

CHAPTER II
LITERATURE REVIEW

2.1 General properties of nanomaterial

A nanoparticle (NPs) is commonly defined as an object with at least one dimension smaller than 100 nm (11, 86, 87). The forms of NPs can be different such as amorphous or crystalline structure. Therefore, NPs should be considered a distinct state of matter, in addition to the solid, liquid, gaseous, and plasma states, due to its distinct properties (2).

Important issues that must be considered in the field of NPs are agglomerates and aggregates of NPs, which represent the strong attractive forces between crystal or single particles causing them to form a tight bond. As a result, the particles become larger in size than a single form of the particles (or primary particle) structure. Therefore, the primary particle size may be explained as the size of an individual particle in suspension. However, the primary particles may characteristically agglomerate because of weak physical interactions (adhesion). The size and shape of particles can be changed after agglomeration. The surrounding physical or chemical conditions (such as temperature, pH, and viscosity) can affect different agglomeration states (88). Primary particles loosely bind together resulting in a total surface area similar to the total specific surface area of the primary particle. In the case of aggregation, it is developed when a common crystal line structure of primary particles is formed. The total specific area of aggregated particles is smaller than the total surface area of the primary particle because particles are aligned together side by side (11, 89). The diagram of interchangeable aggregation and agglomeration states of NPs is shown in figures 2.1 and 2.2.

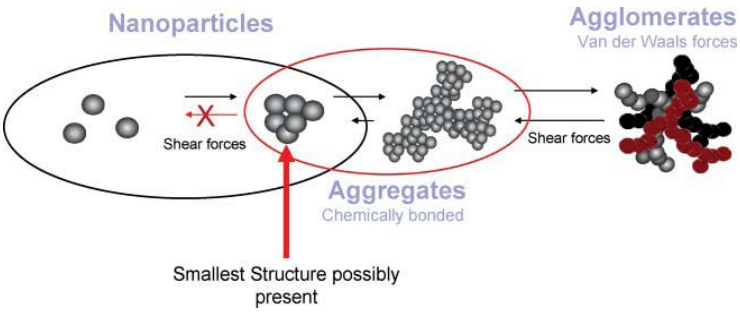

Figure 2.1 The schematic diagram represents the aggregates and agglomerates of NPs. (Reproduced with permission from Schilling *et al*. (11)).

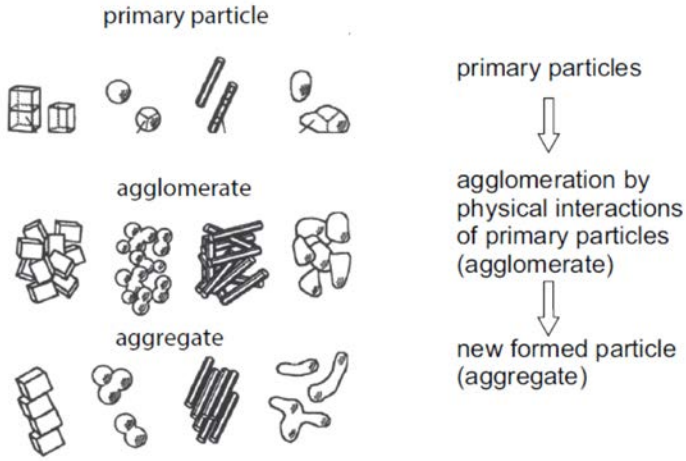

Figure 2.2 The schematic diagram represents the aggregation and agglomeration of NPs. The agglomeration of primary has a weak binding. The aggregation of particles provides a strong binding. (Reproduced with permission from Dirk Walter) (88)).

To break the bonds of agglomerated NPs, a dispersion mechanism such as probe sonication can be applied. The measurement of the agglomeration state of solution-based NPs can be performed by TEM analysis and dynamic light scattering (DLS).

Nanomaterials are generally classified into four major groups based on their dimensionality, morphology, composition, and uniformity and agglomeration state (2).

1) Dimensionality

Dimension can be used to classify nanomaterial types. One dimensional nanomaterials has one dimension that is not in nanoscale. The examples of one dimensional nanomaterials are nanotubes, nanowires, nanorods, and nanoribbons that have been developed and used in various applications.

Two-dimensional nanomaterials have two dimensions that are outside the nanometric size range. Two-dimensional nanomaterials can be defined as an atomic or molecular thickness that has infinite planar dimensions such as nanoplates, nanosheets, and nanofilms (90, 91).

Three-dimensional (or polycrystals) nanomaterials include powders, fibrous, multilayer, and polycrystalline materials in which all of the structural elements contact to each other and form interfaces (92, 93).

Nanoparticles that have all dimensions in nanoscale (not larger than 100 nm) are called zero-dimensional nanomaterials or nanoparticles. Zero-dimensional nanomaterials can be morphous or crystalline. They can provide various shapes and forms. The examples of zero-dimensional nanomaterials are quantum dot and metal oxide nanoparticles (such as TiO_2 and ZnO) (91, 92).

2) Morphology

The morphological characteristics of NPs can be divided into three major categories: flatness, sphericity, and aspect ratio (2) (figure 2.3). A general classification exists between high- and low-aspect ratio particles. High aspect ratio NPs are in the forms of nanotubes, nanowires, and various shapes (such as helices, zigzags, belts). Small-aspect ratio particles have various morphologies such as spherical, oval, cubic, prism, helical, or pillar. Collections of many particles exist as powders, suspension, or colloids (2).

3) Composition

The composition of NPs is the chemical properties of nanomaterials including degree of purity, impurity or additives. NPs can be composed of a single component material or a complex of several materials. NPs found in a nature are often agglomerations due to the mixture of various compositions while a single-component material has a high stability and can be easily synthesized by various methods (2).

4) Uniformity and agglomeration state

Based on their chemistry and electro-magnetic properties, NPs can exist as dispersed aerosols in the form of suspensions/colloids, or in an agglomerate state (figure 2.3). The definition of agglomerate is defined as the cluster of particles rigidly joins together by partial fusion or by growing together. Agglomeration of nanoparticles can change the size of the NPs and their physical and optical properties (87, 94).

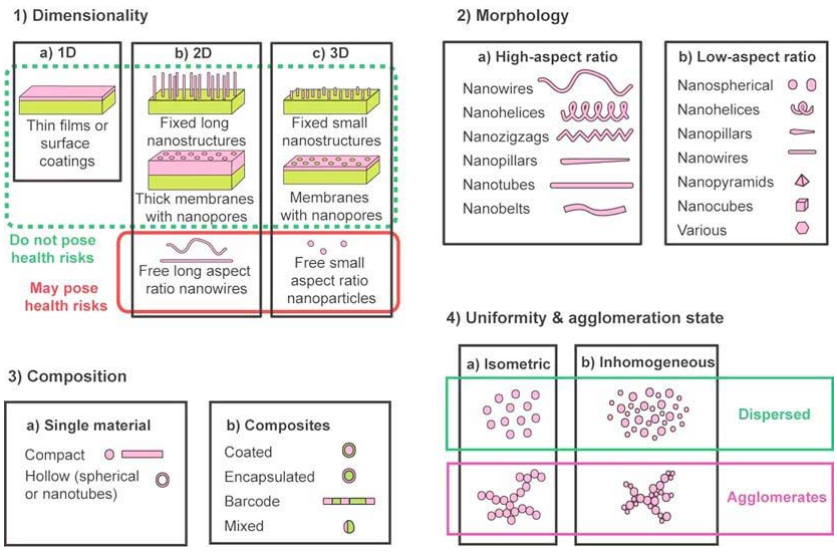

Figure 2.3 Nanomaterial classifications are categorized into four groups based on dimensionality, morphology, composition, and uniformity and agglomeration state. (Reproduced with permission from Buzea *et al.* (2)).

2.2 Properties and applications of TiO_2-NPs and MWCNTs

Due to the small size of NPs and their special properties, the characterization of nanomaterials is needed before employing them. Recently, Berube *et al*. (95) divided the classifications of nanomaterials that can have problematic effects on human health into six groups; they are carbon nanotubes (CNTs), quantum dots, metal oxides, metals, fullerenes, and polymers. In this thesis, titanium dioxide NPs (TiO_2-NPs) and carbon nanotubes were used in the experiment. The properties of both nanomaterials are described as follows.

2.2.1 TiO_2-NPs

TiO_2-NPs are classified as transition metal oxides that have three different main crystallized structures: anatase, rutile, and brookite (7, 96). Depending on its chemical structures, the anatase phase of TiO_2-NPs has a tetragonal structure (as shown in figure 2.4). Rutile TiO_2-NPs have a tetragonal structure as well, containing 6 atoms per unit cell (in figure 2.4a). The rutile phase of TiO_2-NPs is stable at suitable temperatures and pressure levels. Moreover, with a particle size greater than 14 nm, anatase and brookite phases of TiO_2 can transform into the rutile phase after reaching optimal temperature (about 500 ºC to 900 ºC) (7, 97). The refractive indexes of rutile and anatase are approximately 2.75 and 2.54, respectively (97, 98). Because of their high reflective index, macro-scale TiO_2-NPs have been used as a pigment in color manufacturing. They can also be used in ceramic industries due to their excellent chemical properties (99). Due to the great catalytic properties of TiO_2, they have been used as photocatalysts for hydrogen production in solar cells and for organic contaminant degradation (100). TiO_2-NPs have been used to reduce UV light absorption and can be found in everyday life products such as sunscreen, cosmetics, and clothing. Other applications of TiO_2-NPs are in cleaning products, self-cleaning coatings, air filtration devices, electronics (e.g., computer, keyboard, and mouse), and hair styling devices. The use of TiO_2-NPs in solar cells was also reported (11, 98).

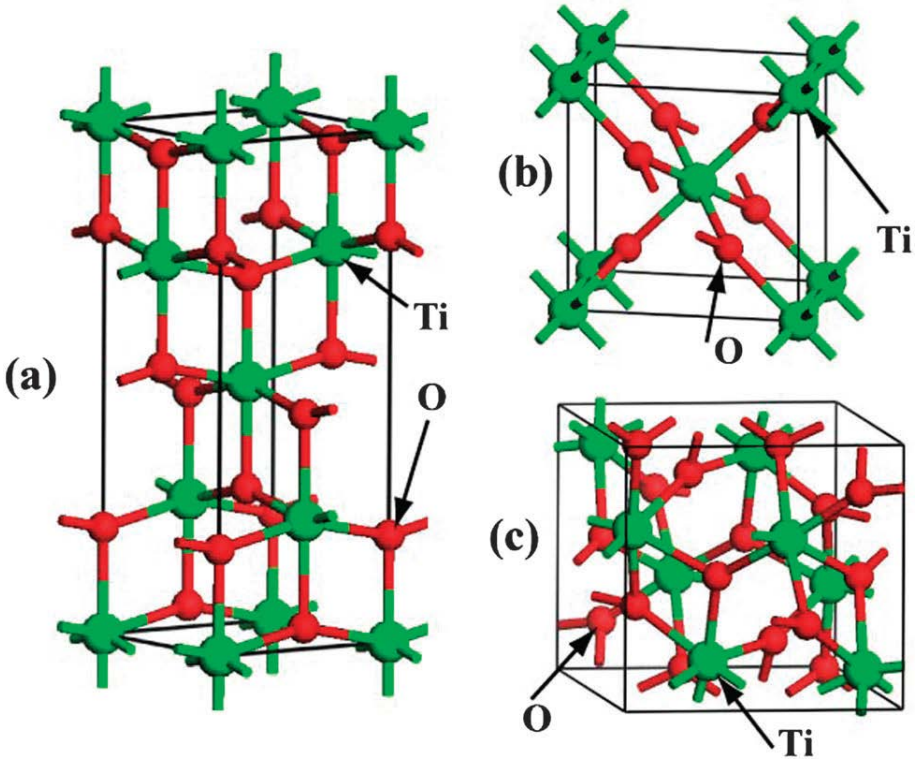

Figure 2.4 Different phase structures of TiO_2: (a) anatase, (b) rutile, and (c) brookite. (Reproduced with permission from Zhang *et al.* (101)).

2.2.2 Carbon nanotubes

Carbon nanotubes are formed from a sheet of graphite rolled into a cylindrical structure. The cylinder structure normally has a length of up to ten microns. The end of the tube is capped with a half part of a fullerene molecule (102). There are two classes of carbon nanotubes: the first one is composed of one atom-thick sheet of graphene and rolled up into a cylindrical shape called single-walled carbon nanotubes (SWCNTs). The other is composed of a number of graphene sheets to form concentric tubes called multi-walled carbon nanotubes (MWCNTs). The MWCNTs are larger than the SWCNTs and consist of many single-walled tubes (figure 2.5) (103-107). Generally, the structures of CNTs containing a lot of carbon atoms arranged in hexagons are similar with that of graphite. CNTs have three main unique geometrical structures (armchair, zigzag, and chiral) and these structures can be classified by the wrapping pattern of a carbon sheet in a tube. Both the structure and composition of CNTs lead them to have outstanding properties such as stability, mechanically storing

energy and high conductivity (103). For these reasons, CNTs open up new perspectives for various applications, such as nanotransistors in circuits, field emission displays, and biomedical applications (106, 108).

(a) (b) (c)

Figure 2.5 The schematic structures of carbon nanotubes. (a) Single layer of grapheme sheet, (b) single-walled carbon nanotubes, and (c) multi-walled carbon nanotubes. (Reproduced with permission from Kreupl *et al.* (109)).

The application of CNTs mainly depends on their properties, including thermal, electronic, and mechanical properties (110). CNTs in composite reinforcement or lubrication are related to their mechanical properties displaying the strong chemical bonds between carbon-carbon in graphene layer. This leads CNTs to be the strongest and stiffest manmade materials on earth (102). CNTs can also be used for absorbing radiation; therefore, they are currently used in stealth paints or coating. Additionally, high strength and low-density properties of CNTs can be used in light weight applications with strong nanotube-based fibers (110).

2.2.3 Characterization of nanomaterials

The characterization of size, morphology, and surface charge of nanomaterials can be done using advanced microscopic techniques such as scanning electron microscopy (SEM), transmission electron microscopy (TEM), and atomic force microscopy (AFM). TEM and SEM can be employed to visualize the physical size, shape, morphology, uniformity, and topography of NPs. Electron microscopy techniques are very useful in ascertaining the overall shape of polymeric NPs, which may determine their toxicity (111). The surface charge of NPs affects the physical stability and re-dispersibility of NPs (103). An analytical tool used with SEM to

identify the elemental composition of samples is energy dispersive X-ray (EDX) microanalysis. EDX (Energy Dispersive X-ray Spectroscopy), is an x-ray technique used to identify the elemental composition of materials. EDX systems are combined with SEM or TEM to do an image and elemental analysis of the specimen of interest. The data generated by EDX analysis consist of spectra showing peaks corresponding to the elements of the analyzed sample. In addition, elemental mapping of a sample and image analysis are performed (112). However, both internal and surface functionalization of NPs in suspension may not always be visualized by these techniques, which rely on the electron density of the functional group. Alternatively, dynamic light scattering (DLS) can be used to measure the hydrodynamic size and surface charge of suspended NPs in different vehicles (103, 113). DLS is a technique for measuring the size of particles typically in the sub-micron region. DLS measures Brownian motion and this motion is linked to the size of the particles. The size of measured NPs was derived from the time-dependent fluctuation of the scattering intensity caused by the interference of the relative Brownian movements of multiple NPs in suspension. Through analysis of these fluctuations, average particle size and polydispersion can be calculated. Additionally, the surface charge of the NPs can indicate the suspension stability. This can be measured by the zeta potential function installed in DLS (113).

2.3 Cytotoxic effect of nanomaterials *in vitro*

Nanotoxicology refers to the study of the adverse effects of nanomaterials on living organisms and the ecosystem. The study of the prevention of such adverse effects is also included (114). Additionally, toxic effects of physical and chemical properties (e.g. size, shape, surface chemistry, composition, and aggregation) on biological systems were emphasized (115). Donaldson *et al*. (116) described how the adverse effect of NPs after exposure to the body has a greater potential to travel through the organism than do microparticles. In addition, when NPs reach the target organ(s), they can trigger mediators that activate inflammatory or immunological responses. NPs can also enter the blood or the central nervous system, where they have a direct potential to affect cardiac and brain functions (116, 117). Moreover, the

exposure of NPs can trigger specific mechanisms of toxicity such as epithelial tissue injury, inflammation, oxidative stress, and allergy. In addition, the exposure of NPs can exert a toxic effect on DNA (called genotoxicity). This might initiate and promote carcinogenesis, or exert teratogenicity (118, 119).

To understand the complete risk of NPs to human health, the comprehensive study of the mechanisms of potential exposures and the toxicokinetic data associated with various portals of entry to the body is important (119). In 2005, Oberdörster *et al.* (5) demonstrated the hypothetical routes of uptake and translocation of NPs into the body, as shown in figure 2.6.

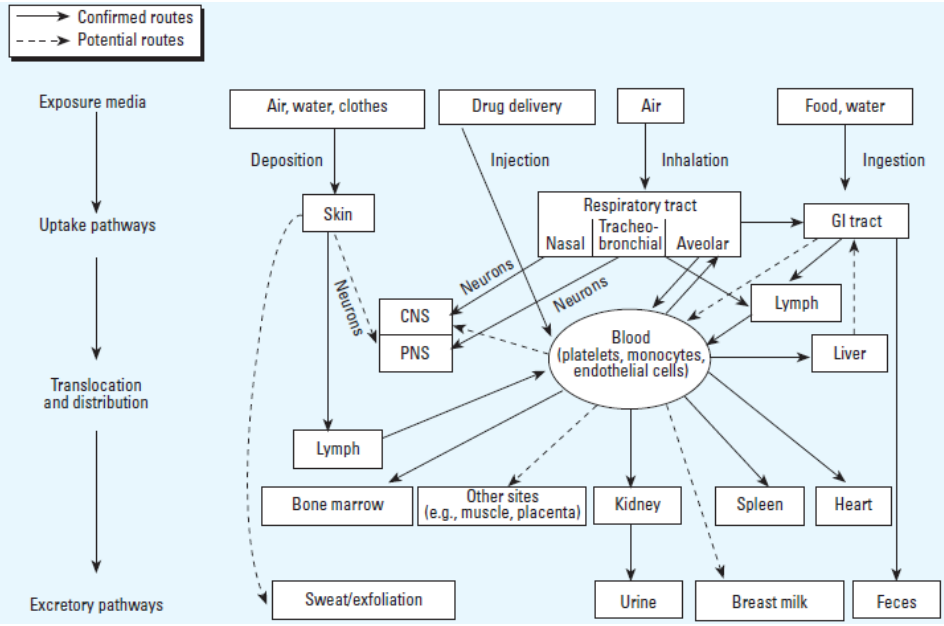

Figure 2.6 Biokinetics of NPs in the human body. (Reproduced with permission from Oberdörster *et al.* (5)).

The possible causes of toxicity produced by nanomaterials were proposed by Fischer and Chan (115). The cause of toxicity was related to the unique structures of nanomaterials including the following reasons: 1) NPs have special physical and chemical properties. Therefore, the breakdown of nanostructures could lead to a specific toxic effect that is difficult to predict. 2) The surfaces of nanomaterials contribute to many catalytic and oxidative reactions. Because of the greater surface

area-to-volume ratio of nanomaterials, these reactions may induce more toxicity than bulk materials. 3) Some nanomaterials may contain toxic metals or compounds, and the breakdown of these materials can elicit similar toxic responses to the components themselves.

TiO_2-NPs have been mostly used in a wide range of applications. Because of the specific properties of TiO_2 (such as catalytic activity) at the nanoscale size, more concern in human health risk is necessary. Several studies revealed that TiO_2-NPs produce cytotoxicity to various cell types and model animals (17). TiO_2 has recently been reclassified by the IARC (International Agency for Research on Cancer) as a group 2B carcinogen that is "possibly carcinogenic to humans" (9, 17, 120).

2.3.1 Oxidative stress-mediated nanotoxicity

Oxidative stress has been defined as an imbalance between the production of an oxidizing molecule (pro-oxidants) and the presence of cellular antioxidants in favor of the pro-oxidants that lead to potential damage (121). The damages occur through the production of peroxides and free radicals which include the superoxide anion radical ($O_2^{\bullet-}$), hydrogen peroxide (H_2O_2), and hydroxyl radical ($^{\bullet}OH$). These free radicals are potentially deleterious products that can damage cellular components including proteins, lipids, and DNA. Therefore, they are referred to as "reactive oxygen species" (ROS) (52, 122). The consequent damage to cell molecules can occur at several pathophysiological states, such as neurodegenaration, cancer, mutagenesis, and cardiovascular diseases (123). The production of ROS in aerobic cells can also associate in aging and degenerative diseases (124, 125). ROS can be generated in many different organelles in response to various stimuli. Major sources of intracellular ROS are generated endogenously, as in the process of mitochondrial oxidative phosphorylation (121, 126, 127). Complexes I and II of the electron transport chain in mitochondria are the most possible sites of superoxide radical formation during oxidative phosphorylation because these complexes are semiquinones with unpaired electrons. Thus, the oxygen molecule may receive these unpaired electrons to form a superoxide radical (128).

The regulation of extracellular ROS generation in mammalian cells occurs through the respiratory burst of phagocytic cells by nicotinamide adenine dinucleotide

phosphate (NADPH) oxidase (121, 129). The mechanism of the immune system by phagocytic cells (such as neutrophils or activated macrophages) defends against foreign organisms by generating superoxide radical anions through NADPH oxidases and myeloperoxidases (38, 122). These phagocytes are capable of generating large amounts of ROS to resist pathogens. Active NADPH oxidase has three subunits (p40phox, p47phox, and p67phox) located in the cytosol, while p22phox and gp91phox are membrane bound. Upon stimulation, all subunits are brought together into one macromolecule complex and this complex can generate several forms of ROS (130).

Exposure to environmental factors is another source of oxidative stress. The exogenous compounds that have proven to be potential sources of ROS are radiation (e.g., UV light and X-rays), toxic chemicals (e.g., paraquat), drugs (e.g., adraiamycin and quinones), and particulate matters (PMs) (131-134). PMs mediated oxidative stress has been reported in recent years. Some particles (such as silica and asbestos) can mediate oxidative stress after being inhaled in the lungs (135, 136). Particulate-mediated oxidative stress is comprised of two distinct mechanisms: non-cellular and cellular particles-mediated ROS generation. The non-cellular ROS generation is occurred from Fenton-like reaction that has iron or other transition metals reacting with hydrogen. On the other hand, the particles-mediated oxidative stress results from simulating of stimulated lung cells by inhaled particles (137). Particle size is an important factor in determining the deposition region of the lung after inhalation (138). In addition, the particle size of the aerosol entering the respiratory tract was determined as inhalable particles, which normally have sizes that range between 1nm to 10μm. The NPs have been determined as respirable dust, which can enter and be deposited on an alveolar region of the respiratory tract (138-140). Therefore, NPs must be closely related to oxidative stress mediated toxicity especially in cells at the alveolar region of the lung (15).

Oxidative stress is considered to be the most important mechanism in the cytotoxic effects of NPs (5, 141-143). NPs may possibly induce the production of ROS both inside and outside of the cell. As reported by Suh *et al*. (144), ROS produced by NPs may affect cell membrane stability and cell survivability. On the other hand, if NPs are internalized, ROS production, particle dissolution, and

mechanical damage to sub-cellular units such as the nucleus are very important and should be considered. Most recently, Manke *et al.* (145) described the mechanisms of oxidative stress induced by NPs. They found that there are two factors involved in this mechanism. The first factor is a cellular factor, which depends on cell interaction with NPs, such as NP-cells interaction and immune-cells interaction. Therefore, this factor mostly relies on NPs properties (such as surface properties, size, composition, and presence of metals). Aydin *et al*. (146) also concluded that three main factors cause oxidative stress by NPs: 1) the surface of NPs (especially metal-based NPs) that plays a role in active redox cycling, 2) the functional groups of NPs which have an oxidative potential, and 3) the interaction between particle and cell.

Several studies have reported on NPs-mediated toxicity *in vitro* through oxidative stress. Pujalte *et al*. (147) demonstrated the cytotoxicity and oxidative stress induced by three types of NPs: TiO_2, ZnO, and CdS on IP15 (glomerular mesangial) and HK-2 (epithelial proximal) cell lines. Their results indicated that the important factors that affected the cytotoxicity of NPs were physicochemical properties of NPs and a type of cell. Only ZnO and CdS caused oxidative stress on those cell lines; in contrast, the effects were not observed with TiO_2-NPs. Moreover, they also suggested that the chemical property of NPs might induce different cellular responses that related to the production of ROS.

Yang *et al*. (148) reported the relationship between particle composition of NPs and the oxidative effect. They reported that different properties of NPs lead to diverse cytotoxicity. The interaction of electron donor or acceptor active sites with molecular dioxygen (O_2) is important. They also provided an example of ZnO-NPs that are more chemically active in nature than SiO_2. The electron capture on the surface of ZnO-NPs can lead to more formation of the superoxide radical ($O_2^{\bullet -}$), which culminates in ROS accumulation and oxidative stress. In addition, the decreased nanoparticle size might create discontinuous crystal planes that could increase the number of structural defects as well as disrupt the well-structured electronic configuration of the material. Thus, the electronic configuration on the particle surface might change. This would establish specific ‘surface groups’ that could function as reactive sites. ‘Surface groups’ can make NPs hydrophilic or hydrophobic, lipophilic or lipophobic, or catalytically active or passive. As suggested by De Berardis *et al.*

(149), electron capture on the surface of metal NPs could increase the formation of superoxide radicals ($O_2^{\bullet-}$), leading to ROS accumulation and oxidative stress.

The major routes that NPs can enter the body are inhalation, trans-dermal, and ingestion. However, inhalation is the most potentially harmful route for humans (146). Therefore, the lungs are a major target organ and the most sensitive organ of inhaled NPs. Due to their size, NPs can be distributed throughout the whole respiratory tract and reach the alveoli (15). Immediately after exposure, NPs are translocated to blood circulation and distributed to other organs (150, 151). Therefore, NPs can induce a potential oxidative stress as described previously. Oxidative stress damage by NPs in the respiratory-related cells has been evaluated both *in vivo* and *in vitro*. Park and Park (152) presented their study of the oxidative stress and pro-inflammatory response of silica NPs on RAW 264.7 cell lines. Treatment of silica NPs on the cultured RAW 264.7 cells led to ROS generation and decreased intracellular glutathione (GSH). In several other studies, NPs altered ROS production and interfered with biological antioxidant defense responses mentioned in the investigation by Park *et al*. (153) and the oxidative stress was increased after treatment of cells with TiO_2-NPs. They also discussed that ROS is an important factor of the apoptotic process. The excess generation of ROS can induce mitochondrial membrane permeability and damage the respiratory chain, resulting in the induction of the apoptotic process.

Manke *et al*. (145) reported the mechanisms of oxidative stress mediated toxicity of NPs in the mitochondrial respiration, immune cell activation, and NADPH oxidase system. Furthermore, excessive production of oxidative stress could also activate cytokines and upregulated interleukin (IL), kinases, and tumor necrosis factor-α (TNF-α). Therefore, these biomolecules can be used as indicators of inflammation signaling processes to oxidative stress (146, 151).

Recently, the mechanisms of TiO_2-NPs induce oxidative stress and apoptosis has been reported by Shukla *et al.* (154). Their study investigated the toxic effect of TiO_2-NPs (1 to 80 µg/ml) on HepG2 (human liver) cells. The cytotoxicity was found in cells treated with TiO_2-NPs at concentrations of 20, 40, and 80 µg/ml. The loss of mitochondrial membrane potential (MMP) was detected after for 24 h incubation. However, the significant increase of apoptosis (in both early and late

stage) was found in cells treated with TiO_2-NPs at concentrations of 20, 40, and 80 µg/ml for 48 h. It seems that mediated cytotoxicity of TiO_2-NPs in HepG2 cells was occurred by ROS production. Their results showed the increase of pro-apoptotic proteins (BAX) and the decrease of anti-apoptotic protein (Bcl-2) after treating cells with TiO_2-NPs. This resulted in a high ratio of Bax/Bcl-2 that later could lead to cytochrome c production. The cytochrome c could bind to Apaf-1 (apoptotic protease activating factor) and caused an apoptosome formation. Moreover, their results showed that caspase-9 and caspase-3 could generate the death of cells treated with TiO_2-NPs. In overall, TiO_2-NPs could induce cell death by ROS mediated DNA damage pathway (154). The involvement of ROS mediated apoptosis cell death by TiO_2-NPs was also reported by Meena *et al*. (34). Their results indicated that TiO_2-NPs induced apoptosis of HEK-293 cells through ROS-mediated oxidative stress with a similar pathway mentioned previously. The apoptosis cell death caused by TiO_2-NPs was recently reported by Sheng *et al*. (155). Rat primary cultured hippocampal neuron cells were treated with TiO_2-NPs at concentrations between 5-30 µg/ml. Their results revealed that the death of hippocampal neuron cells treated with TiO_2-NPs occurring from MMP reduction, cytochrome c up-regulation, Bax and caspase-3 protein expression, and down regulation of Bcl-2 protein, which are associated with mitochondria-mediated apoptosis cell death pathway.

It is well-known that TiO_2-NPs can be activated into an excited state under UV irradiation. This can also induce ROS generation and trigger oxidative stress (156). Xiong *et al*. (157) reported that the surface area of TiO_2-NPs was a main factor of toxicity in cells both with and without UV irradiation. The hydroxyl radical molecules occurred after UV irradiation could be adsorbed on the surface of TiO_2-NPs. These hydroxyl radicals and hydroxide ion generated on the surface of TiO_2-NPs can damage cells (157, 158). In this case, the higher toxicity could be found in cells treated with high surface area particles than ones treated with low surface area particles (157). Micron-size particles may enter the cells via phagocytosis, however, nano-size particles can internalize and incorporate with various biomolecules (such as protein, lipid, and DNA) and may lead to cytotoxicity.

2.3.2 NPs induce inflammatory responses

Inflammation is the defense mechanism in the body that responds to pathogens or foreign materials and promotes the repair of injured tissue (159). Excessive or persistent inflammation can contribute to numerous pathophysiological states and the exacerbation of diseases. The inflammation of living tissues may be caused by microorganisms, noxious stimuli (such as chemicals), or physical injury (119, 159). The chronic inflammatory responses with the surface, chemical, or physical reactivity of NPs lead to the stimulation of neutrophils and macrophages that can cause inflammation to persist. The prolonged inflammation results from many processes that can contribute to an induction of fibrosis and carcinogenesis (160, 161). During the inflammatory process, various chemical markers such as adhesion molecules, chemotactic factors, and pro-inflammatory factors are released. As described previously, NPs have an ability to trigger oxidative stress. ROS are known to cause many forms of injury and inflammation. Gilmour *et al*. (162) showed the correlation between ROS and inflamed cells as a three stage model. At the first level, oxidative stress is at a low level. The induction of antioxidant enzymes ((NAD(P)H: quinone oxidoreductase (NQO1), glutathione-S-transferase M1 (GSTM1), and heme oxygenase-1 (HO-1)) is able to restore cellular redox homeostasis. With continued oxidative stress, these enzymes become overwhelmed and can no longer neutralize the effect of ROS. At the second level: MAPK (mitogen-activated protein kinase) and NF-κB activations produce proinflammatory responses. At the third level of oxidative stress, the permeability of the mitochondria is compromised and disrupted, resulting in cellular apoptosis and necrosis. Immune effects from NPs are also thought to be due to oxidative stress through the presence of surface free radicals that are generated by the interaction between NPs and the aqueous milieu. Released reactive species and free radicals can interfere with the numerous cellular signaling pathways, resulting in the expression of altered cytokine release profiles.

Oberdörster *et al*. (5) reported four primary pathways involved in inflammation and oxidative stress mediated by NPs (figure 2.7). In the first pathway, the particle surface causes oxidative stress, resulting in the increase of intracellular calcium and gene activation. In the second pathway, transition metals are released from NPs, resulting in oxidative stress. In the next pathway, cell surface receptors are

activated by transition metals released from particles, resulting in subsequent gene activation. Lastly, the intracellular distribution of NPs to mitochondria generates oxidative stress.

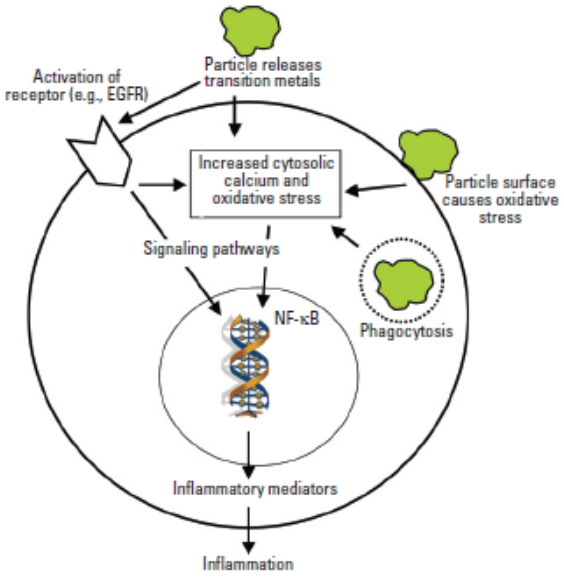

Figure 2.7 Intracellular mechanism of oxidative stress and inflammation induction by TiO_2-NPs. (Reproduced with permission from Oberdörster *et al.* (5)).

Recently, Nishanth *et al.* (159) showed the inflammatory response of RAW 264.7 macrophages cells after exposure to NPs at different types and sizes. These NPs are silver (Ag), aluminum (Al), carbon black (CB), carbon-coated silver (CAg), and gold (Au). Their results showed that significant increases in IL-6, ROS, NF-κB, cyclooxygenase-2 (COX-2), and tumor necrosis factor-alpha (TNF-α) expression were observed in macrophages exposed to Ag NPs followed by Al, CB, and CAg.

The signaling pathway involved in inflammatory responses causes by NPs has been studied recently by Cui *et al.* (163). They investigated the signaling pathway of inflammation in a mouse's liver after treating mice with TiO_2-NPs by intragastric administration. The accumulation of TiO_2-NPs was found in the liver. The histopathological changes and hepatocyte apoptosis of mice liver and the liver functions damaged by TiO_2-NPs were observed. Their results showed that TiO_2-NPs can significantly increase the mRNA and protein expression of TLR2, TLR4, and

several inflammatory cytokines (IKK1 (Inhibitor of nuclear factor kappa-B kinase subunit alpha or IKK-α), IKK2 (or IKK-β), NF-κB, NF-κBp52, NF-κBp65, TNF-α, and NIK (NF-κB-inducing kinase)). TiO_2-NPs can also significantly suppress the mRNA and protein expression of IκB and IL-2. The signaling pathway of inflammation of mouse liver caused by TiO_2-NPs may occur via the activation of mRNA molecules for TLR2 (Toll-like receptor 2) and TLR4 (Toll-like receptor 4) and protein expression. Moreover, their results also indicated that TiO_2-NPs can significantly increase the mRNA and protein expression of several inflammatory cytokines, including NIK, IKK1, IKK2, NF-κB, NF-κBp52, NF-κBp65, and TNF-α.

During the primary stage of inflammation, residential macrophages are the first immune cell type to be activated to generate an immune response (164). The effects of various types of NPs on immune cells were reported by various studies. Park *et al*. (165) showed the pro-inflammatory cytokine released from the RAW 264.7 macrophages cell. Their results showed that TNF-α was released significantly while other cytokines (including IL-1α, IL-1β, IL-6, and IL-10) were slightly increased (151, 165). Interestingly, Choi *et al*. (166) reported the decrease of IL-6 and TNF-α productions of RAW 264.7 cells after treatment with silicon NPs (SNs) found at concentrations greater than 20 μg/ml. In contrast with silicon microparticles (SMs), the productions of both cytokines were increased when the concentration of SMs increased. They also explained that because of their small size, macrophages might not recognize the small size particles. It is possible that SNs enter macrophage cells through the pores of the cell membrane, while the SMs are large enough to be recognized and were phagocytized by the macrophage. The exposure of TiO_2-NPs to RAW 264.7 macrophage cells induced the secretion of TNF-α, which has been recently reported by Kim and Tao (167). They showed that the inflammation responses of TiO_2-NPs on macrophage cells were involved in the MAPK/NF-κB signaling cascade.

Due to inflammatory effects induced by TiO_2-NPs, the inhalation of TiO_2-NPs is one of the major routes that raise the contamination of TiO_2-NPs in the human body as described previously. Especially in people who are often in contact with TiO_2-NPs at a high volume (17), some particles can be cleared out from the respiratory tract by mucociliary escalator. Alveolar macrophages are responsible for the particles that

cannot be cleared by mucociliary escalator. Amounts of oxygen radicals, proteolytic enzymes, and proinflammatory cytokines are released depending on phagocytized activity of macrophages. These mediators may lead to acute and chronic lung inflammation (151).

2.3.3 Role of COX-2 and NPs in inflammation

Cyclooyxgenase (COX), also known as prostaglandin H synthase, is an important enzyme in prostaglandin (PG) biosynthesis of from arachidonic acid. The expressions of COX are encoded by two genes, COX-1 and COX-2. Both of which participate in the expression of several proteins including PGD_2, PGE_2, PGI_2, $PGF_{2\alpha}$, and thromboxane A.

Prostaglandin biosynthesis starts after the release of arachidonic acid from membrane phospholipids by phospholipase A_2. Arachidonic acid is then metabolized by the sequential actions of prostaglandin H synthase, or COX, into the unstable intermediate PGH_2. PGH_2 is a common substrate for a series of specific isomerase and synthase enzymes that produce PGE_2, PGI_2, PGD_2, $PGF_{2\alpha}$, and TXA_2 (168, 169).

COX-1 is normally expressed in many tissues of the body (such as stomach, kidneys). It is involved in the cytoprotection of mucosa. On the other hand, COX-2 is an inducible isoform of COX that is upregulated by several stimuli such as mitogens, cytokines, growth factors, and tumor promoters (170, 171). The pathway of COX-2 in cancer development is shown in figure 2.8. These prostaglandins promote cell division, metastasis, and angiogenesis, but inhibit apoptosis. This can lead to tumor growth induction (169).

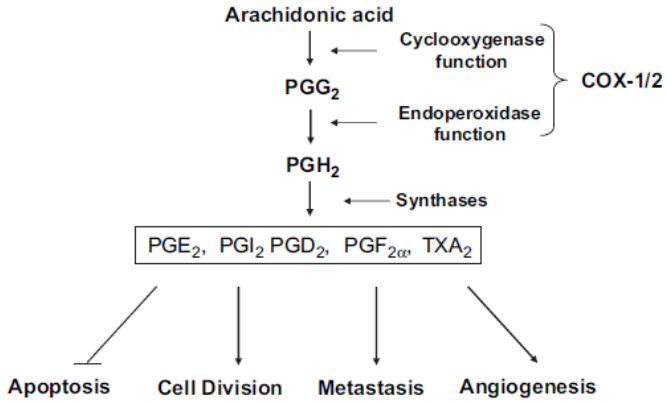

Figure 2.8 The involvement of Cyclooxygenase-2 (COX-2) enzyme in cancer development and apoptosis cell death. (Reproduced with permission from Grosch *et al.* (169)).

COX-2 is important in the regulation of prostaglandins production. The expression of COX-2 is strongly induced by several pro-inflammatory cytokines and growth-promoting stimuli (172). COX-2 has been described as an inducible isoform expressed during the inflammatory process (173). The study of COX-2 and NPs involved in genotoxic effects was performed by Xu *et al.* (174). They measured mutant fractions of redBA/gam loci in MEF cells exposed to either TiO_2 particles or fullerene-60 (C_{60}) at different doses. Their results showed that in the presence of COX-2 inhibitor (NS-398), the genotoxic effects of nano-sized TiO_2 and C_{60} were reduced dramatically. Their results imply that COX-2 is involved in mediating the genotoxic events induced by TiO_2-NPs and C_{60}-NPs. Nishanth *et al.* (159) also reported the toxicity of various types of NPs. Their studies revealed that Ag-NPs exhibit a higher propensity for inducing inflammation, mediated by ROS and NF-κB signaling pathways and leading to the induction of COX-2. COX-2 has been determined to be involved in the allergic airway inflammation following exposure to MWCNTs into COX-2 deficiency mice by oropharyngeal aspiration. Sayers *et al.* (175) reported that MWCNTs significantly enhance allergen-induced cytokine release, including IL-13, IL-5, CXCL10, and IL-17A.

2.4 Toxicity of nanomaterials *in vivo*

Because of the aerodynamic properties of NPs, they have a greater potential to reach the deep part of the lungs than microparticles do (5). Furthermore, NPs deposited in the lungs may interact with macrophages, resulting in the activation of a clearance mechanism. These NPs may also have directly contact with other respiratory cells such as fibroblasts, endothelial cells, or cells of the immune system (87). For high bio-persistence (such as NPs), they may cause chronic and pulmonary fibrosis. After NPs are deposited at the lungs, the initiation of inflammatory response can occur by the interaction with cells of the immune system (28, 161, 176).

There are various studies that examine the potential adverse health effects of NPs in animal models by inhalation. Here, the effects of TiO_2-NPs and CNT *in vivo* are the main focus. The neurotoxic potential of TiO_2-NPs has been reported by Wang *et al*. (71). TiO_2-NPs were intranasally instilled into mice for 30 days. Following this, the pathological changes of mice brain tissue were examined. Their results showed that TiO_2-NPs were translocated to the central nervous system and caused brain lesions. The toxicity of TiO_2-NPs on the respiratory system was reported in 2002 by Bermudez *et al*. (177). Three species of laboratory rodents were selected for examining subchronic effects of TiO_2-NPs. Their results revealed that inhaled TiO_2-NPs caused lung burden and induced a pulmonary inflammatory response. Moreover, the development of fibroproliferative lesions was found in the rats after 90 days of exposure with high concentrations of TiO_2-NPs. Size-specific toxicity of TiO_2-NPs was tested *in vivo* by Sager *et al*. (178). They compared the inflammagenic and cytotoxic level between fine (micron-sized) and ultrafined (nano-sized) TiO_2 particles. Their results indicated that TiO_2-NPs induce more inflammation and more cytotoxicity than do micron-sized TiO_2 particles. The report by Park *et al*. (179) showed that the elevation of proinflammatory cytokines, such as IL-1, TNF-α, and IL-6, was observed after 24 h in mice intratracheally instillation with TiO_2-NPs. In mice's lungs tissue, they also found the increase of inflammatory proteins such as macrophage inhibitory protein (MIP) and monocyte chemotactic protein (MCP) after 1 and 14 days after instillation respectively. The mechanism of TiO_2-NPs that induces lung fibrosis was explained by Li *et al*. (151). After TiO_2-NPs exposure into the lungs, NPs can induce high ROS expression. The overproduction of ROS can induce the activation of

cytokine growth cascades. Then, tyrosine kinases, MAPK, and transcriptional factors (such as NF-κB) are activated. Therefore, the genes involved in inflammation and fibrosis (such as TGF-β) are also transcribed and expressed. Meanwhile, this can promote the formation of immature collagenous tissue within the lung. Moreover, several studies have reported the inflammation of tested animal's lungs after treatment with TiO_2-NPs (99, 180, 181).

In vivo toxicity of CNTs on the respiratory system was reported by Muller *et al*. (182). Carbon nanotubes were administered intratracheally to Sragues-Dawley rats and examined for inflammatory responses in the lungs. After 60 days of CNTs exposure, CNTs were still present in the rat lungs. The formation of collagen-rich granuloma in the bronchial lumen, which is an indicator of pulmonary lesion, was observed after exposure the rat with CNTs. Their results indicated that the exposure of CNTs in the lungs of animals could stimulate of TNF-α production. The mechanisms of CNTs for toxicity induction *in vivo* were reported by Chou *et al*. (183). Macrophage cells in the alveoli secreted various inflammatory cytokines after intratracheal instillation of CNTs. Similar results of inflammation induced by CNTs were reported by Hsieh *et al*. (184). They examined the toxicity mechanism of CNTs in mice. Their results indicated that after providing a single dose of CNTs (at the concentration 0.1 or 0.5 mg/mouse) by intratracheal instillation, the air ways were obstructed and granulomatous was observed in lung parenchyma. Moreover, they found that the expression of cathepsin K and MMP12 (the proteinase that plays an important role in tissue remodeling) increased and may induce pulmonary injury. The oxidative stress-mediated toxicity in animals after treatment with CNTs was reported by Han *et al*. (185). MWCNTs at amounts of 20 and 40 μg suspended in 40 μl sterile phosphate-buffered saline were exposed to mice lungs by oropharyngeal aspiration. Their results revealed that total proteins (LDH, TNF-α, IL-1β, and surfactant protein-D) in the mice's broncho alveolar lavage (BAL) fluid significantly increased, after the mice were treated with MWCNTs at both amounts for 1 day. Moreover, the level of 8-hydroxy-2'-deoxyguanosine (8-OHdG) in urine was elevated. This could indicate that systemic oxidative stress is caused by the exposure of MWCNTs.

CHAPTER III
MATERIALS AND METHODS

3.1 Chemicals and reagents

Chemicals and reagents used for this study were purchased from various sources. Dulbecco's Modified Eagle's Medium (DMEM), Nutrient Mixture Ham's F-12 medium, antibiotics-antimycotic (100×), Dulbecco's phosphate buffer saline, and trypsin-ethylene diamine tetra acetic acid (EDTA) were purchased from Gibco (Grand Island, NY, USA). Fetal bovine serum (FBS) was purchased from Hyclone (Perbio, Cramlington, UK). Trypan blue solution (0.4%) (JR Scientific, Woodland, CA), 3-(4,5-Dimethylthiazol-2-yl)-2,5-diphenyltetrazolium bromide (MTT), Dimethyl sulfoxide (DMSO), and 2'7'-dichlorofluorescin diacetate (H_2DCFDA) were purchased from Sigma-Aldrich (St. Louis, Mo, USA). Bradford protein assay reagent, alkaline phosphatase conjugate substrate, non-fat dry milk, tris(hydroxymethyl)-aminomethane, SDS-PAGE standard, glycine, and bis-acrylamide were purchased from Bio-Rad (USA). Rabbit anti COX-2 antibody was purchased from Cayman (MI, USA). AP-conjugated secondary antibody and rabbit anti β-actin antibody were purchased from Cell Signaling Technology® (Beverly, MA, USA). CellTiter-Glo® Luminescent cell viability assay kit was purchased from Promega (WI, USA). AnnexinV-FITC's apoptosis detection kit was purchased from BD pharmingen™ (Franklin Lakes, NJ, USA).

3.2 Experimental procedure

3.2.1 Preparation of nanomaterials

TiO_2-NPs from Wan Jing New Materials Co. Ltd. (Hangzhou Zhejiang, China) were kindly provided by Assist. Prof. Dr. Toemsak Srikhirin (Material Science and Engineering program, Faculty of Science, Mahidol University). TiO_2-NPs from the supplier were dispersed in deionized water (DW) to prepare the stock of suspension at a concentration of 37,500 µg/ml. The stock of TiO_2-NPs suspension in culture medium was freshly prepared by diluting the stock of TiO_2-NPs suspension in DW with culture medium (without serum) to have a concentration of 5,000 µg/ml and then sonicated at 80% amplitude for 30 seconds (10 times) plus 10 seconds with a high intensity ultrasonic processor (Sonic, model VCX 130). For the preparation of TiO_2-NPs, testing concentration was prepared by diluting the TiO_2-NP suspension in culture medium (stock concentration at 5,000 µg/ml) with serum free medium at the desired concentrations for each experiment. Vortex was applied before applying TiO_2-NP suspensions to cultured cells to avoid sedimentation and aggregation.

MWCNTs were purchased from Sigma-Aldrich (St. Louis, MO). The outside diameter (O.D.), inner diameter (I.D.), and length obtained from the supplier were 10-15 nm, 2-6 nm, and 1-10 µm. respectively. The preparation of MWCNT stock solution was done by weighing 1 mg of MWCNTs and dissolving it in 1 ml of 100% fetal bovine serum (FBS) to form a concentration of 1 mg/ml. MWCNTs stock suspension (in 100% FBS) at the concentration of 1 mg/ml was sonicated at 80% amplitude for 30 seconds (10 times) plus 10 seconds pulse. The series of MWCNTs testing concentration was prepared by diluting the MWCNTs stock suspension (1 mg/ml in 100% FBS) with the culture medium containing 1% D-glucose plus 10% FBS. Each concentration of MWCNTs suspended in medium containing 0.1% D-glucose plus 1% FBS was sonicated before being applied to cultured cells as described previously.

3.2.2 Characterization of nanoparticles

3.2.2.1 Size measurement and shape investigation

The hydrodynamic sizes of the NPs (dispersed in water and cell culture media) were measured by Malvern Zetasizer 3000 (Malvern Instrument Inc., London, UK). This technique is based on the principles of dynamic light scattering (DLS). Suspensions of each NP at a volume of 3 ml were prepared and then transferred to a cuvette for DLS measurements. The concentration of TiO_2-NP suspension dispersed in DW and in culture medium free FBS was 5,000 µg/ml. For MWCNTs, the concentration used for measuring was 0.1 mg/ml. They were dispersed in 1 culture medium containing 1% FBS plus 0.1% D-glucose. Before measurement, a 10 minute-ultrasonication was performed to make the nanoparticles well dispersed. The average hydrodynamic size of the suspended NPs was calculated by the instrument software.

The sizes and shapes of TiO_2-NPs and MWCNTs were measured using scanning electron microscopy (SEM, LEO model LEO 1450 VP) or transmission electron microscope (TEM). Both nanoparticles were dissolved in DW and sonicated by ultrasonication before being dropped onto a silicon wafer. After the DW evaporated, samples were observed by SEM at the Microscopic Center, Faculty of Science, Burapha University. In the case of TEM, samples were dropped onto TEM copper grids. The images were obtained using TEM (Philips, Models TECHNAI 20) with the assistance of the staff at the Center of Nanoimaging (CNI), Faculty of Science Mahidol University.

3.2.2.2 Zeta (ζ) potential

TiO_2-NPs were diluted with DMEM to reach a concentration of 5,000 µg/ml. MWCNTs were suspended in DMEM containing 1% FBS plus 0.1% D-glucose. Immediately, the suspensions of NPs were injected into a capillary cell of Malvern Zetasizer 3000. The measurements were carried out in triplicate for the time interval of 30s for each measurement.

3.2.2.3 Crystalline phase characterization with X-rays powder diffraction (XRD)

TiO_2-NPs were dispersed in DW to reach a concentration of 1 mg/ml. The solution was dried at 103-105 ºC, and then crushed into a fine powder. In the case of MWCNTs, a commercial powder form was used for this characterization. The crystallographic studies of all NPs powders were analyzed by XRD. The diffraction patterns were taken in 2θ geometry.

3.2.3 Cell lines and culturing procedure

3.2.3.1 Rat glioma cells (C6) were kindly provided by Assoc. Prof. Dr. Sukumal Chongthammakun. C6 cells were grown in a mixture of DMEM and Nutrient Mixture Ham's F-12 medium (at a ratio of 1:1) and were supplemented with 10% FBS and 1% antibiotic-antimycotic. Cells were propagated in 25-cm^2 culture flasks under a 95% humidified air incubator at 37 ºC and 5% CO_2. The culture medium was changed 2-3 days/week. Cells were sub-cultured every 4-5 days by using 0.25% trypsin-EDTA to detach the cells.

3.2.3.2 Murine macrophage cells (RAW 264.7) were kindly provided by Prof. Dr. Pawinee Piyachaturawat. Cells were maintained in DMEM and were supplemented with 10% FBS and 1% antibiotic-antimycotic. Cells were propagated in 25-cm^2 culture flask under a 95% humidified air incubator at 37 ºC and 5% CO_2. Culture medium was changed every 2-3 days. RAW 264.7 cells were sub-cultured after 80% of cell confluences by using the cell scraper method. Only cells in the exponential phase under twenty passages were used in the experiments.

3.2.4 Cells viability assay

3.2.4.1 Trypan Blue Exclusion Test

The trypan blue exclusion assay can also be used to determine the cell viability. It is based on the principle that cell membranes of the viable cells do not take up certain dyes (blue cells), whereas non-viable cells do. Briefly, a cell suspension was simply mixed with 0.4% trypan blue dye and then examined by microscopy. The number of dead and alive cells was counted. The calculation of relative cell viability is shown in following equation (186):

$$\text{Viable cells (\%)} = \frac{\text{total number of viable cells per ml of aliquot}}{\text{total number of cells per ml of aliquot}} \times 100$$

In this study, cells were seeded in 35mm culture dishes and incubated for 24 hours at 37 ºC with 5% CO_2. Cells were treated with different concentrations of TiO_2-NPs for 24 h under a 95% humidified air incubator at 37 ºC and 5% CO_2. Cells were then detached (by scrapped off or trypsinized) and transferred to a test tube. The trypan blue dye (JR Scientific, Woodland, CA) with the same volume of cell suspension was added into the cell suspension. Next, cells and dye were incubated for 5 min at room temperature. The viable cells (cells without dye) were counted using a hemocytometer.

3.2.4.2 CellTiter-Glo® Luminescent cell viability assay

The CellTiter-Glo® Luminescent cell viability assay is a luminescent cell viability technique that determines the number of viable cells. This test is based on luciferase reactions that can measure ATP production in cells. In live cells, ATP is used as their energy supplier. For this reason, the presence of ATP can be used as an indicator of metabolically active cells (187). CellTiter-glo® reagent can cause cell lysis after adding reagent into cells. Following this, the ATP is released and the enzyme luciferase can interact with the compounds in the CellTiter-glo® reagent to form a luminescence signal. The signal detected is proportional to the concentration of ATP and the amount of ATP is proportional to the number of viable cells (188). Therefore, the percent of relative cell viability can be measured. With this assay, RAW 264.7 cells and C6 cells were plated in 96 well plates at 1×10^5 cells per well. Plated cells were incubated for 24 h at 37 ºC with 5% CO_2. After this, cells were treated with different concentrations of TiO_2-NPs for 24 and 48 h at the same incubating conditions as cell culture. After incubation, treated cells were determined for cell viability using the CellTiter-Glo® assay following the protocol provided by the manufacturer. The luminescence was read at the wavelength of 542 nm at an integration time of 1,000 milliseconds per well with a microplate reader (Molecular devices, SpectraMax® M series, CA, USA).

3.2.5 Measurement of intracellular ROS

Intracellular ROS was monitored using the fluorescent probe 2',7'-dichlorodihydrofluorescein diacetate (H_2DCFDA) by following the approach from manufacturer's protocol with slight modification. H_2DCFDA is a dye that easily diffuses into cells. The dye is deacetylated by cellular esterase to form non-fluorescent DCFH that can be further oxidized by ROS inside cells to form a high fluorescent compound; dichlorofluorescein (DCF) (189).

In this study, cells were plated onto 96-well plates at a density of 9.5×10^3 cells/well (for RAW 264.7 cells) and 1.9×10^4 cells/well (for C6 cells) and allowed to adhere overnight in 95% humidified air incubator at 37 ºC and 5% CO_2. After incubation, media was removed and cells were further incubated in 10 µM solution of H_2DCFDA for 30 minutes in dark incubation. Next cells were rinsed twice with PBS and treated with NPs. Immediately after treatment, the fluorescence intensity of DCF molecules (from the oxidation of dyes) was read using a microplate reader (Molecular devices, SpectraMax® M series, CA, USA) with the excitation and emission wavelengths at 492 nm and 535 nm respectively. The hydrogenperoxide (H_2O_2) at the concentration of 100 µM was used as a positive control. The DCF fluorescence intensities were measured at 5, 15, and 30 min after treating cells with TiO_2-NPs at various concentrations. The percentage increase of fluorescence intensity was calculated by the formula below, as explained by Subramaniam and Ellis (190).

$$\%\ increase\ in\ fluorescence\ intensity = \left[\frac{(Ft_{30} - Ft_0)}{Ft_0} \times 100\right]$$

Where;

Ft_{30} = fluorescence intensity at desirable time (5, 15, and 30 min)

Ft_0 = fluorescence intensity at initiate time (0 min)

3.2.6 Protein isolation and western blot analysis

3.2.6.1 Determination of protein concentration

In this study, cells were plated onto petri dishes at a density of approximately 1×10^6 cells/ml and were allowed to adhere overnight in a 95% humidified air incubator at 37 ºC and 5% CO_2 before experimentation. After treatment with NPs, the media was removed and washed three times with cold PBS. Then the exposed cells were harvested by adding ice-cold lysis buffer (50 mM Tris-HCl pH 7.4, 150 mM NaCl, 1% Triton X-100, 1 mM EDTA, 1 mM Na_3VO_4, 1 mM PMSF, and 1 mM NaF) containing EDTA-free protease inhibitor cocktail (Roche Diagnostics, Basel, Switzerland). Samples were mixed and left on ice for 30 min. Next, the cultured cells were immediately scraped off by using a cell scraper. The lysates were collected into microcentrifuge tubes and centrifuged at 1,200 rpm, 4 ºC for 20 min. The supernatants were collected and stored at -80 ºC. The collected protein concentrations were determined by the Bradford method using a Bio-Rad protein assay kit (BioRad, Richmond, CA, USA) and then the absorbance was measured at 595 nm by spectrophotometer (Molecular devices, SpectraMax® M series, CA, USA).

3.2.6.2 Western blotting analysis

Western blot is an analytical technique used to detect specific proteins in cell samples and tissue homogenates or extracts. The proteins are separated based on their molecular weight by using sodium dodecyl sulfate-polyacrylamide gel electrophoresis (SDS-PAGE). In this thesis, the expression of inflammatory associated proteins in C6 and RAW 264.7 cells was observed. Protein samples (those were collected from 3.2.6.1) were treated with 5× sample buffer containing 1 M Tris-HCl (pH 6.8), glycerol, 10% SDS, β-mercaptoethanol, and 1% bromophenol blue. After this, the samples were boiled at 95 °C for 5 min to denature proteins. The solubilized proteins were loaded into 10% SDS-PAGE containing with 40% acrylamide, 1.5 M Tris-HCl (pH 8.8), 10% APS, and TEMED, total volume 20 µl/well. Thereafter, the proteins were constantly electrophoresed through 80-100 volts for 90 min. Then, the proteins were transferred to a 0.45 µm nitrocellulose membrane (Bio-Rad Laboratories, Hercules, CA, USA) with transfer buffer containing Tris glycine buffer (25 mM Tris HCl, 192 mM glycine, and 0.1% SDS) and 10% methanol. The running condition was set at 220 mA for 90 min. The membrane was blocked with 5% w/v

non-fat dry milk (Bio-Rad Laboratories, Hercules, CA, USA) in Tris-buffered saline containing 0.1% Tween-20 (TBST) for 1 h. After washing with TBST, the membrane was probed with a primary antibody overnight at 4 ºC. The specific primary antibodies used in this study were anti COX-2 antibody from Cayman Chemical (MI, USA), anti-β-catenin (H-102) antibody from Santa Cruz Biotechnology (CA, USA), and anti-β-actin antibody from Cell Signaling Technology (MA, USA). The membrane was washed five times with 1×TBST containing with 1 M Tris-HCl (pH 7.5), 5 M NaCl, and Tween 20 to remove any residual primary antibody. After washing, the membrane was incubated with the alkaline phosphatase (AP) conjugated goat anti-rabbit secondary antibodies (Cell Signalling Technology, MA, USA) for 1 h. The membrane was washed five times with TBST. The signal of proteins was detected by chemiluminescence technique using an alkaline phosphatase (AP) conjugate substrate Kit (Bio-Rad, Hercules, CA, USA). After the colors were developed, the membrane that contains interested protein was visualized by gel documentation (Syngene, UK). The intensity of protein bands was measured by GeneSnap software on gel documentation.

3.2.7 Determination of apoptosis cell death

3.2.7.1 The detection of DNA fragmentation by DNA laddering pattern on the agarose gel assay was used to determine cell apoptosis.

Apoptosis can be defined as the specific morphological pattern of cell death characterized by nuclear and cytoplasmic condensation, plasma membrane blebbing, and nuclear pyknosis, leading to nuclear DNA breakdown into multiples oligonucleosomal fragments (approximately 180-200 bp). These fragments were appeared on an agarose gel (191-193).

In this study, RAW 264.7 and C6 cells were seeded into petri dishes at a density of 1×10^5 cells/ml. Cells were treated with different concentrations of NPs at various periods. Treated cells were resuspended in 10 mM TE buffer pH 8.3 and then lysed with lysis buffer (100 mM Tris-HCl pH 8, 10 mM EDTA and 1% SDS). Following this, cells were incubated in a shaking water bath at 50 ºC for 1 h. Next, the ribonuclease A (20 µg/ml) was added and incubated for 1 h at 37 ºC. Thereafter the proteinase K (0.1 mg/ml) was added and further incubated overnight at

50 ºC. The mixture of phenol/chloroform/isoamyl alcohol (PCI) was added for chromosomal DNA extraction and then precipitated in ethanol at -20 ºC overnight. DNA samples were separated by 1.8% agarose gel. The apoptotic DNA fragmentation was detected by staining with ethidium bromide and was visualized under UV light of gel documentation system (194, 195).

3.2.7.2 Analysis of cell death by flow cytometric method

The combination of two different fluorochromes (FITC-conjugated Annexin V and propidium iodide (PI)) was used to detect the loss of membrane integrity that causes cell death either from apoptotic or necrotic processes. Non apoptotic (Annexin V-FITC negative, PI negative), early apoptotic (Annexin V-FITC positive, PI negative), and late apoptotic or necrotic cells (Annexin V-FITC positive, PI positive) were presented by this double staining. This mechanism of this staining is based on the exposure of phosphatidylserine to the outer cell membrane and the membrane permeability of the cells (196). For example, phosphatidylserine (PS) is located at the inner layer of cell membrane lipid bilayer for live cells. However, the early stage of apoptosis, there is a breakdown of cell membrane. Thus, the PS is translocated to the outer layer of the cell membrane. Therefore, the binding of Annexin V (which have high affinity to PS) can be detected (Annexin V-FITC positive). At this stage, the plasma membrane excludes the PI, therefore, the PI staining is negative (196).

In this study, 10,000 cells were prepared for flow cytometry analysis. Cells were washed with cold PBS and resuspended in 1× binding buffer. The concentration of cells was at 1×10^6 cells/ml. Cells were stained with FITC-conjugated annexin V and propidium iodide for 15 min at room temperature according to the protocol provided by BD pharmingen™ Annexin V-FITC apoptosis detection kit. The stained cells were monitored by BD FACSCanto™ flow cytometer using BD FACSDiva software. Annexin V-FITC and PI were detected at 488/520 nm and 488/585 nm of excitation and emission, respectively.

3.2.8 Cytokine assay

Enzyme-linked immunosorbent assay (ELISA) was used to measure cytokine production of cells with and without NPs treatments. Commercial ELISA kits (eBioscience, San Diego, CA) were used for TNF-α and IL-6 detections by following the specific manufacturer's instructions for each cytokine detection. Briefly, at the end of incubation time, the cultured cells in 96 well plates were centrifuged to collect the supernatant and stored at -75 ºC until assayed. A monoclonal antibody that specifically detects cytokine was pre-coated onto a 96 well plate and incubated overnight at 4 ºC. Standard cytokines and samples were pipetted into the wells. The specific cytokine molecules bound to the immobilized antibody. After washing to remove unbound substances, an enzyme-linked polyclonal antibody specific to each cytokine was added into each well. Following this wells were washed and a substrate solution was added to each well. The color development was measured after adding stop solution using a microplate reader (Molecular devices, SpectraMax® M series, CA, USA) at a wavelength of 450 nm. The concentration of cytokines was calculated from the linear portion of the generated standard curve.

3.2.9 Statistical analysis

Data of representative experiments were expressed as mean ± standard error of mean (SE). The statistical significance of individual treatment was analyzed by one-way analysis of variance (ANOVA) followed by Dunnett's multiple comparison test to compare differences between all groups of data (GraphPad Prism®, Version 5.0).

CHAPTER IV
NANOMATERIALS CHARACTERIZATION

4.1 Introduction

NPs have unique properties that are different from bulk (or micron size) particles (2). For understanding the potential of NPs in their exclusive application, a deeper knowledge of their structure and characteristics is needed. Characterization is done by using a variety of different techniques. For characterizing NPs, the parameters considered include: surface area and porosity, solubility, particle size distribution, aggregation, hydrated surface analysis, zeta (ζ) potential, wettability, adsorption potential, shape, and size (197, 198). Consequently, there are several techniques used to understand these characterization parameters in NPs. These include electron microscopy (Transmission Electron Microscopy (TEM) and Scanning electron microscopy (SEM)), atomic force microscopy (AFM), dynamic light scattering (DLS), x-ray photoelectron spectroscopy (XPS), powder X-ray diffraction (XRD), Fourier transform infrared spectroscopy (FTIR), matrix-assisted laser desorption/ionization time-of-flight mass spectrometry (MALDI-TOF), ultraviolet-visible spectroscopy, dual polarization interferometry, nuclear magnetic resonance (NMR), and NPs tracking analysis for tracking of the Brownian motion (103, 198, 199).

DLS is a technique that is used for measuring the hydrodynamic size, size distribution, and polydispersity of NPs in colloidal suspensions of the nano- and submicro-size of particle ranges (200). This technique can determine the distribution of particles, hydrodynamic size, and agglomeration state of the nanoparticles (201). A colloidal solution is exposed by a laser beam. Later, DLS can analyze scattered light intensity modulation that can provide characteristics of particles. Determination of the agglomeration of nanoparticles is indicated by the level of polydispersity index (PDI). The PDI value is high if the particles are agglomerated (103, 113, 202). The zeta potential presents the magnitude of the electrostatic or charge repulsion or attraction between particles. The range of zeta potential is typical in between +100 mV to -100

mV. The zeta potential value has been used for prediction of NPs stability in suspension. In general, NPs with the zeta potential that is higher than +30 mV or less than -30 mV are normally considered to be stable. The aggregation of particles suspension with a low zeta potential normally causes by the action of the Van der Waals force. The zeta potential measurement can help provide the information of nanoparticle dispersion long-term stability (203-205). SEM is an analytical instrument that has been most widely used for characterizations of morphology, surface structure, and size of nanomaterials. This technique based on electron microscopy that offers several advantages in investigation of particles in nanoscale level (103, 206).

In this chapter, the determination of NPs sizes was done by using DLS measurement of hydrodynamic size, zeta potential, and PDI of NPs dispersed in different vehicle media. The characterization of shape and surface structure of NPs was done by electron microscope techniques (TEM and SEM). The crystalline phase characterization in 2θ geometry of TiO_2-NPs and MWCNTs was characterized by X-ray diffraction (XRD) technique.

4.2 Materials and methods

4.2.1 Size and shape characterizations

The hydrodynamic sizes of TiO_2-NPs and MWCNTs dispersed in de-ionized water (DW), PBS, and fetal bovine serum (FBS)-free cell culture media were measured by a Malvern Zetasizer 3000 (more information on this technique is presented in Chapter 3 section 3.2.2.1). For TiO_2-NPs, the stock solution of TiO_2-NPs at a concentration of 37,500 µg/ml was diluted to 5,000 µg/ml with DW and DMEM (without serum). The 5,000 µg/ml TiO_2-NPs suspension was sonicated for 10 min to assure the dispersion state. Following this, TiO_2-NPs (3 ml) were transferred into a cuvette for size measurements. For MWCNTs, the suspension's concentration for size characterization was 0.1 mg/ml, which was dispersed in 1% FBS plus 0.1% D-glucose in culture medium. Before measurement, the 1 mg/ml concentration of stock suspension of MWCNTs was sonicated for 10 min and diluted 10 times with the appropriate media to become 0.1 mg/ml. The 3 ml of MWCNTs final dilution (100

µg/ml suspended in 1% FBS plus 0.1% D-glucose in culture medium or PBS) was vigorously mixed with a vortex and transferred into a cuvette for hydrodynamic size measurements. The average hydrodynamic sizes of the suspended particles were calculated by the instrument software. The sizes and shapes of TiO_2-NPs and MWCNTs were measured by following the approach explained in Chapter 3, section 3.2.2.1

4.2.2 Zeta (ζ) potential and crystalline phase characterization

The zeta potential of TiO_2-NPs and MWCNTs was also measured by a Malvern Zetasizer 3000. The TiO_2-NPs suspension was similarly prepared as described in the size characterization section. The suspension of TiO_2-NPs (at concentration of 5,000 µg/ml) was suspended in DW and DMEM (without serum) and was directly injected into the capillary cell of a Malvern Zetasizer 3000. The measurements were carried out three times (at intervals of 30s) for each injection. For MWCNTs, zeta potential was determined in 3 different types of suspension media: 1) 100% FBS, 2) 1% FBS, 0.1% D-glucose in PBS, and 3) 1% FBS 0.1% D-glucose in DMEM. The stock suspension was prepared as described in section 4.2.1. The 3 ml of MWCNTs (100 µg/ml suspended in 1% FBS plus 0.1% D-glucose in culture medium or PBS) was vigorously mixed with a vortex and transferred into a cuvette for zeta potential measurements. The measurements were carried out as explained in Chapter 3, section 3.2.2.2. The crystalline phase characterization was measured by following the approach explained in Chapter 3, section 3.2.2.3.

4.2.3 Chemical characterization by EDX analysis

Chemical characterization of TiO_2-NPs was measured by using EDX of scanning electron microscopy (SEM, LEO model LEO 1450 VP), as described in Chapter 3, section 3.2.2.1

4.3 Results

4.3.1 Shape and size characterization by TEM and SEM

In this study, two different types of nanomaterials: 1) TiO_2-NPs (metal based NPs), and 2) MWCNTs (carbon based nanomaterials) were investigated.

4.3.1.1 TEM analysis

The morphology and size of both nanomaterials were examined using TECHNAI 20 TEM. The preparation of TEM samples was carried out as mentioned in section 4.2.1. TEM micrographs of the TiO_2-NPs, and $MWCNT_S$ are shown in figure 4.1.

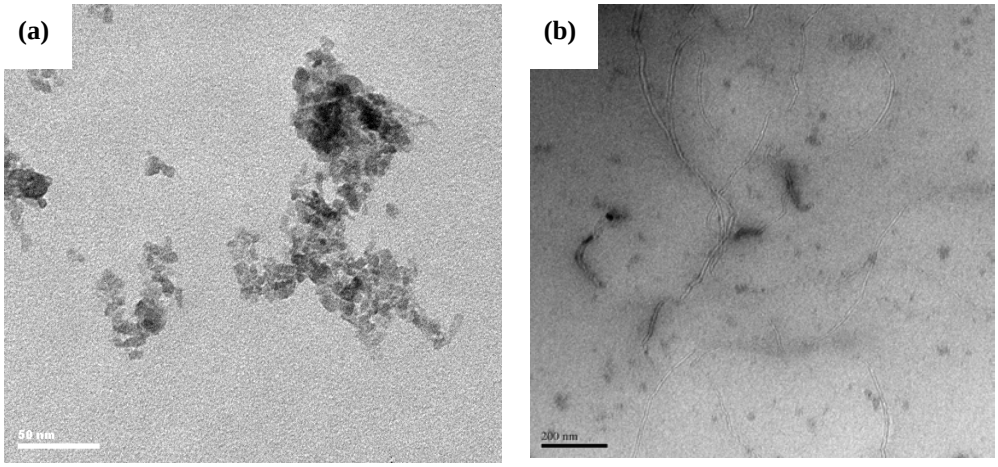

Figure 4.1 TEM images of TiO_2-NPs (a), and MWCNTs (b).

TEM micrographs (figure 4.1a) show that TiO_2-NPs used in this study are at the nanoscale level. Their size is around 13.9 ± 1.8 nm. The TEM image of MWCNTs (figure 4.1b) shows that they are several microns long with a tube-like structure that has an average outside diameter of 10-15 nm and length around 1-10 μm (data from the supplier).

4.3.1.2 SEM analysis

Microstructures of NPs were characterized by a scanning electron microscope (SEM) as illustrated in figure 4.2. TiO_2-NPs showed a spherical shape (Figure 4.2a). The particles were clumped together. This might have resulted from poor optimization of the sample preparation technique. For example, the concentration used for preparation was too high. Figures 4.2b and c show the tube-like structures of MWCNTs.

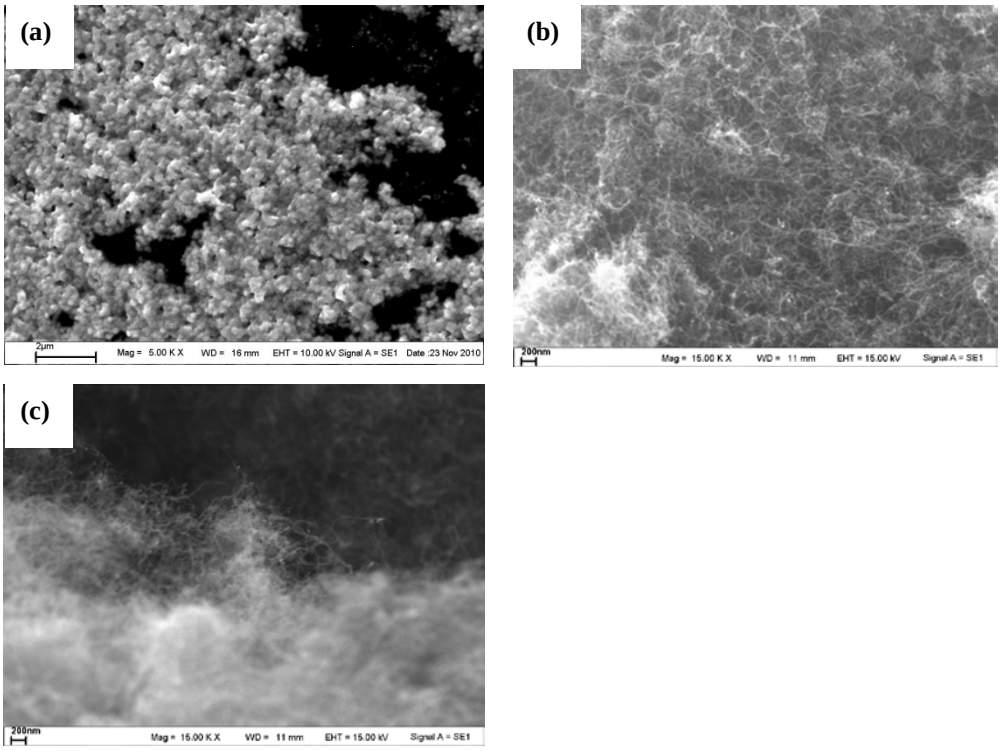

Figure 4.2 SEM images of TiO_2-NPs (a) and MWCNTs (b and c).

4.3.2 Zeta potential of TiO_2-NPs and MWCNTs

The zeta potentials of both NPs were measured by DLS. The zeta (ζ)-potential of TiO_2-NPs in DW was approximately 46 mV. However, the zeta potential of TiO_2-NPs dispersed in culture medium was approximately -3 mV. The surface charge is one of the major physical properties of the NPs that play a major role in various applications. It is commonly measured through the zeta (ζ) potential (30). The zeta potential of TiO_2-NPs dispersed in DW had a strong zeta potential (greater than 30 mV). However, TiO_2-NPs dispersed in culture medium had a weak zeta potential

(between -10 and +10 mV). These ranges can be considered to be neutral. The decrease of the zeta-potential of TiO_2-NPs suspended in the culture medium was due to the fact that the environment of the culture medium is different from DW. The absorption of protein in the medium on the surface of TiO_2-NPs can occur and the electrolyte condition of the medium can affect the surface charge of the particles (207). The PDI is one of the parameters that can be used to determine the distribution of particles in aqueous solution. The PDI of TiO_2-NPs dispersed in DMEM was similar to the PDI value of TiO_2-NPs dispersed in DW; those were 0.38 and 0.37 respectively. The PDI value measured from DLS can use to indicate the size distribution and the stability of TiO_2-NPs (208).

MWCNTs dispersed in 1% FBS plus 0.1% D-glucose showed agglomeration of the carbon fiber. The PDI of MWCNTs was quite high (0.72, on a scale of 0-1). This high PDI value reflects the inhomogeneous size distribution of MWCNTs. The zeta potential of MWCNTs in 1% FBS plus 0.1% D-glucose was -11.40 ± 0.95 mV and the stability of MWCNTs dispersed in medium was low.

4.3.3 Structure characterization of TiO_2-NPs and MWCNTs

4.3.3.1 Phases characterization of TiO_2-NPs and MWCNTs by XRD

The bulk crystalline phases of TiO_2-NPs were determined using powder x-ray diffraction (XRD) measurements. XRD can determine the crystalline phases of particles. The XRD pattern of TiO_2-NPs (Figure 4.3) exhibited strong diffraction peaks at 2θ of 25.30º, 37.82º, 48.00º, and 63.32º. These peaks were described as the crystallographic structure anatase phase (TiO_2, JCPDS card #84-1286). However, diffraction peaks at 25.43º, 27.26º, 30.76º, 36.14º and 54.23º were also detected. The presence of these diffraction peaks indicates that the TiO_2-NPs were present in the form of mixed phases. The diffraction peaks can also be assigned to a mixture of rutile (TiO_2, JCPDS card #82-0514) and brookite phases (TiO_2, JCPDS card #76-1936) (184-187). Thus the crystalline phases of the TiO_2-NPs used in this study are the mixed forms of anatase, rutile, and brookite.

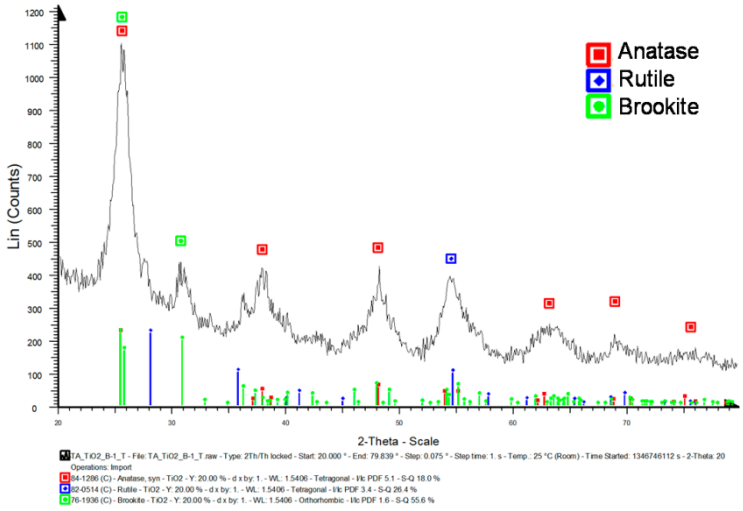

Figure 4.3 The XRD pattern of TiO_2-NPs shows the mixture of anatase, rutile and brookite phases.

In order to determine the XRD pattern of MWCNTs, the 2θ peak positions at 25.9º and 43.2º were used as the characteristic pattern of graphitized carbon, whose results are reported elsewhere (209-211). The XRD pattern of CNTs is shown in figure 4.4

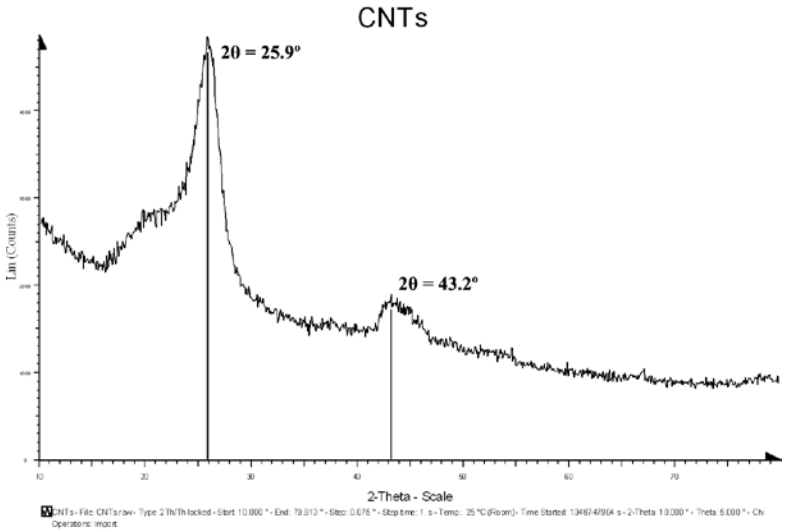

Figure 4.4 The XRD pattern of MWCNTs. The characteristic peaks for CNTs at the positions of 2θ = 25.9º and 43.2º were used to analyze the MWCNT sample.

4.3.4 EDX characterization of TiO_2-NPs

An investigation of the elements of TiO_2-NPs was performed. The corresponding energy dispersive X-ray (EDX) spectral analysis of TiO_2-NPs is shown in figure 4.5. From the spectra, it is shown that the TiO_2-NPs composites contain the peaks of Ti and O, though there are also some impure elements which might have formed during the preparation procedure. The EDX elemental microanalysis (wt%) showed that TiO_2-NPs contained 41.76% titanium, 55.6% oxygen and 2.58% chloride.

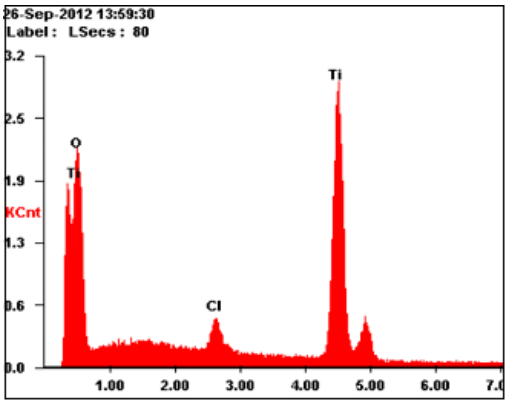

Figure 4.5 Energy dispersive X-ray (EDX) profile of TiO_2-NPs suspended in DW

4.4 Discussion

In this chapter, two types of nanomaterials have been characterized by using different techniques, which were TEM, SEM, DLS, and XRD to characterize size, shape, zeta potential, PDI, and crystalline phase of NPs. Both size and shape of TiO_2-NPs and MWCNTs are different; the size of TiO_2-NPs is in nanoscale level with a spherical shape. The structure of MWCNTs is a tube-like structure. The crystalline phases structure of TiO_2-NPs was confirmed to be the mixed forms of anatase, rutile, and brookite. Because of the high reflective index of rutile and anatase phases presenting in TiO_2-NPs, they have been currently used as a pigment to enhance the brightness of various industrial products and used as a UV light protection in sunscreen (as described in section 2.2.1). Consequently, the XRD pattern of MWCNTs was revealed as the characteristic pattern of graphitized carbon. The characterization of nanomaterials used in this thesis could provide useful information and more

understanding of toxic responses mediated by both nanomaterials. As mentioned previously, the zeta potential is an electrical potential that can be used to indicate the particle surface charge. It can also be used to specify the stability of nanoparticles in aqueous medium. The degree of interaction between particle and cell membrane can rely on the zeta potential of nanoparticles. In this thesis, the zeta potential of TiO_2-NPs suspended in DMEM (without serum added), which normally contains electrolytes was approximately -3.0 mV, on the other hand, the zeta potential of MWCNTs suspended in PBS supplemented with 1% FBS plus 0.1% D-glucose was approximately -11.4 mV. The different degrees of the zeta potential imply that both types of NPs may produce different toxic effects.

CHAPTER V
CYTOTOXICITY AND INFLAMMATORY EFFECTS OF TIO2-NPs ON RAW 264.7 CELLS

5.1 Introduction

Macrophages play an important role in the host defense mechanism especially in the inflammatory process that responds to exogenous substances including inhaled particles (164, 212). The important functions of the macrophage are phagocytosis, cytokine secretion, and the production of reactive oxygen species (213-215). During inflammation, macrophages play a central role in managing many different immune pathological phenomena, including the overproduction of pro-inflammatory cytokines and inflammatory mediators such as IL-1β, IL-6, NO, iNOS, COX-2, and TNF-α (212, 216-218). Depending on the duration of inflammatory response, inflammation can be divided into two stages as acute inflammation and chronic inflammation.

There are several types of macrophages; some migrate throughout the body, while others are permanently located in certain tissues. In the case of the lungs, alveolar macrophages are mainly responsible for phagocytosis and eliminating inhaled pathogens/foreign materials (215). This macrophage gets involved in the early inflammation process by engulfing foreign materials and cell debris. Inflammatory macrophages are transformed from monocytes that are recruited to the site of inflammation in response to inflammatory chemical mediators (164, 215). Inhalation of nanoparticles can effect on macrophages and epithelial cells (219, 220). Ultrafine particles or nanoparticles have a small size; therefore, they can reach the deep part of the respiratory tract and alveoli (70, 87) and then can be circulated in the body. After inhalation of ultrafine particles into the lungs, alveolar macrophages are responsible for the clearance and phagocytosis of those inhaled particles (219, 221-223). However, excessive uptake of particles may cause harmful effects produced by macrophages, especially since alveolar macrophages are the primary sources of inflammatory

cytokine production in the lungs (217). Extensive research in recent years has shown that the NPs can induce the production of inflammatory response by macrophage cells. The primary inflammatory cytokines secreted from macrophages are IL-1β, IL-6, and TNF-α (152, 166, 212, 224-227).

According to the study of NPs inflammation induction in alveolar macrophages, the underlying mechanisms of pro-inflammatory cytokines released need to be examined. One of the main mechanisms that is involved in the production of inflammation is the arachidonic acid (AA) pathway. With this pathway, cyclooxygenease-2 (COX-2) is a key enzyme that regulates the production of active lipid called prostaglandins (173). These prostaglandins involve in pain and inflammation mediation of the immune systems (168, 228). NPs could associate in the arachidonic acid pathway and could induce inflammation in macrophage cells, as recently reported by Lee *et al*. (229). Their results showed the involvement of the cyclooxygenases (COX) enzyme on cell inflammation and cell growth of RAW 264.7 cells after treatment with MWCNTs. The expression of COX-2 is induced by a variety of stimuli related to inflammatory response (172, 174, 230) including pro-inflammatory cytokines production such as tumor necrosis factor-α (TNF-α), interleukin-1β (IL-1β), and β-catenin (168, 172, 173, 175, 231-234). Although there are many studies on how NPs induce inflammation, the involvement of COX-2 in a critical signaling event for TiO_2-NPs in the inflammation of RAW 264.7 cells is still understudied Therefore, the objectives of this chapter are described follows:

1. To determine the toxicity effects of TiO_2-NPs on RAW 264.7 cells.

2. To determine the effects of TiO_2-NPs on ROS production in RAW 264.7 cells

3. To evaluate the production of pro-inflammatory cytokine produced by RAW 264.7 cells after treatment with TiO_2-NPs

4. To investigate whether TiO_2-NPs can induce COX-2 expression in RAW 264.7 cells

5.2 Materials and methods

5.2.1 The preparation of TiO_2-NPs

The preparation of TiO_2-NPs was explained in Chapter 3, section 3.2.1. The TiO_2-NPs in culture medium were freshly prepared by diluting 5,000 µg/ml of a suspension stock of TiO_2-NPs. The TiO_2-NP suspension was mixed well before being applied to cells.

5.2.2 Cell culture procedure

RAW 264.7 murine macrophage cells were maintained in Dulbecco's modified Eagle's medium (DMEM) supplemented with 10% FBS plus 1% antibiotic-antimycotic. The details of cell preparation were presented in Chapter 3, section 3.2.3.

5.2.3 Cell viability assay

The viability of RAW 264.7 macrophage cells was measured by the CellTiter-glo® Luminescent assay. More information on this technique has been provided in Chapter 3, section 3.2.4.2. RAW 264.7 cells at a concentration of 1×10^5 cells/well (100 µl) in RPMI 1640 (Nacalai Tesque, Kyoto, Japan) were seeded into a 96-well plate and incubated at 37 °C with 5% CO_2. After incubating for 24 h, the old medium was removed and replaced with 50 µl of fresh medium (without serum). An equal volume (50 µl) of serum-free medium with different concentrations of TiO_2-NPs (5, 25, 250, and 500 µg/ml) was added into each well. After RAW 264.7 cells were treated with TiO_2-NPs for 24 h, 100 µl of CellTiter-glo® reagent was added to the treated cells and mixed with an orbital shaker for 2 min. Following this, the 96-well plate was incubated at room temperature for 10 min. The luminescence was recorded with an ELISA plate reader at the emission of 542 nm. The blank wells (medium with each concentration of TiO_2-NPs without cells) were also measured to check the luminescence from TiO_2-NPs alone. These values were subtracted from sample values of this experiment. The values of the cell viability of treated cells were expressed as percentages relative to untreated cells.

5.2.4 Intracellular ROS measurement

Intracellular ROS was quantified by measuring the amount of dichlorofluorescein diacetate molecules oxidized (H_2DCFDA) to fluorescent dichlorofluorescein (DCF). More details of ROS measurement are provided in Chapter 3, section 3.2.5. RAW 264.7 cells were plated onto 96-well plates at a density of 9.5×10^3 cells/well and incubated overnight in 95% humidified air incubator and 5% CO_2. After incubation, cells were further incubated with 10 µM H_2DCFDA for 30 minutes as explained in Chapter 3, section 3.2.5. Then cells were rinsed twice and treated with TiO_2-NPs at concentrations of 25, 250, and 500 µg/ml. Immediately after treatment, the fluorescence of DCF molecules from the oxidation of dyes was read using a microplate reader with the set condition shown in section 3.2.5. The DCF fluorescence intensities were measured at 5, 15, and 30 minutes after treating cells with TiO_2-NPs at various concentrations. The percentage increase of fluorescence intensity was calculated by the below formula as explained by Subramaniam and Ellis (190).

$$\%\ increase\ in\ fluorescence\ intensity = \left[\frac{(Ft_{30} - Ft_0)}{Ft_0} \times 100\right]$$

Where;

Ft_{30} = fluorescence intensity at desirable time (5, 15, and 30 min)

Ft_0 = fluorescence intensity at initiate time (0 min)

5.2.5 Western blotting

RAW 264.7 cells were seeded on 100 mm culture dishes at a density of 6×10^6 cells/dish and allowed to adhere overnight in a 95% humidified air incubator at 37 ºC plus 5% CO_2. After incubation, medium was removed and TiO_2-NPs at the concentrations of 25, 250, and 500 µg/ml were added into the cells. After treatment, the cells were washed three times with cold PBS. Then the exposed cells were harvested by adding ice-cold lysis buffer (50 mM Tris-HCl pH 7.4, 150 mM NaCl, 1% Triton X-100, 1 mM EDTA, 1 mM Na_3VO_4, 1 mM PMSF, and 1 mM NaF) containing EDTA-free protease inhibitor cocktail. Equal amounts of protein were loaded and separated on a 10% SDS-PAGE (total volume 20 µl/well). Next, the proteins were

transferred to nitrocellulose membrane and followed the approach presented in Chapter 3, section 3.2.6.2.

5.2.6 Determination of apoptosis cell death

5.2.6.1 DNA fragmentation analysis

RAW 264.7 cells were seeded into cell culture dishes at a density of 4×10^5-6×10^5 cells/dish (each set of experiment had the same cell number). Cells were treated with TiO_2-NPs at concentrations of 25, 250 and 500 µg/ml. Treated cells were scraped off, the DNA of cells was extracted and gel electrophoresis was performed to determine cell apoptosis, following the method written in Chapter 3, section 3.2.7.1.

5.2.6.2 Flow cytometry analysis of cell death

Double staining of RAW 264.7 cells with the combination of AnnexinV-FITC and PI was used to detect membrane integrity. More information on this technique has been presented in Chapter 3, section 3.3.7.2. RAW 264.7 cells at a density of 4×10^5-6×10^5 cells/dish (each set of experiment had the same cell number) were treated with TiO_2-NPs at 25, 250, and 500 µg/ml for 24 h. Next, cells were washed twice with cold PBS and then were suspended in binding buffer to have a final concentration of 1×10^6 cells/ml. Thereafter, 100 µl of the cell suspension was transferred to a 5 ml culture tube. Following this, 5 µl of FITC-Annexin V and 5 µl of PI were added into the tube. The mixture of cells and dyes was gently shaken and dark-incubated for 15 minutes at room temperature. Then, 400 µl of binding buffer was added to each tube and analyzed by flow cytometry within 1 h. 10,000 total events of the cells were analyzed by a BD FACSCanto^{TM} flow cytometer using BD FACSDiva software. Annexin V-FITC and PI were detected as mentioned in Chapter 3, section 3.2.7.2.

5.2.7 Cytokine assay

Pro-inflammatory cytokine productions (TNF-α and IL-6) of RAW 264.7 cells were measured using a commercial ELISA kit. More details have been presented in Chapter 3, section 3.2.8. RAW 264.7 cells were plated onto 96-well plates at a density of 1×10^5 cells/well and incubated overnight in 95% humidified air incubator and 5% CO_2. After incubation, cells were rinsed once with serum free medium (for removing the residue serum) and treated with TiO_2-NPs at concentrations of 25, 250, and 500 µg/ml. After 24 h, the supernatant was collected and centrifuged at 4,000 rpm for 5 min. The supernatant were stored at -80 °C until usage.

5.3 Results

5.3.1 Effects of TiO_2-NPs on cell viability of RAW 264.7 cells

After RAW 264.7 cells were treated with different concentrations of TiO_2-NPs for 24 h, cell viability was determined by CellTiter-glo® assay. The concentrations of TiO_2-NPs used in this experiment were 5, 25, 250, and 500 µg/ml. The results illustrated that at 24 h post-treatment, cell viability decreased in a dose-dependent manner (figure 5.1). The viability of cells decreased when the concentration of TiO_2-NPs increased compared to that of untreated cells. The positive control was prepared by treating cells with ellipticine. As expected, the cell viability decreased significantly. Cell viability of cells treated with 5 µg/ml TiO_2-NPs was similar to that of the control group. It showed a slightly higher percentage of cell viability than untreated cells but no significant difference.

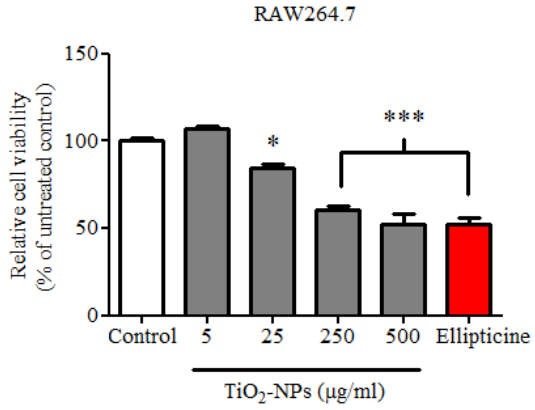

Figure 5.1 Cell viability of RAW 264.7 cells after treatment with different doses of TiO_2-NPs. The ellipticine at a concentration of 0.125 µg/ml was used as a positive control. *, *** Significant difference of cell viability from untreated cells (control) TiO_2-NPs at $^{*}p< 0.05$ and $^{***}p< 0.001$

5.3.2 DNA fragmentation assay of RAW 264.7 cells treated with TiO_2-NPs

The effect of TiO_2-NPs on the DNA of RAW 264.7 cells was investigated. Typical DNA fragmentation, which indicates cell apoptosis, was not observed in untreated cells (lane 1 of figure 5.2). However, after cells were treated with various concentrations of TiO_2-NPs for 24 h, DNA fragmentation was detected in cells treated with TiO_2-NPs at concentrations of 25, 250, and 500 µg/ml (shown in lanes no. 2-4 of figure 5.2, respectively). Compared with the results from the viability assay (section 5.3.1), a high percentage of dead cells was found in cells treated with 250 and 500 µg/ml TiO_2-NPs. Strong DNA fragmentation was also found at the same concentrations. Therefore, it can be concluded that TiO_2-NPs at 250 and 500 µg/ml have cytotoxic effects on RAW 264.7 cells via an apoptosis cell death mechanism.

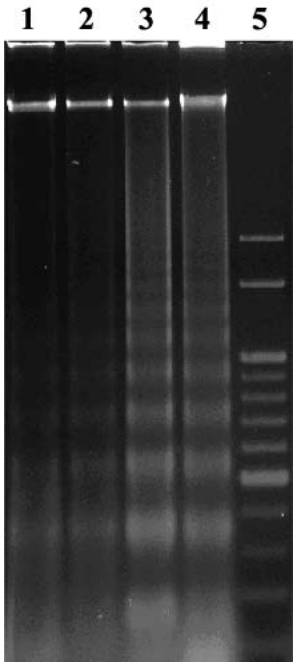

Figure 5.2 DNA laddering pattern on the agarose gel of RAW 264.7 cells treated with TiO_2-NPs for 24 h. RAW 264.7 cells were treated with different doses of TiO_2-NPs without FBS for 24 h (1) untreated cells. (2-4) Cells treated with TiO_2-NPs at concentrations of 25, 250, and 500 µg/ml respectively. (5) DNA ladder marker. Results are representative of a triple slit experiment.

5.3.3 Investigation of apoptosis/necrosis cell death of RAW 264.7 cells treated with TiO_2-NPs

To confirm and quantify the induction of cell apoptosis by TiO_2-NPs, the investigation of cell apoptosis/necrosis was performed by the double staining of Annexin V-FITC conjugated with PI. After flow cytometry analysis, untreated cells showed the percentages of cells in the period of early apoptosis and late apoptosis/necrosis of 1.18% and 8.40% respectively. RAW 264.7 cells treated with 25 µg/ml TiO_2-NPs for 24 h, showed the percentage of cells in periods of early apoptosis and late apoptosis/necrosis of 2.27% and 13.8% respectively. The increase of cells in the late apoptosis/necrosis period was also found in cells treated with 250 (19.63%) and 500 µg/ml (22.27%) TiO_2-NPs. At these two concentrations, the percentages of cells in early apoptosis were 2.13 and 2.67%. The significant difference of cells in late apoptosis/necrosis was found in cells treated with 500 µg/ml TiO_2-NPs.

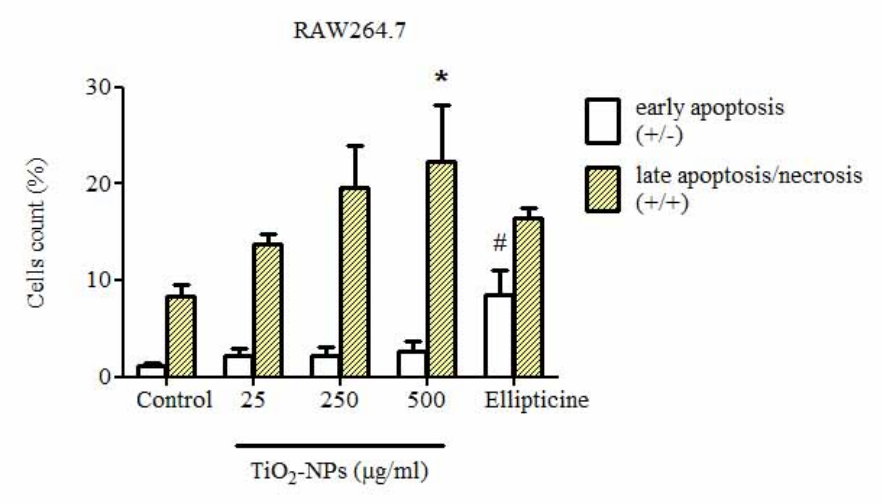

Figure 5.3 The effect of TiO_2-NPs on cell death stages of RAW 264.7 cells. Significant difference of cell death stages (* early apoptosis; $^{\#}$ late apoptosis/necrosis) from untreated cells at $p< 0.05$.

5.3.4 Effect of TiO_2-NPs on intracellular ROS induction in RAW 264.7 cells

The generation of ROS by TiO_2-NPs was measured from the fluorescence intensity of DCF molecules after treating cells with TiO_2-NPs for 5, 15, and 30 min. The results showed that a significant change of DCF-fluorescence intensity was not found in RAW 264.7 cells treated with 25-500 µg/ml TiO_2-NPs for 5 min. However, RAW 264.7 cells treated with 500 µg/ml TiO_2-NPs for 15 ($p< 0.01$) and 30 ($p< 0.001$) min showed a significant increase in DCF-fluorescence intensity compared with untreated cells. At $p< 0.01$, the induction of DCF-fluorescence intensity in cells treated with 250 µg/ml TiO_2-NPs for 30 min was significantly different from untreated cells (figure 5.4). These results imply that the exposure time and the high concentration of TiO_2-NPs had an effect on the induction of ROS.

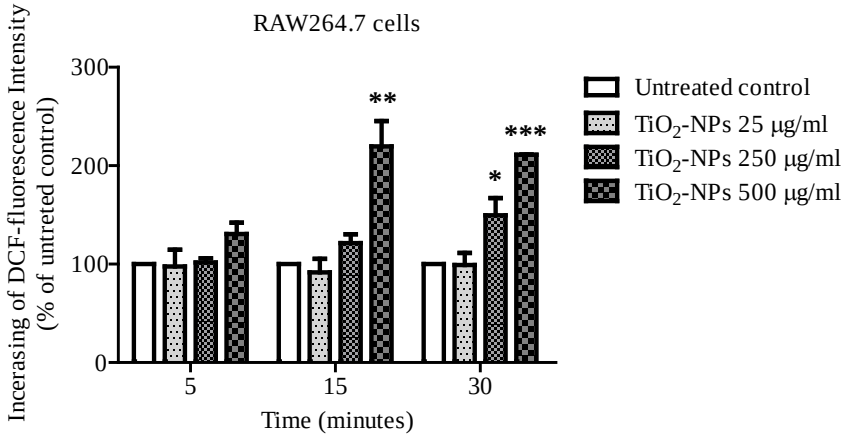

Figure 5.4 The induction of ROS (detected from DCF-intensities) in RAW 264.7 cells treated with various concentrations of TiO_2-NPs from 25-500 μg/ml for 5, 15, and 30 min. *, **, *** Significant difference of ROS production compared with control at $^{*}p< 0.05$, $^{**}p< 0.01$, $^{***}p< 0.001$.

It is well-known that ROS play an important role in apoptosis cell death (235, 236). From the previous section (DNA laddering assay and flow cytometric analysis), the results in this thesis showed that TiO_2-NPs at 25 μg/ml caused significant cell toxicity because of the significant decrease of cell viability. Late apoptosis was also increased when increasing the concentration of TiO_2-NPs. The significant induction of ROS and DNA fragmentation was clearly found in cells treated with 250 μg/ml TiO_2-NPs for 30 min ($p< 0.05$). At a higher concentration (500 μg/ml) with a lower exposure time (15 min), cells can be enhanced to produce high ROS levels.

5.3.5 The effect of TiO_2-NPs on pro-inflammatory cytokine production

To study the effect of TiO_2-NPs on cytokine production of RAW 264.7 cells, the cytokines released in cell culture assay were measured. The release of TNF-α and IL-6 cytokines was investigated in this study. Tumor necrosis factor-α (TNF-α) has a key role in inflammatory response. This cytokine plays a crucial role in the innate and adaptive immunity, cell proliferation, and apoptotic processes. Increased concentrations of TNF-α were found in acute and chronic inflammatory conditions. The cytokine is produced by different kinds of cells, including macrophages,

monocytes, T-cells, smooth muscle cells, adipocytes, and fibroblasts (237, 238). Several studies have reported the involvement of TNF-α in NPs-mediated toxicity (239, 240). However, the molecular mechanism of NPs-mediated inflammation through TNF-α is still unclear. IL-6 is one of the major mediators of the immune system involved in an acute-phase response from infection or injury (241, 242). Moreover, IL-6 exhibits an important role in an inflammatory response. The evidence of IL-6 involved in the pathogenesis of chronic diseases was reported (243, 244).

The results of the study in this chapter showed that the production of TNF-α released from cells treated with 25 μg/ml TiO_2-NPs for 24 h increased significantly. At this concentration, the cell viability also decreased significantly. It has been reported that the high concentration of TNF-α can cause cell death (245). Therefore, the increase of TNF-α by treating cells with TiO_2-NPs at a concentration of 25 μg/ml might also be involved in cell death. Other reports of cellular toxicity from proinflammatory cytokine production were also described by Schmalz *et al.* (246, 247).

At higher concentrations of TiO_2-NPs, the reduction of TNF-α was found. This might be due to the increase in the number of dead cells after treating cells with 250 and 500 μg/ml TiO_2-NPs, resulting in low secretion of TNF-α. The degree of agglomeration of high concentrations of TiO_2-NPs might also be involved (161). As expected, the positive control, cells treated with LPS (5 μg/ml), showed a high concentration of TNF-α (figure 5.5). The production of IL-6 in untreated RAW 264.7 cells was much lower than TNF-α. After treating cells with TiO_2-NPs at concentrations of 25 to 500 μg/ml for 24 h, it was revealed that TiO_2-NPs had no significant effect on inducing IL-6 secretion of RAW 264.7 cells. In contrast, significant production of IL-6 was found in cells treated with LPS (figure 5.6).

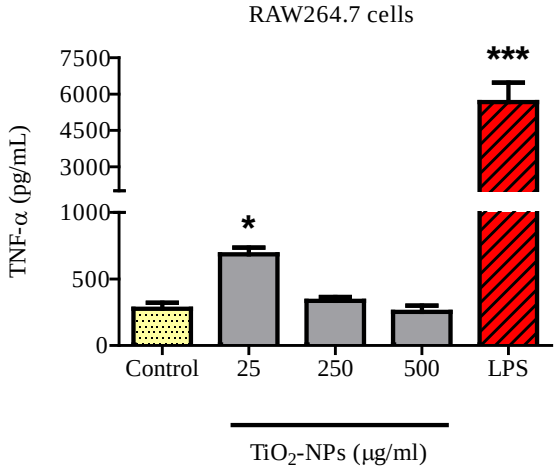

Figure 5.5 Effect of TiO_2-NPs at concentrations of 25-500 μg/ml on TNF-α production of RAW 264.7 cells after treatment with TiO_2-NPs for 24 h. *, *** Significantly different from control (untreated cells) at $^{*}p< 0.05$ and $^{***}p< 0.001$. Cells treated with LPS (5 μg/ml) were used as a positive control.

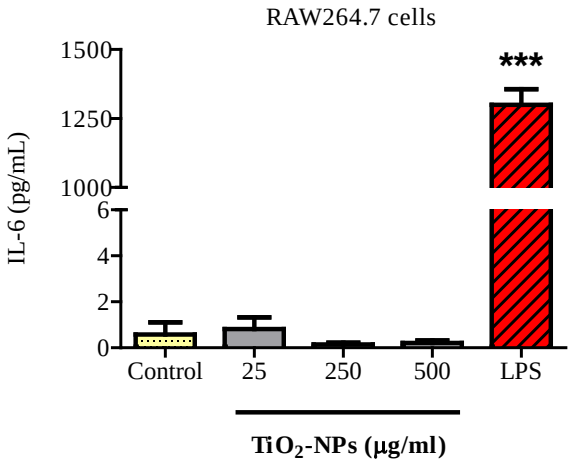

Figure 5.6 Effect of TiO_2-NPs at concentrations of 25-500 μg/ml on IL-6 production of RAW 264.7 cells after treatment with TiO_2-NPs for 24 h. *** Significantly different from control (untreated cells) at $^{***}p< 0.001$. LPS (5 μg/ml) was used to treat cells as a positive control. Only LPS shows a significant induction of IL-6.

5.3.6 Effect of TiO_2-NPs on COX-2 expression in RAW 264.7 cells

The expression of COX-2 protein, which can be up-regulated during cell inflammation, was analyzed by Western blot analysis. Compared with untreated cells, the level of COX-2 expression in RAW 264.7 cells exposed to 250 µg/ml TiO_2-NPs for 24 h increased significantly ($p< 0.01$). When the concentration of TiO_2-NPs was at 500 µg/ml, a significant increase of COX-2 was also found ($p< 0.05$). Therefor TiO_2-NPs at a concentration of 250 µg/ml were selected to investigate the effect of exposure time on the induction of COX-2 levels. The results showed that short exposure times at 1 and 6 h did not have a significant induction of COX-2 expression in RAW 264.7 cells.

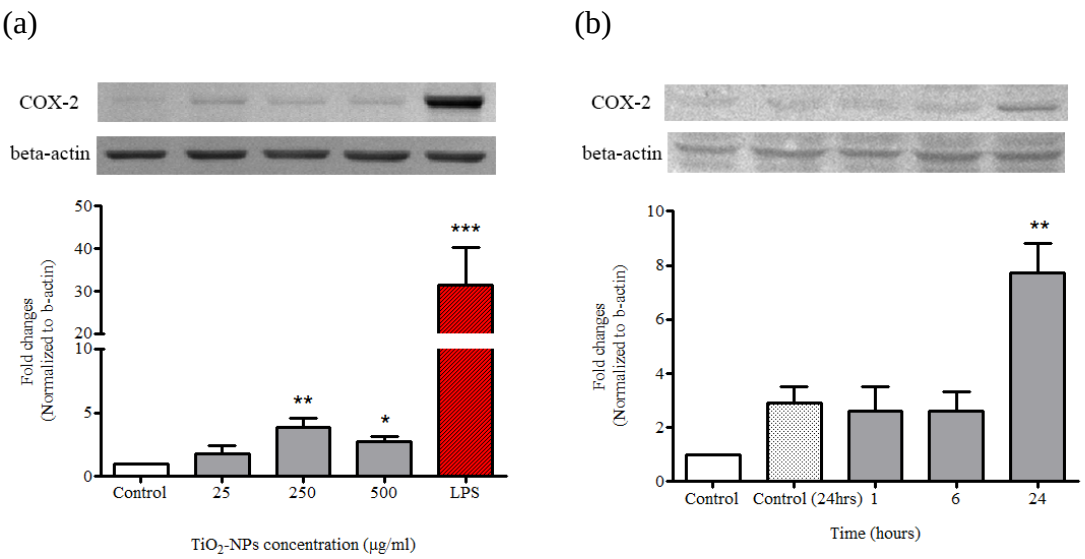

Figure 5.7 Effect of TiO_2-NPs at concentrations of 25-500 µg/ml on COX-2 expression in RAW 264.7 cells. (a) COX-2 expression in cells treated with TiO_2-NPs for 24 h. (b) Cells treated with 200 µg/ml TiO_2-NPs at various exposure times (1, 6, and 24 h). Cells treated with LPS (5 µg/ml) were used as a positive control. The data were normalized with β-actin expression. *, **, *** Significantly different from untreated cells (24 h incubation) at $^{*}p< 0.05$; $^{**}p< 0.01$ and $^{***}p< 0.001$.

5.3.7 Effect of TiO_2-NPs on the inhibition of β-catenin expression in RAW 264.7 cells

The cytoplasmic protein β-catenin is a central molecule that plays a key role in the Wnt signaling pathway (248). This Wnt pathway has been used in an *in vitro* model of inflammatory macrophage activation, as reported by George (249). The study here investigated the expression of β-catenin after treating RAW 264.7 cells with various concentrations of TiO_2-NPs. The expression of β-catenin was assessed by Western blot analysis. RAW 264.7 cells were incubated with different doses of TiO_2-NPs (25, 250, and 500 µg/ml) for 24 h. The expression of β-catenin (after normalized with β-actin) decreased significantly at 250 and 500 µg/ml of TiO_2-NPs (figure 5.8a). Next, the TiO_2-NPs at a concentration of 250 µg/ml were chosen to further investigate the effect of exposure time of TiO_2-NPs on cells. After cells were incubated with 250 µg/ml TiO_2-NPs for 1, 6 and 24 h, a significant decrease of β-catenin expression was found at 24 h incubation (figure 5.8b). These results demonstrated that the 250 µg/ml TiO_2-NPs reduced β-catenin expression in RAW 264.7 cells.

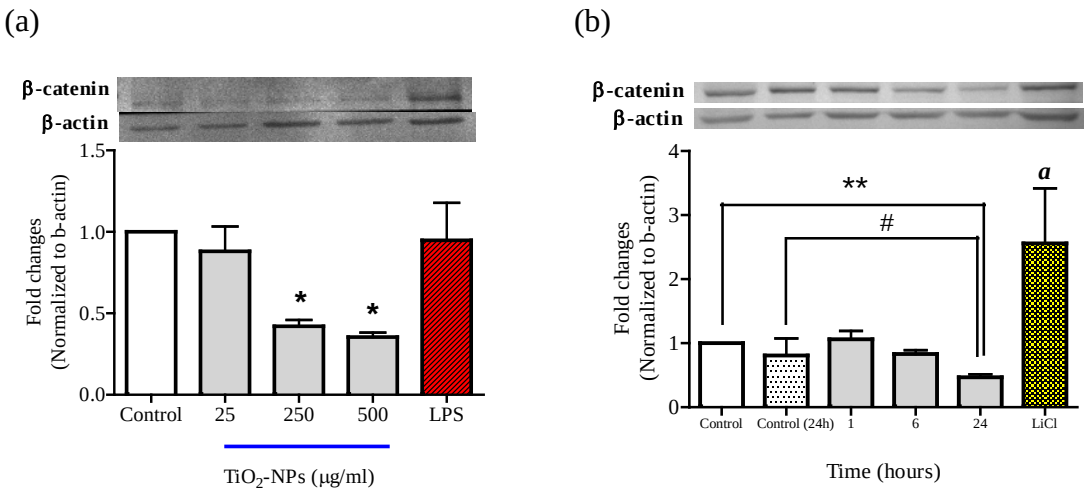

Figure 5.8 Effect of TiO_2-NPs on the induction of β-catenin expression in RAW 264.7 cells Western blot analyses show β-catenin expressions of (a) cells treated with TiO_2-NPs (25-500 µg/ml) for 24 h and LPS at 5 µg/ml was used as a positive control. (b) Time course of β-catenin expression in cells treated with 250 µg/ml TiO_2-NPs at 1, 6, and 24 h. Lithium chloride (LiCl) at a concentration of 10 mM treated for 24 h was used as a positive control. *, ** Significantly different from untreated cells (0 h) at $^{*}p< 0.05$ and $^{**}p< 0.01$ (for graph a) and at $^{\#}p< 0.05$ and $^{a}p< 0.01$ (for graph b).

5.4 Discussion

5.4.1 Effect of TiO_2-NPs on cell viability, apoptosis cell death, and ROS production of RAW 264.7cells

TiO_2-NPs at concentrations of ≥ 25 µg/ml caused cell death. Around 15.8% of dead cells were detected after treating cells with 25 µg/ml TiO_2-NPs. The percentage of dead cells increased when the concentration of TiO_2-NPs increased. The recent report of Palomaki *et al*. (250) indicated that RAW 264.7 cells were sensitive to TiO_2-NPs in a dose-dependent manner. Therefore, the contamination of TiO_2-NPs in the environment and the use of these nanoparticles must be taken into account (251)

because a high concentration of TiO_2-NPs may enter the human body and induce toxicity.

The primary function of macrophages is well-known. They are responsible for clearing particles and other foreign pathogens through the phagocytosis process (223). During the phagocytosis of NPs, macrophage cells commonly go through different pathways depending on the types of particles. This is accompanied sequentially by the up-regulated inflammatory production of ROS, RNS, chemokines, and cytokines (167, 252, 253). All of these events are linked to cell death (214). The results of this chapter showed a significant toxicity of TiO_2-NPs on macrophage cells that were involved in ROS-mediated cell death through apoptosis. The toxicity of TiO_2-NPs was also reported by Park *et al*. (22). They found that TiO_2-NPs at concentrations between 5-200 μg/ml induced apoptosis cell death in lung epithelial cells and toxicity of TiO_2-NPs increased in a dose-dependent manner. Jin *et al.* (21) also found that TiO_2-NPs can generate ROS. The uptake of TiO_2 particles by alveolar macrophage cells (NR8383 cells) leading to intracellular ROS generation was reported by Scherbart *et al*. (28). Moreover, the association between cytotoxicity and surface area of TiO_2-NPs was recently reported by Xiong *et al.* (157). Their results indicated that TiO_2-NPs with a large surface area had a higher cytotoxic effect on RAW 264.7 cells than a small surface area.

5.4.2 Effect of TiO_2-NPs on the induction of cell apoptosis

TiO_2-NPs at a concentration of 500 μg/ml could significantly induce late apoptosis/necrosis of RAW 264.7 cells (figure 5.3). Kang *et al*. (33) studied the effect of TiO_2-NPs on apoptosis cell death in human peripheral blood lymphocytes. They found that two classes of MAPKs, p38 and JNK were involved in apoptosis cell death of human lymphocytes induced by TiO_2-NPs. Their results showed that the collapse of mitochondrial membrane potential (MMP) and the early event in the mitochondrial pathway of apoptosis were induced by TiO_2-NPs. Apoptosis cell death in macrophages induced by nano-sized TiO_2 particles was also reported by Moller *et al.* (254). Their finding showed that murine macrophage (J774A.1) cells treated with ultrafine TiO_2 for 24 h resulted in the induction of both apoptosis and necrosis cell death. Similar effects were also observed in white blood cells; in particular, an increase in both early stage

apoptosis and late apoptosis/necrosis cell death depending on the concentration was observed. Vamanu *et al*. (255) studied human histiocytic lymphoma cells (U937) treated with TiO_2-NPs (particle size less than 100 nm) at concentration ranges between 0.005 to 4 mg/ml for 24 and 48 hours. Different stages of apoptosis were observed after treatment for 24 h where at most concentrations (0.005 to 1 mg/ml), the apoptosis cell death sign was observed. The necrosis cell deaths were detected only at high concentrations (2 and 4 mg/ml) after 24 h post-treatment. Producing controversial results, Goncalves *et al*. (256) investigated the toxicity of TiO_2-NPs on human neutrophiles. They found the inhibition of apoptosis cell death in neutrophils at concentrations that were higher than 20 µg/ml. In their case, TiO_2-NPs might help delay apoptosis and prolong the life span of polymorphonuclear neutrophils. Recently, Wilhelmi *et al*. (26) reported the interfering effect of TiO_2-NPs on RAW 264.7 cells. There were no apoptotic effects detected in RAW 264.7 cells treated with TiO_2-NPs at concentrations of 10, 40, and 80 µg/cm^2 for 4 and 24 h. DNA fragmentation was detected at the concentrations of 10, 40, and 80 µg/cm^2 for 24 h of incubation. With these previously published results, it seems that the roles of TiO_2-NPs in the induction of either apoptosis or necrosis cell death on immune cells need clarification (20).

ROS generation may also be a key factor leading to cytotoxicity. The oxidative stress-mediated cytotoxicity and apoptosis cell death of immune and neuron cells induced by TiO_2-NPs have been variously reported in the last few years (17, 257-260). A key finding of this thesis was that ROS generation in RAW 264.7 cells increased significantly (when compared with the untreated cells) after treatment with 500 µg/ml of TiO_2-NPs for 15 min. The mechanism of TiO_2-NPs leading to ROS-mediated cytotoxicity was reported by Jin *et al*. (21). After TiO_2-NPs were dispersed in medium solution, the abundance of surface hydroxyl groups were induced large quantity of superoxide and hydroxyl radicals by electron capture which can recombine into H_2O_2 in aqueous solution (6, 21, 261). Cells exposed to TiO_2-NPs can exhibit cytotoxicity and genotoxicity by phagocytosis and internalization of TiO_2-NPs into the cytoplasm (262). Jin *et al*. (21) showed that the toxic effect of NPs was produced by the generation of ROS and oxidative stress in the mitochondria of healthy cells. After cells were exposed to TiO_2-NPs, ROS was increased at the membrane of mitochondria without clearance mechanism. This could lead to mitochondrial disruption. In

addition, the role of ROS-mediated apoptosis and necrosis cell death has been investigated by several studies (235, 263). Alveolar macrophage cells were treated with substances that produce oxidants that were though to exclusively cause necrosis (252). The conclusion here is based on the results of this study showing that the concentration and exposure time of TiO_2-NPs are the major factors that affect on ROS production.

In this thesis, the investigation of apoptosis cell death induced by TiO_2-NPs in RAW 264.7 cells was conducted. Data from this thesis revealed the presence of late apoptosis/necrosis stages in cells treated with TiO_2-NPs. Furthermore, the fragmentation of DNA was observed in cells treated with high concentrations (250 and 500 µg/ml) of TiO_2-NPs for 24 h. The results showed that TiO_2-NPs (250 and 500 µg/ml) could induce oxidative stress in cells at 30 min post incubation. This induction might involve in the process of apoptosis cell death. The similar incident of TiO_2-NPs mediated cell death was reported by Shukla *et al*. (154). Overall, TiO_2-NPs could generate ROS in cells resulting in cell apoptosis via two possible mechanisms: 1) mitochondrial independent pathway or extrinsic pathway (also known as death-receptor pathway and 2) mitochondrial dependent pathway (235, 264, 265).

With the extrinsic pathway, TNF receptors involve in transmitting the death signal from the cell surface to inside the cell. The TNF-α could be used to indicate the extrinsic pathway of apoptotic cells. In mitochondrial dependent apoptosis or intrinsic pathway, mitochondria play a key role in intracellular integration and circulation of death signals (266). The promotion of caspase 9 and 8 in this pathway results in cell apoptosis induction (264, 267). The modulation of oxidative stress is a major effect of this pathway. It was reported that this apoptotic mitochondrial event is regulated by Bcl-2 (B-cell lymphoma 2) family proteins. These proteins can be pro-apoptotic (such as Bax, Bak) and anti-apoptotic (such as Bcl-2, Bcl-X_L, Bcl-w) proteins. Therefore, the balance of these 2 types of proteins is important for cell fate. (266, 268-270). Especially, the activation of Bax and Bak located at the outer mitochondrial membrane can lead to membrane permeabilization and cause the release of intracellular proteins such as cytochrome c that has an ability to enhance caspase activation. It was reported that caspase 9 was activated in macrophages and lead to cell apoptosis (271).

5.4.3 Effect of TiO_2-NPs on macrophage cell inflammation induction

IL-6 and TNF-α are two key mediators in inflammation and fibrosis that are produced by macrophages. Both inflammatory cytokines, IL-6 and TNF-α, are multi-functional cytokines that play a central role in diverse host defense mechanisms such as acute and chronic inflammatory response (272). For the investigation of the inflammatory response in macrophage cells induced by TiO_2-NPs, the levels of cytokines released in culture medium were measured by ELISA. The results in figure 5.5 showed that the secretion of TNF-α in culture medium increased significantly 25 µg/ml TiO_2-NPs. On the other hand, the secretion of IL-6 in cultured medium was similar in all treatments (figure 5.6). The effects of TiO_2-NPs on the secretion of inflammatory cytokines from RAW 264.7 macrophage cells has been reported in the last few years by Kim and Tao (167) and Palomaki *et al*. (250) Their results exhibited that TiO_2-NPs induced both types of cytokine (IL-6 and TNF-α) production. The results from Kim and Tao showed that TiO_2-NPs (50 µg/ml) significantly induced the TNF-α from RAW 264.7 cells. This concentration is close to the result found in the lowest concentration (25 µg/ml) used in this study. The results are similar to those reported by Morishige *et al*. (273), who observed the high TNF-α secretion by the human acute monocytic leukemic cell line (THP-1) when exposed to 100 µg/ml TiO_2-NPs (in the rutile phase) for 24 h. However, at the higher dose (500 µg/ml), the release of TNF-α is generally declined. The effect of NPs concentration on cytokines induction might depend on the agglomeration state of the nanoparticles at a higher concentration. The agglomeration size determined by DLS also showed that the nanoparticle suspension was found to have a large hydrodynamic diameter; therefore, they may behave like large particles (micron-sized particles), which show a low potency of inflammation (161). The low detection of cytokines released in culture media might result from the interfering effect of TiO_2-NPs. As reported by Kobach *et al*. (274), cytokines released in culture media may be absorbed on the surface of NPs, leading to the misinterpretation of *in vitro* studies (274, 275).

Park *et al*. (153) studied the mRNA expression of various oxidative stress and related genes (including IL-6) in the human bronchial epithelial cell line (BEAS-2B cells). Their results indicated that an increase of IL-6 mRNA expression was observed after treating cells with TiO_2-NPs at concentrations of 5 to 40 µg/ml for 3 h.

However, the expression level of the IL-6 gene decreased after increasing the exposure time from 3 to 24 h. Park *et al.* (153) suggested that the decrease of IL-6 expression at 24 h, might be due to the fact that the gene transcription system was disturbed by TiO_2-NPs. This distribution could have induced the generation of ROS. The low production of IL-6 in cells treated with TiO_2-NPs was recently reported by Dekali *et al.* (276) IL-6 secretion was measured after human alveolar epithelial cells (A549) and human macrophage cells (THP-1) were exposed to TiO_2-NPs at concentrations of 2.5 and 39 $\mu g/cm^3$ for 6 h. Their results indicated that TiO_2-NPs did not significantly induce IL-6 release in culture medium of either cell type. Oxidative signaling is also linked to the up-regulation of the inflammatory response genes, including COX-2. Federico *et al.* (277) reported that free radicals might correlate with inflammation processes in inflammatory response cells.

From results in this thesis (as shown in figure 5.7), it is demonstrated how the expression of the COX-2 enzyme increased significantly at 250 µg/ml TiO_2-NPs with 24 h exposure. Cyclooxygenase, also known as prostaglandin H synthase, is the rate-limiting enzyme that converts arachidonic acid into prostaglandin H2, thromboxanes, and prostacyclins. There are two isoforms of the COX enzyme, they have been characterized as COX-1 and COX-2. COX-2 protein is an inducible isoform that can rapidly and transiently induce inflammatory cytokines and various stimuli (278). In contrast to COX-1, which is expressed in most tissues, COX-2 is detected during inflammation of inflammatory response cells and some tumor cells (279, 280). The upregulation of COX-2 expression might be related to various sources (including ROS). Recently, Sang *et al*. (281) reported the effect TiO_2-NPs on COX-2 enzyme induction, which could mediate spleen injuries in mice. TiO_2-NPs were exposed to mice by intragastric administration every day for 15, 30, 45, 60, 75, and 90 days at the concentration of 10 mg/kg BW. Their results indicated that TiO_2-NPs significantly increased the level of COX-2 gene and protein expression in the mouse spleen following an increase of exposure duration. Moreover, the levels of AP-1 and CRE, the transcription factors responsible for COX-2 expression, were increased in both RT-PCR and ELISA analysis. β-catenin is a protein that is involved in the Wnt signaling pathway, which is associated with the proliferation and metabolism of many cancer cells (282, 283). The Wnt signaling pathway not only plays a critical role in cell

proliferation and the development of tumors but also plays a distinct role in inflammation, immunity and apoptosis (249, 283). Figure 5.8 shows how, the levels of β-catenin in RAW 264.7 macrophage cells after treatment with 250 and 500 µg/ml TiO_2-NPs decreased significantly. The inhibition of β-catenin can occur by the phosphorylation and ubiquitin-mediated degradation of β-catenin. This mechanism is associated with the phosporylation of GSK-3β (284, 285). The involvement of β-catenin signaling in cancer cell apoptosis was recently reported by Jiang *et al*. (286). Their results indicated that the apoptosis cell death of breast cancer cells was associated with a decreasing β-catenin level.

β-catenin signaling appears to play a positive role in cell survival (249, 283). Deletion of β-catenin or inhibition of Wnt signaling has been shown to induce apoptosis in several *in vivo* and *in vitro* models (287-290). RAW 264.7 cells treated with high concentrations of TiO_2-NPs (250 and 500 µg/ml) can increase the expression of the COX-2 enzyme and increase apoptosis/necrosis cell death. Consequently, the inhibition of β-catenin expression has also been found at high doses of TiO_2-NPs. Therefore, the results in this study can possibly conclude that the decrease of β-catenin expression in RAW 264.7 cells is involved in the increase of COX-2 expression and later, in the induction late apoptosis/necrosis cell death.

To summarize, the possible mechanism of cell inflammation mediated by TiO_2-NPs is shown in figure 5.9. The generation of intracellular ROS might be a key factor for TiO_2-NPs mediated cytotoxicity in RAW 264.7 macrophage cells. The induction of ROS could lead to overexpression of several mitogen-activated protein kinases (MAPKs). MAPKs are divided into three subgroups as ERKs, JNKs, and p38 (291). They can be activated through the phosphorylation process. The activation of MAPKs may phosphorylate several of signal protein including transcription factors (such as AP1 and Nf-κB) resulting in regulation of various cellular activities (for example; proliferation, inflammatory responses, and apoptosis) (17, 163, 167, 174, 238, 256, 281, 292-298). ROS also involve in MAPK activation. However, the mechanism underlying ROS activate MAPK is still unclear. Some proposed mechanisms could be 1) Activation of MAPK pathway by ROS through the oxidative modification of MAP3Ks, which is intracellular kinases involved in MAPK signal cascade and 2) Activation of MAPK pathway by ROS through the processes of

inhibition of degradation of MKPs (MAPK phosphatases). This mechanism occurs after activation of ROS by cytokines, growth factors, and some other stresses (299).

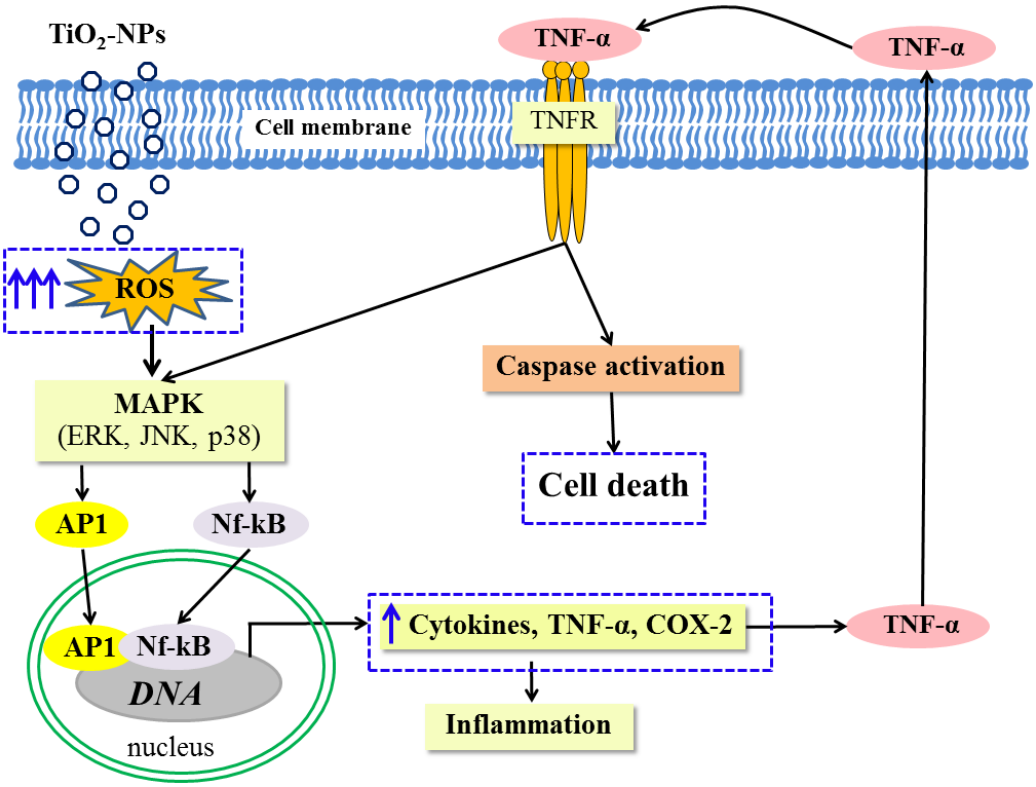

Figure 5.9 Schematic of the hypothetic pathways of inflammation mediated by TiO_2-NPs in RAW 264.7 cells. (Modified from Bianchi *et al*. (296)).

5.4.4 Possible cytotoxicity mechanisms from TiO_2-NPs in macrophage cells

Several studies have pointed out that the induction of oxidative stress molecules by NPs can cause toxicity (17, 145, 295, 300). The mechanisms of oxidative stress mediated toxicity of NPs are mitochondrial dysfunction and damage (33, 155, 301), activation of NADPH oxidase system (302), alteration of calcium homeostasis (303-305), and depletion of antioxidant enzymes (155). In the case of inhalation, inhaled NPs could activate professional phagocytic cells in the lung. These cells are a key cell involving in intracellular ROS production. The generation of ROS can be induced by phagocytosis of macrophages or by stimulation of macrophages with pathogens (such as bacteria or foreign materials) (306). The results from this

chapter showed that free radicals containing oxygen molecules were generated by TiO_2-NPs and caused DNA damage, which later mediated cell death as previous discussion. The possible mechanism or pathway of cell death is summarized in figure 5.10. DNA damage mediated by TiO_2-NPs was also reported by Kang *et al*. (260). They examined the genotoxicity of TiO_2-NPs in human lymphocytes. Their results indicated that the damage of DNA in human lymphocytes treated with TiO_2-NPs was from ROS generation. Endoproteases called caspases have an important role in regulating cell death and cell inflammation. It is well-known that caspase-3, -6, -7, -8, and -9 involve in apoptosis of mammalian cells (307). The apoptosis cell death induction by TiO_2-NPs through the activation of caspases (caspase-3, -8, and -9) were reported by Kang *et al*. (33). Their results presented that TiO_2-NPs induced apoptosis through mitochondrial pathway because of changing of mitochondrial membrane potential (MMP). The decrease of MMP by TiO_2-NPs and later lead to apoptosis cell death was also reported by Hussain *et al*. (19). They reported that the generation of ROS could cause MMP reduction resulting in releasing of cytochrome c and activating of caspase-9 and caspase-3. These incidents lead to DNA fragmentation. The diagram presents apoptosis induction that could occur by TiO_2-NPs in RAW 264.7 cells is shown in figure 5.10.

In figure 5.10, two major pathways of apoptosis (intrinsic and extrinsic pathway) as discussed previously may involve in apoptosis of cell treated with TiO_2-NPs at concentration 250 and 500 μg/ml. The generation of ROS could damage DNA. The elevation of ROS levels may lead to the transcription of inflammatory cytokines (such as TNF-α) in Nf-κB transcriptional pathway as discussed in the section of inflammation. The TNF-α molecules might further secrete and bind to their receptors (TNFR) on cell membrane. Upon stimulation of TNF-α with their receptors may further activate the apoptotic pathway through the activation of caspases as previous discussion (17, 19, 20, 31, 154, 155, 300).

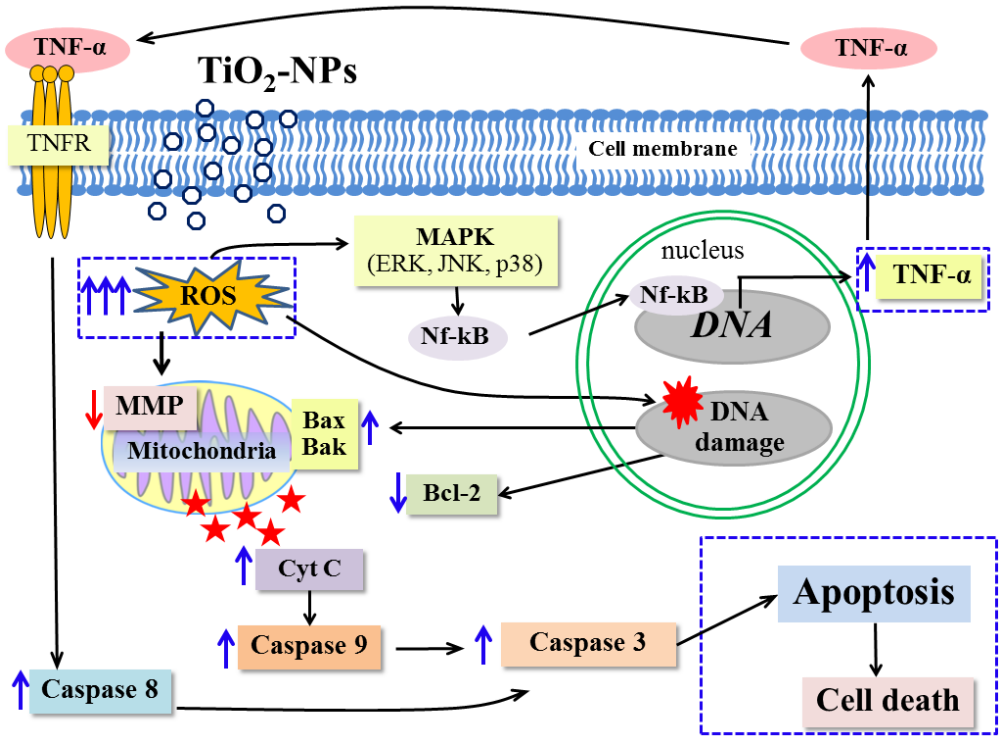

Figure 5.10 The possible mechanism of cell death pathways of RAW 264.7 cells treated with TiO_2-NPs. (Modified from Shukla *et al*. (154))

CHAPTER VI
INVESTIGATION OF CYTOTOXICITY EFFECTS OF TiO2-NPs ON BRAIN TUMORS

6.1 Introduction

Cancer is the most common cause of death in many countries. Central nervous system (CNS) tumors are an important cause of morbidity and mortality worldwide (308). Although the primary brain cancers are relatively uncommon cancers, they are often associated with high mortality rates (309). Gliomas are the most common primary brain tumors in adults, with an incidence of 3-5 cases per 100,000 populations. Malignant gliomas are defined by the World Health Organization (WHO) classification as anaplastic gliomas and glioblastomas (GBM) (310).

The treatment of malignant gliomas includes the use of chemotherapeutic drugs, radiotherapy, and interventional surgery. However, both chemotherapy and radiotherapy give inconsistent results in terms of prolonging survival and positive responses to treatment (308). In addition, the candidate drugs for therapy have low treatment efficiency because of their insufficient access to the central nervous system (CNS) due to the presence of the blood-brain barrier (BBB) blocking the passage from blood to the brain (311). Since nanotechnology has expanded its applications to biomedicine and biomedical areas, this nanotechnology is attractive for the diagnosis and treatment of malignant gliomas (308). Bouzier-Sore *et al.* (312) used maghemite (the magnetic particles) (~ 7.5 nm in size) for tracking the TK-GFP gene (suicide gene) in microglial cells. Their results indicated that the transfected microglia with the TK-GFP gene for cell therapy and maghemite NPs for cell tracking are a good candidate for brain cancer therapy. The benefit of applying NPs is to delivery therapeutic materials across the BBB without any damage of the barrier. This means that NPs can pass through the junctions between endothelial cells (313, 314). There are several routes to transport specific molecules or nanoparticles through the BBB. These routes are paracellular transport of hydrophilic molecules through the tight

junction between brain endothelial cell, transcellular lipophilic diffusion, carrier-mediated transcytosis, and adsorptive-mediated endocytosis. However, the mains entry routes of NPs to the brain via BBB are adsorptive or receptor-mediated endocytosis (314). Wu *et al*. (74) studied the distribution, accumulation, and toxicity of SiO_2-NPs in rats' brain after intranasal instillation. Their results revealed that the SiO_2-NPs at the size of 15 nm were deposited in striatum and impaired function of the brain. Ze *et al*. (73) also reported that TiO_2-NPs at sizes between 5 to 6 nm could pass BBB of mice after intranasal administration. Recently, Shilo *et al.* (75) have reported that insulin-targeted gold nanoparticles (INS-GNPs) at the size of 20 nm could across the BBB via the receptor-mediated endocytosis mechanism. Their results indicated that NPs integrated with the receptor-mediated endocytosis can be used for brain therapy.

The respiratory tract is the primary route of exposure of inhaled particles into the body (87, 262). NPs can translocate to all regions of the respiratory tract after entering the body by inhalation. The possibility of NPs at the sizes of ≤ 155 nm to enter the brain through an olfactory epithelium and systemic blood circulation was reported (70, 315, 316). After nanomaterials enter blood circulation, they may breakdown the tight junctions of endothelial cells and the blood-brain barrier and then enter the brain. Therefore, the NPs may impact tumor cells in the brain. In this chapter, the effect of TiO_2-NPs on glial tumor cells was investigated. C6 glioma cells were used as a model cell in this study. If TiO_2-NPs could destroy this brain tumor cell, it would help open a new approach for brain cancer therapy. In contrast, if TiO_2-NPs induce the growth of C6 glioma cells or inflammatory cytokines, the limited use of TiO_2-NPs becomes an area of concern.

6.2 Materials and methods

6.2.1 Cell preparation

Rat glioma cells (C6 cells) were grown as described in Chapter 3, section 3.2.3.1.

6.2.2 Cell viability assay

The viability of C6 glioma cells was measured by the CellTiter-Glo® Luminescent assay. More information on this procedure has been provided in Chapter 3, section 3.2.4.2. C6 cells at the concentration of 1×10^5 cells per well (for 100 µl) in DMEM/Ham's F-12 (Nacalai Tesque, Kyoto, Japan) were seeded into 96-well plates and incubated at 37 °C with 5% CO_2. After being incubating for 24 h, the old medium was removed and replaced with 50 µl of fresh medium (without serum). An equal volume (50 µl) of serum free medium with different concentrations of TiO_2-NPs (25, 125, 250, and 500 µg/ml) was added into each well. After treating C6 cells with TiO_2-NPs for 24 h, 100 µl of CellTiter-glo® reagent was added to the treated cells and mixed with an orbital shaker for 2 min. The following steps including the incubation conditions, measurement of the luminescence, and the cell viability calculation were described in Chapter 5, section 5.2.3.

6.2.3 Western blotting analysis

C6 cells were seeded on 100 mm culture dishes at a density of 2.5×10^6 cells/dish and allowed to adhere overnight in a 95% humidified air incubator at 37 ºC, and 5% CO_2. After incubation, cell media were removed and TiO_2-NPs at concentrations of 25, 250, and 500 µg/ml were added into the cells. After treatment for 24 h, cells were washed three times with cold PBS. Then the exposed cells were harvested by adding ice-cold lysis buffer. The lysis buffer preparation and more details have been presented in Chapter 5, section 5.2.5.

6.2.4 Determination of apoptosis cell death

6.2.4.1 DNA fragmentation analysis

C6 cells were seeded into 65 mm culture dishes at a density of 1×10^6 to 1.5×10^6 cells/well (the same cell number was used in each set). Cells were treated with TiO_2-NPs at 25, 250, and 500 µg/ml for 24 and 48 h. Treated cells were scraped off and cell DNA was extracted for running on gel electrophoresis to determine cell apoptosis, following the method written in Chapter 3, section 3.2.7.1.

6.2.4.2 Analysis of cell cycle and quantification of apoptosis

C6 cells were stained with PI to detect membrane integrity. C6 cells at a density of 1×10^6 to 1.5×10^6 cells/well (each set uses the same cell number) were treated with TiO_2-NPs at 250, 500, and 1,000 µg/ml for 24 h. After the C6 cells were treated with TiO_2-NPs for 24 h, cells were washed twice with ice-cold PBS and trypsinized by 0.05% trypsin EDTA. Next, the cells were centrifuged at 800 rpm for 5 min at 4 °C. The supernatant was discarded and adjusted the cell concentration to 2×10^6 cell/100 µl of PBS. Thereafter, 900 µl of 70% ethanol was added into cells and was gently mixed. Cells were fixed in ethanol overnight at 4 °C and centrifuged again to collect cell pellets. Cell pellets were suspended in 1 ml of ice-cold PI staining buffer solution (1 mg/ml of PI dissolved in Ca^{2+}/Mg^{2+} free PBS plus 2% fetal bovine serum). 20 µl of RNAse stock solution (1 mg/ml in PBS) were added and incubated at 37 °C for 30-45 min in a dark chamber. Cell suspension was transferred to FACs tubes and analyzed by flow cytometer.

6.3 Results

6.3.1 Effect of TiO_2-NPs on cell viability of C6 cells

After C6 cells were treated with different concentrations of TiO_2-NPs for 24 h, cell viability was determined by CellTiter-glo® assay. TiO_2-NPs concentrations used in this experiment were 5, 25, 250, and 500 µg/ml. The results demonstrated that TiO_2-NPs were toxic to C6 cells at all concentrations used in this study. When the concentration of TiO_2-NPs increased, the number of dead cells also increased.

However, the exposure times of 24 and 48 h showed a similar effect on cell viability (as shown in figure 6.1).

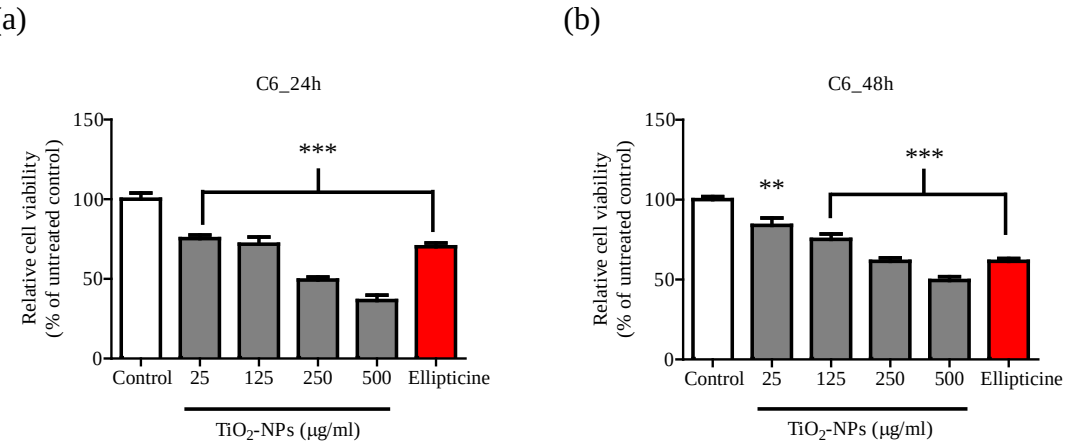

Figure 6.1 Cell viability of C6 glioma cells after treatment with different doses of TiO_2-NPs in the range of 25-500 µg/ml. Cells treated with ellipticine treated at a concentration of 0.5 µg/ml were used as a positive control. **, *** Significant difference of cell viability from untreated cells at $^{**}p< 0.01$, and $^{***}p< 0.001$.

6.3.2 Effect of TiO_2-NPs on DNA fragmentation of C6 glioma cells

C6 cells were treated with TiO_2-NPs for 24 and 48 h; the typical pattern of DNA fragmentation was determined by agarose gel electrophoresis and the DNA bands were detected under UV light. At 24 h post-incubation, DNA fragmentation was not observed (the data are not shown). However, after C6 cells were treated with TiO_2-NPs for 48 h, the laddering pattern was detected in cells treated with 250 and 500 µg/ml TiO_2-NPs (number 4 and 5 of figure 6.2) and a positive control (1,000 µM of H_2O_2), as seen in lane number 7 of figure 6.2.

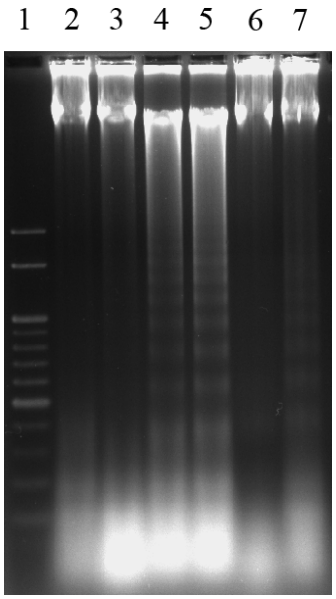

Figure 6.2 DNA laddering pattern of C6 cells after treatment with TiO_2-NPs for 48 h. C6 cells were treated with different doses of TiO_2-NPs in media without FBS. (1) DNA ladder marker. (2) Untreated cells. (3-5) Cells were treated with TiO_2-NPs at doses of 25, 250, and 500 µg/ml respectively. (6-7) Cells were treated with H_2O_2 at doses of 500 and 1,000 µM respectively. These results are representative of a triple slit experiment.

6.3.3 Effect of TiO_2-NPs on cell cycle analysis of C6 cells

To confirm the apoptotic effect of TiO_2-NPs (at a high concentration ≥ 250 µg/ml) on C6 cells, cell cycle analysis was performed. After C6 cells were treated with TiO_2-NPs at 250, 500, and 1,000 µg/ml for 24 h, the subG_0 population of cells (hypodiploid cells with DNA content less than G_1 in cell cycle distribution) increased when the concentration of TiO_2-NPs increased. The percentage of hypodiploid cells was 3.0, 3.2, and 7.8% after exposure to TiO_2-NPs at 250, 500, and 1,000 µg/ml respectively. The most significant difference of subG_0 cycle was found at the highest dose of TiO_2-NPs (figure 6.3d). Moreover, a significant depletion of G_0/G_1 populations was detected at 1,000 µg/ml of TiO_2-NPs treatment (figure 6.3f).

(a) Untreated control

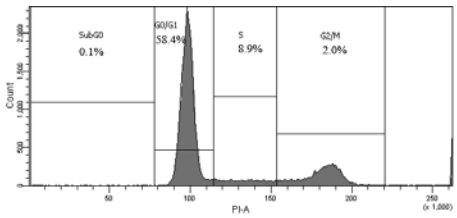

(b) TiO_2-NPs 250 µg/ml

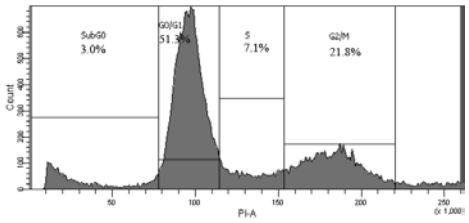

(c) TiO_2-NPs 500 µg/ml

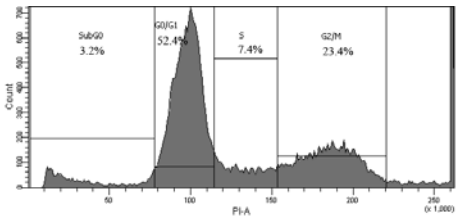

(d) TiO_2-NPs 1,000 µg/ml

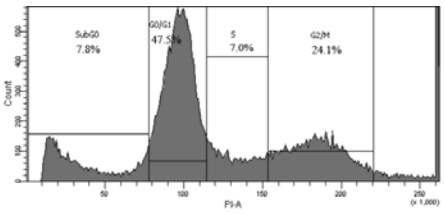

(e) Vinblastine 5 µM

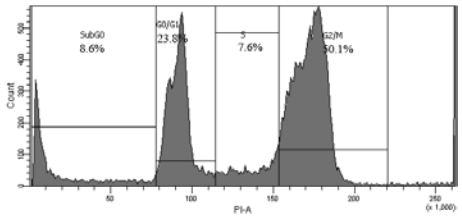

(f)

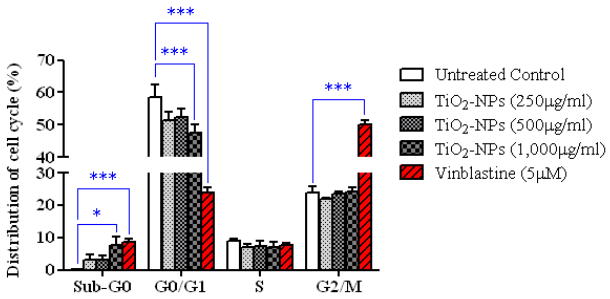

Figure 6.3 The effect of TiO_2-NPs on C6 cell cycle profile examined by flow cytometry analysis after treatment with TiO_2-NPs at 250, 500, and 1,000 µg/ml for 24 h. The significant differences of each cell cycle phase from untreated control group were presented at $^{*}p< 0.05$ and $^{***}p< 0.001$ compared to the untreated cells.

The activation of the endonuclease that cleaves DNA into a small fraction is considered to be a hallmark result of apoptosis. Thus, after staining DNA with PI dye, hypodiploid cells with DNA content less than G_0/G_1 in the cell cycle distribution were counted as apoptosis cells (317, 318). From the results in figure 6.3, we can conclude that TiO_2-NPs at high doses (≥ 250 μg/ml) have a high potential to induce fragmentation of DNA of C6 cells.

6.3.4 Effect of TiO_2-NPs on β-catenin and COX-2 expression of C6 glioma cells

In the brain, GSK3 is a downstream component of several signaling pathways including Wnt-β-catenin signaling (319). Besides that, β-catenin is an essential component of the Wnt signaling pathway, which is involved in a large variety of developmental processes and in tumor formation (282, 320, 321). The protein expression of β-catenin and COX-2 in C6 cells after treatment with different concentrations of TiO_2-NPs for 24 h were detected by western blot analysis. The protein expression of COX-2 (figure 6.4a) slightly increased but not significantly in cells treated with 500 and 1,000 μg/ml, but this was not significantly different from untreated cells. However, the expression of β-catenin dramatically decreased (after being normalized with the protein expression of β-actin) when the concentration of TiO_2-NPs increased as shown in figure 6.4b. Therefore it is not likely that the COX-2 protein has a major role in the toxicity induction of C6 glioma cells treated with TiO_2-NPs. These results revealed that there is no clear relationship between COX-2 and β-catenin expression after treating C6 cells with TiO_2-NPs. Since COX-2 expression was slightly increased, on the other hand, the expression of β-catenin was significant decrease. However, both COX-2 and β-catenin expressions play an important role in cells proliferation, cell cycle, and apoptosis in several tumor cell types (234, 283, 322-324). The further investigation of the relationship between COX-2 and β-catenin in glioma cells in a future study may provide more information to clarify the mechanism of cell death.

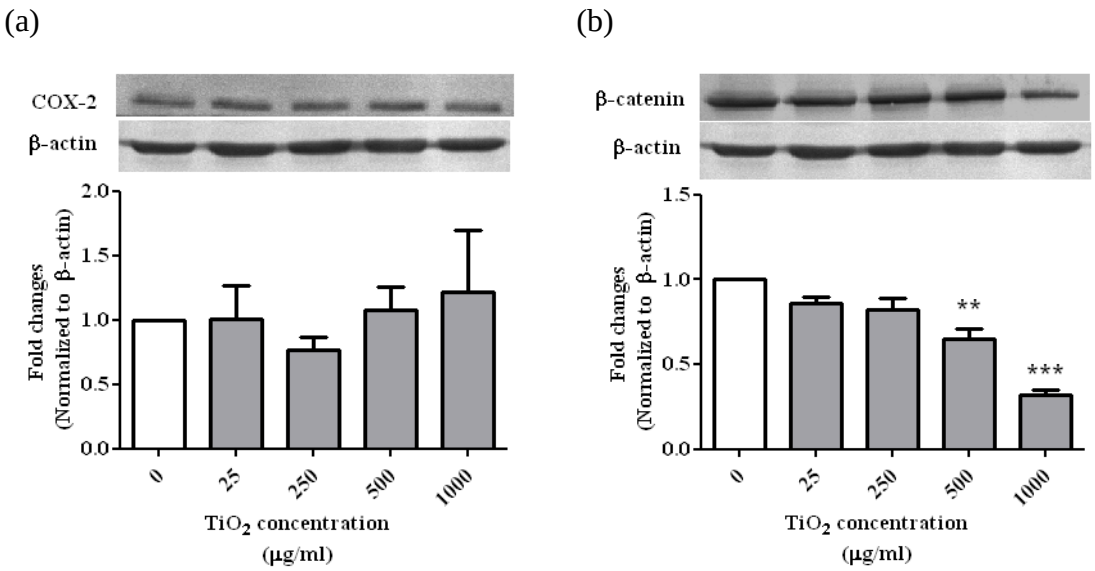

Figure 6.4 Effect of TiO_2-NPs on the expressions of (a) COX-2, and (b) β-catenin. Cells were treated with TiO_2-NPs (25-1000 μg/ml) for 24 h. **, *** Significantly different from untreated cells at $^{**}p< 0.01$ and $^{***}p< 0.001$

6.4 Discussion

6.4.1 Cytotoxicity of TiO_2-NPs to C6 glioma cells

The results of the present study indicate that TiO_2-NPs at concentration ranges of 25-500 μg/ml can induce toxicity to C6 glioma cells. To further prove that the TiO_2-NPs mediated the toxicity of C6 cells, apoptosis cell death was investigated. DNA fragmentation was detected in C6 cells after treatment with 250-500 μg/ml of TiO_2-NPs for 48 h. There have been many reports of cell apoptosis induction by TiO_2-NPs. TiO_2-NPs seem to be toxic to neuronal cells, especially glial cells (142). It was reported that 2.5 to 120 ppm TiO_2-NPs that had an aggregated sized around 330 nm in a culture medium could induce ROS, inflammation, and cell apoptosis of microglia cells (BV2). In 2008, Lai *et al*. (53) reported the information of cell death in neuronal cells (U87 cells) after treatment with 1 to 100 μg/ml TiO_2-NPs at a size of less than 25 nm for 48 h. Both apoptosis and necrosis were detected in cells after treating TiO_2-NPs at concentrations > 1 μg/ml.

Oxidative stress has been purported to be a key mediator in TiO_2-NPs induced brain damage in animal models. A recent study by Ze *et al.* (73) reported that after intranasal administration of TiO_2-NPs to mice for 90 days, lesions in the mice's brain were observed. They also indicated that TiO_2-NPs induced oxidative stress and the activation of the oxidative stress-gene, which resulted in lesions in the mice's brain. The oxidative stress mediated toxicity in glial cells was reported recently by Huerta-García *et al*. (325). They selected C6 glial cells as a model to determine the effects of TiO_2-NPs on brain cells. Their results indicated that C6 cells treated with 20 $\mu g/cm^2$ TiO_2-NPs (< 50 nm) for 2, 4, 6, and 24 h produced a strong oxidative stress in C6 cells. Therefore, as comparing with my results in this thesis, the viability of C6 cells was decreased as a dose dependent manner (shown in figure 6.1). The apoptosis cell death was confirmed by two different assays: 1) DNA fragmentation assay (in figure 6.2) and 2) Flow cytometric analysis of cell cycle with propidium iodide DNA staining (in figure 6.3). With these results and results from studies by others as mentioned above, TiO_2-NPs might generate ROS and lead to cytotoxicity of C6 cells.

Nanoparticles can travel to the central nervous system via two major routes: olfactory nerves and the blood-brain-barrier (2, 70, 316, 326). Because of their small size and unusual properties, nanoparticles can pass through the blood brain barrier and enter the brain (67, 68). After entering to the brain, the surface charge of TiO_2-NPs may generate either oxidative stress or ROS, causing apoptosis cell death to neuron cells (142, 257, 258). The oxidative stress and the generation of ROS produced by TiO_2-NPs not only induce apoptosis cell death of neuron cells, but also increase the permeability of the brain protection mechanism, such as the blood-brain-barrier, which allows nanoparticles to enter the brain. ROS generation, coupled with the loss of cell viability, inflammatory cytokine release, and the damaged of DNA, is probably a key factor that leads to cytotoxicity. The oxidative stress-mediated cytotoxicity and apoptosis cell death of immune and neuron cells induced by TiO_2-NPs have been variously reported in the last few years (17, 257-260).

The mechanism of TiO_2-NPs leading to ROS-mediated cytotoxicity was reported by Jin *et al*. (21). After TiO_2-NPs dispersion, a large amount of surface hydroxyl groups has been found by X-ray absorption fine structure spectrometry (XAFS). Those surface hydroxyl groups can induce superoxide and hydroxyl radicals

by electron capture, which can recombine into H_2O_2 in aqueous solution (6, 21, 261). Cells exposed to TiO_2-NPs may exhibit cytotoxicity and genotoxicity by phagocytosis and internalization into the cytoplasm (262). Jin *et al.* (21) also explained the toxic effect of nanoparticles produced by the generation of ROS and oxidative stress in the mitochondria of normal cells, as ROS is generated and neutralized by glutathione and antioxidant enzymes (such as GPx, SOD, and CAT). After exposure to cells with TiO_2-NPs, ROS increased at the membrane of the mitochondria without a clearance mechanism, therefore leading to mitochondrial disruption. The apoptosis and necrosis cell death were initiated through the mitochondrial membrane permeability transition pore (21, 327). The role of ROS-mediated apoptosis and necrosis cell death has been investigated by several studies (235, 263). Alveolar macrophage cells were treated with substances that produce oxidants that were thought to exclusively cause necrosis; however, ROS can act as signaling molecules to trigger apoptosis under certain conditions (252). When pro-oxidants overwhelm anti-oxidant defense mechanisms, oxidative stress occurs. Although the toxicity of TiO_2-NPs on glial cells has been thoroughly studied, the link between oxidative stress and apoptosis cell death has not been confirmed. In the present study, TiO_2-NPs induced cytotoxicity in C6 glioma cells, as demonstrated by 1) dose-dependent reduction cell viability by CellTiter-Glo® and trypan blue dye exclusion assay, 2) the evidence of DNA fragmentation as dose-dependent determined by DNA laddering pattern on the agarose gel, and 3) the increase of C6 glioma cells in subG_0 population as dose-dependent. All of the toxicity determination assays are correlated with the increase of intracellular ROS levels determined by DCF-florescence intensity (in chapter 5). Therefore the results from those experiments provided convincing evidence that the mechanism cell death induced by TiO_2-NPs was involved in the increase of intracellular ROS-mediated apoptosis in glioma cells.

6.4.2 TiO_2-NPs decreased β-catenin expression in C6 cells

In this study, the mechanism of how TiO_2-NPs induce toxicity of C6 glioma cells was also reported. As shown in figure 6.4, the results in this thesis demonstrate how, the expression of COX-2 enzyme was different from untreated cells. An insignificant increase of COX-2 expression was found in cells treated with 1,000

µg/ml of TiO_2-NPs. Cyclooxygenase, also known as prostaglandin H synthase, is the rate-limiting enzyme that converts arachidonic acid into prostaglandin H2, thromboxanes, and prostacyclins. There are two isoforms of the COX enzyme that have been characterized as COX-1 and COX-2. COX-2 protein is an inducible isoform that can rapidly and transiently induce inflammatory cytokines and a variety of stimuli (278). In contrast to COX-1, which is expressed in most tissues, COX-2 is not detected under resting conditions, except for inflammatory response and in some tumor cells (279, 280). The expression of COX-2 in glioma was reported by Badie *et al.* (280). Their study demonstrated the expression of COX-2 in brain tumor cells involved in brain edema patients. Consequently, COX-2 expression in C6 cells detected in our study is at normal levels, so the toxicity of TiO_2-NPs to C6 cells may be caused by other mechanisms rather than COX-2. The up-regulation of COX-2 expression might be related to various sources (including ROS). In his dissertation, Kitz (328) discussed how the depletion of NAPDH oxidase blocked the expression of COX-2 in rat mesangial cells, whereas increased Ca^{2+}-dependent mitochondrial ROS production was associated with prostaglandin production in human chondrocytes.

This thesis also found that the expression of crucial protein β-catenin was inhibited by the induction of TiO_2-NPs. β-catenin is a protein that is involved in the Wnt signaling pathway. This pathway is associated with the proliferation and metabolism of many cancer cells (282, 283). The Wnt signaling pathway not only plays a critical role in cell proliferation and the development of tumors, but also plays a distinct role in inflammation, immunity and apoptosis (249, 283). In figure 6.4, the levels of β-catenin in C6 glioma cells after treatment with TiO_2-NPs at concentration ranges of 25-1000 µg/ml were decreased in a dose-dependent manner with a significant decrease at concentrations of 500 and 1,000 µg/ml. However, the expression of COX-2 enzyme, was not significantly changed. These data suggest that TiO_2-NPs might effectively impact the Wnt/β-catenin pathways. However, it seems that there is no association between the expressions of β-catenin and COX-2. The mechanism of this is not clearly understood and further study would be interesting for future research.

CHAPTER VII
INFLAMMATORY EFFECTS OF TIO2-NPS AND MWCNTS IN ALVEOLAR LAVAGE FLUID OF MICE

7.1 Introduction

Due to an increase of the use of nanomaterials in daily life, the impact of using NPs on human health has become an area of serious concern. Inhalation is considered to be the most important and critical exposure route of human exposure to engineered nanoparticles. These particles have a high deposition efficiency to the respiratory system after inhalation (5). Therefore, human health can be affected, when nanomaterials are aerosolized (87). Inhalation of NPs can cause various lung responses and lead to the development of lung diseases such as chronic bronchitis, chronic obstructive pulmonary disease (COPD), and pulmonary fibrosis (49, 329). Research on nanosafety, especially *in vivo,* is still lacking. The mechanisms behind the toxicological effects of NPs are still debated; therefore, further investigations of the toxicity of NPs involved in reactive oxygen species (ROS) the result in oxidative stress, inflammation and consequent damage to proteins, membranes and DNA are required (49, 152, 330, 331).

As mentioned previously, NPs have aerodynamic properties that can reach and deposit in the distal parts of the lungs during inhalation (5, 161). Depending on the size of NPs, after being deposited to the lungs, the agglomerate/aggregate of NPs may deposit at the lung surface and interact with lung epithelial cells or lung macrophage cells. On the other hand, NPs can be distributed from the lungs to other organs (332). After NPs interact with macrophages, chemotactic signals can be triggered to activate and attract neutrophils to help clean up the invading particles (138, 227). Once the particles have been deposited in the lungs, the particles will then initiate an inflammatory response by interacting with the cells of the immune system. In the case of high bio-persistence, the particles may cause chronic inflammation and pulmonary fibrosis (49). Inflammation is a vital process to eliminate pathogens and promote the

repair of injured tissue (333, 334). However, excessive or persistent inflammation can contribute to tissue injury and the pathogenesis and exacerbation of diseases, including inflammatory lung diseases such as chronic obstructive pulmonary disease (227, 335). Inflammation can be monitored by observing the influx of inflammatory cells, primarily macrophages and neutrophils, or by measuring markers such as proinflammatory cytokines, total protein and LDH in the lung fluid after lavaging the lungs.

TiO_2-NPs have been widely used in various household products including air and water cleaning, cosmetics, and pharmaceuticals (179). Thus, TiO_2-NPs have a potential to impact daily life. However, before using TiO_2-NPs in a form that has a chance to directly contact humans, an investigation of toxicity *in vivo* exposure should be performed. Another type of NPs that has been used a lot recently is carbon nanotubes (CNT). They are unique carbon-based NPs that have significant characteristics in size, strength, and surface chemistry (336). In particular, their length/width (aspect) ratios, reactive surface chemistry, and poor solubility are noteworthy (337). CNT can be prepared in a multi-walled form (called MWCNTs). More details are shown in Chapter 2, section 2.2.2. MWCNTs have shown to have the capability to induce allergic, inflammatory, and fibrotic pulmonary responses (338). These effects have associated with significant increases in various pro-inflammatory cytokines (337, 339).

In this thesis, the focus will be on *in vivo* testing for toxicity and inflammatory responses of two different types of nanomaterials (TiO_2-NPs and MWCNTs). Therefore, the objective of this chapter is to investigate the toxicity effects and inflammatory responses after intranasal instillation of TiO_2-NPs and MWCNTs into mice.

7.2 Materials and methods

7.2.1 Animals and treatments

The preparations of TiO_2-NPs and MWCNTs were explained in Chapter 3, section 3.2.1. Adult male ICR mice (approximately 7 weeks old), with body weights ranging from of 25-30 grams, were purchased from the National Animals Center of Thailand, Mahidol University, Salaya campus, Nakhonpathom. They were housed in translucent plastic cages with sawdust bedding in the animal room, Faculty of science, Mahidol University, Bangkok. They were allowed to acclimatize for one week before use. All animals were maintained in a controlled room with a 12 h light-dark cycle, temperature 21-22 ºC and relative humidity of approximately 50-60%. All animals had free access to water and food. The use of experiment animals and the experimental design was approved and carried out by following the protocol of the Animal Care and Use Committee, Faculty of Science, Mahidol University, Thailand (MUSC54-033-243).

To determine the toxicity effect of TiO_2-NPs and MWCNTs, the animals were instilled with TiO_2-NPs or MWCNTs suspension through their nostrils. Prior to instillation, all the mice were anesthetized with intraperitoneal injections of pentobarbital at the concentrations of 30-50 mg/kgBW. After the mice were deeply anesthetized (confirmed by the absence of reflexes on the footpad), they were injected with TiO_2-NPs or MWCNTs. The TiO_2-NPs or MWCNTs and a vehicle control suspension (50 ul for each mouse) were gradually released into the nostrils using a micropipette. The rate of injection was carefully adjusted to allow the mice to inhale the NP suspension without bubbles. The mice were then held for a couple of minutes until their breathing rates gradually returned to normal.

The treatments were grouped into five conditions as shown in the following lists:

Group 1 : Intact control group

Group 2 : Vehicle control group (for TiO_2-NPs); mice were treated by intranasal instillation with PBS 50 µl per mouse

Group 3 : Vehicle control group (for MWCNTs); mice were treated by intranasal instillation with 1% serum plus 0.1% D-glucose dissolved in PBS 50 µl per mouse

Group 4 : Positive control group; mice were treated with lipopolysaccharide (30 µg per mouse)

Group 5-7 : TiO_2-NPs Treatment groups; mice were treated by intranasal instillation with TiO_2-NPs suspended in PBS at the concentration of 50, 500, and 1,000 µg/kgBW (50 µl/mouse)

Group 8-10 : MWCNTs treatment groups; mice were treated by intranasal instillation with MWCNTs suspended in 1% serum plus 0.1% D-glucose dissolved in PBS at the concentration of 50, 500, and 1,000 µg/kgBW (50 µl/mouse)

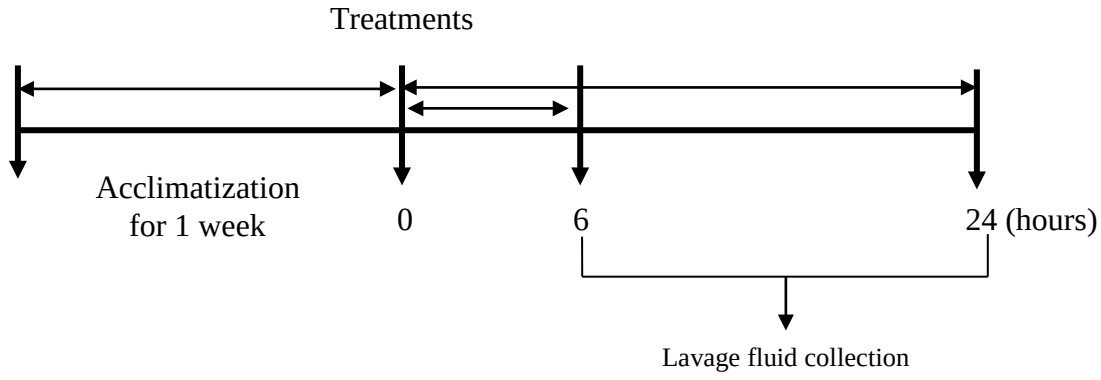

Figure 7.1 Schematic diagram showing the time course of treatment and sample collection.

At the end of the treatment period, all mice were euthanized by intraperitoneal injection with 50 mg/kg pentobarbital and exsanguinated through the heart. The trachea was cannulated with a catheter attached to a 1 ml syringe; the lungs were infused gently with a sterile 0.9% sodium chloride solution (1 ml) and the solution was drawn back. The lavage process was performed three times. The lavage fluid was clarified by centrifugation at 1,500 g for 15 min at 4 ºC. The total protein, lactate dehydrogenase (LDH) activity, cytokines, and chemokines were analyzed from broncho alveolar *lavage* fluid (BALF).

7.2.2 Protein assay in BAL fluid

The total protein concentration was measured by the Bradford method (340) using a BioRad Assay Kit (BioRad, Richmond, Ca, USA) according to the manufacturer's instruction and read at 595 nm using a spectrophotometer. Bovine serum albumin (BSA) was used as a standard protein.

7.2.3 LDH level in BAL fluid

Activity of LDH in BAL fluid supernatant was measured by using the commercially available LDH-Cytotoxicity Assay kit II (Abcam, Cambridge, MA, USA). All processes followed the manufacturer's instructions.

7.2.4 Cytokine assay

Pro-inflammatory cytokine production (TNF-α, and IL-6) of BAL fluid was measured using commercially available enzyme-linked immunosorbant assay (ELISA) kits (eBioscience, San Diego, CA). The ELISA analysis was performed according to the manufacturer's instructions. After incubation, the supernatants of all samples were collected and stored at -75 ºC until assay. A monoclonal antibody specific for each cytokine was pre-coated onto a microplate and incubated overnight at 4 ºC. The standard and samples were pipetted into the wells, and any cytokine present should have bound to the specific immobilized antibody. After removing unbound substances, an enzyme-linked polyclonal antibody specific to the cytokine was added to the wells and incubated for 1 h at room temperature. After washing to remove any unbound antibody-enzyme reagent, a substrate solution was added to the wells. The

solution was then incubated for 30 min and washed with buffer at least 7 times. The substrate solution was added to each well and incubated at room temperature. The stop solution was added after 15 min. The intensity of color development was read at 450 nm with a microplate reader. The amount of cytokine was calculated from the linear portion of the generated standard curve.

7.2.5 Statistical analysis

Statistical analysis was conducted by using the statistical software package, GraphPad Prism version 5.0. For more than two experimental groups, the statistical difference among different groups was first compared using one-way analysis of variance (one-way ANOVA). Then, the significant difference between groups was further examined by Dunnett's Multiple Comparison Test. Values of $p< 0.05$ were considered to be significantly different.

7.3 Results

After 6 and 24 h of TiO_2-NPs and MWCNTs intranasal instillation, all mice were euthanized by intraperitoneal injection with 50 mg/kg pentobarbital. Lungs were lavaged three times with 1 ml of sterile 0.9% sodium chloride solution. The lavage supernatants were analyzed for total protein, lactate dehydrogenase (LDH) activity and cytokine levels. The concentrations of cytokines and chemokines including interleukin IL-1β, IL-6, and tumor necrosis factor alpha (TNF-α) were measured in the supernatants of BAL fluids. Finally all mice were exsanguinated through the heart. Lungs, livers, and kidneys were weighed to determine the organ weight per body of the mice.

7.3.1 Mouse`s body and organ weight investigation

Compared to a vehicle control, TiO_2-NPs did not affect the body weight and the organ weigh of the mice. However, the positive control group (treated with LPS 30 µg/mouse) showed significant differences in the lung weight after treating mice with LPS for 24 h (Table 7.1).

Mice treated with MWCNTs had a similar body weight to the control mice at both 6 and 24 h. In the case of the lung weight, there was significant increase of the weight of the 500 µg/kgBW treatment group at 6 h, but at a longer exposure time (24 h) there was no difference. Interestingly, the group of mice treated with a vehicle control (1% FBS in 0.1% D-glucose) for 6 h had a significant increase in the weight of the kidney, both left and right, when compared with an intact control. However, at 24 h of treatment, mice in this group had no difference in kidney weight (Table 7.2).

Table 7.1 Changes in relative organ weight and body weight following a single instillation of TiO_2-NPs

Time (hours)	TiO_2-NPs (µg/kgBW)	Body weight (g)	Organ Weight (g/100g bodyweight)			
			Lung	Liver	Kidney	
					Left	Right
6	Intact control	35.72 ± 1.70	1.13 ± 0.11	5.66 ± 0.34	0.81 ± 0.07	0.87 ± 0.08
	Vehicle control	35.43 ± 1.47	1.19 ± 0.11	5.74 ± 0.26	0.81 ± 0.02	0.88 ± 0.04
	50	35.06 ± 1.93	1.23 ± 0.07	5.84 ± 0.36	0.85 ± 0.03	0.90 ± 0.08
	500	35.20 ± 1.43	1.19 ± 0.05	5.91 ± 0.31	0.77 ± 0.10	0.84 ± 0.08
	1,000	34.96 ± 1.62	1.14 ± 0.09	5.75 ± 0.32	0.77 ± 0.05	0.90 ± 0.09
	LPS (30µg/mouse)	34.95 ± 1.07	1.29 ± 0.11	5.98 ± 0.29	0.80 ± 0.07	0.91 ± 0.05
24	Intact control	35.00 ± 1.76	1.14 ± 0.09	6.26 ± 0.42	0.90 ± 0.05	0.93 ± 0.10
	Vehicle control	34.64 ± 1.47	1.18 ± 0.11	6.39 ± 0.74	0.85 ± 0.07	0.88 ± 0.09
	50	34.32 ± 0.99	1.25 ± 0.19	6.07 ± 0.31	0.88 ± 0.09	0.90 ± 0.06
	500	34.85 ± 0.47	1.20 ± 0.14	6.51 ± 0.67	0.91 ± 0.16	0.90 ± 0.08
	1,000	33.75 ± 1.50	1.21 ± 0.09	6.17 ± 0.40	0.80 ± 0.08	0.88 ± 0.06
	LPS (30µg/mouse)	33.23 ± 1.47	**1.51 ± 0.18*****	6.25 ± 0.57	0.81 ± 0.10	0.90 ± 0.07

Note: 1) Vehicle control was groups that were treated with PBS.

2) Weight of each group was calculated. The data presents the mean value ± SD of at least of four independent experiments.

3) $^{***}p < 0.001$ denotes significant differences between mean values measured in the indicated group compared to their vehicle control.

Table 7.2 Changes in relative organ weight and body weight following a single instillation of MWCNTs

Time (hours)	MWCNTSs (µg/kgBW)	Body weight (g)	Organ Weight (g/100g bodyweight)			
			Lung	Liver	Kidney	
					Left	Right
6	Intact control	35.72 ± 1.70	1.13 ± 0.11	5.66 ± 0.34	0.81 ± 0.07	0.87 ± 0.08
	Vehicle control	35.24 ± 0.91	1.09 ± 0.06	5.90 ± 0.18	**0.97 ± 0.16**$^{\#}$	**1.11 ± 0.17**$^{\#\#}$
	50	34.54 ± 0.58	1.21 ± 0.06	6.05 ± 0.38	0.90 ± 0.05	**0.97 ± 0.09***
	500	34.47 ± 0.54	**1.26 ± 0.09***	6.25 ± 0.44	0.84 ± 0.07	0.90 ± 0.07
	1,000	34.41 ± 0.51	1.20 ± 0.09	6.16 ± 0.47	0.90 ± 0.05	0.99 ± 0.06
24	Intact control	35.00 ± 1.76	1.14 ± 0.09	6.26 ± 0.42	0.90 ± 0.05	0.93 ± 0.10
	Vehicle control	34.34 ± 0.25	1.30 ± 0.08	6.35 ± 0.22	0.91 ± 0.06	0.94 ± 0.01
	50	34.15 ± 0.94	1.28 ± 0.09	6.51 ± 0.38	0.87 ± 0.07	0.89 ± 0.07
	500	34.83 ± 1.12	1.28 ± 0.12	6.47 ± 0.29	0.89 ± 0.09	0.91 ± 0.04
	1,000	33.03 ± 0.86	1.33 ± 0.14	6.70 ± 0.57	0.91 ± 0.10	0.99 ± 0.10

Note: 1) Vehicle control was groups that were treated with 1% FBS in 0.1% D-glucose.

2) Weight of each group was calculated in term of mean ± SD of at least of four independent experiments.

3) $^{*}p< 0.05$ denotes significant differences between mean values measured in the indicated group compared to their vehicle control.

4) $^{\#}p< 0.05$, $^{\#\#\#}p< 0.001$ denote significant differences between mean values measured in the indicated group compared to their intact control.

7.3.2 LDH from mouse BAL fluid treated with nanoparticles

For the examination of whether TiO_2-NPs can cause pulmonary toxicity, after administration of TiO_2-NPs (50 and 500 µg/kgBW) for 6 and 24 h, broncho alveolar lavage fluid was obtained from mice administered with PBS, TiO_2-NPs and LPS (30 µg/mouse). BAL fluid activity, a marker of cell toxicity, increased significantly after treating mice with TiO_2-NPs for 6 and 24 h. The LDH production of mice treated with a low dose of TiO_2-NPs (50 µg/kgBW) for 6 h was lower than the ones treated with 500 µg/kgBW TiO_2-NPs (figure 7.2a). On the other hand, at 24 h treatment exposure, significant induction of LDH was found in mice injected with 500 µg/kgBW TiO_2-NPs (figure 7.2b). Mice injected with LPS (positive control mice) significantly produced LDH compared to control mice.

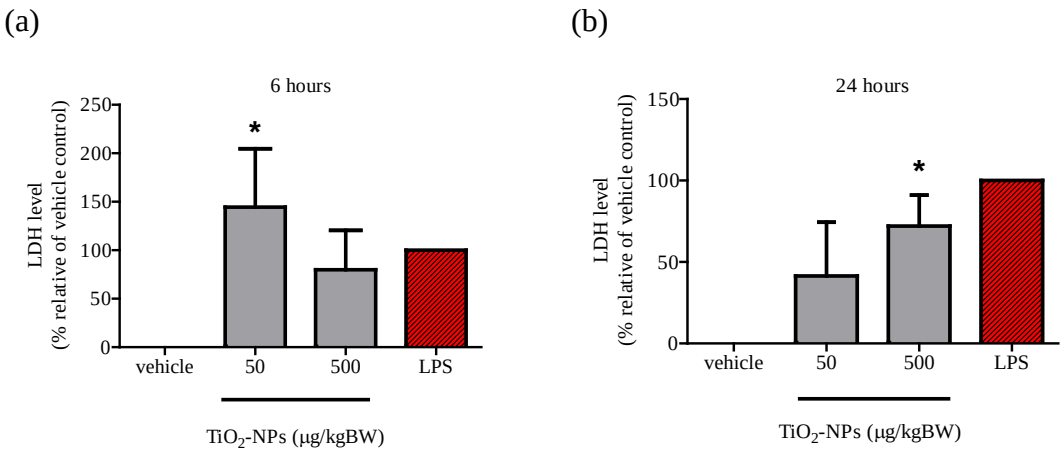

Figure 7.2 The expression of LDH detected in BAL of ICR mice at 6 and 24 h after intranasal instillation with PBS (as a vehicle control), titanium dioxide nanoparticles and LPS 30 µg in 50 µl PBS/mouse (as a positive control). Data are means ± SE of at least three independent experiments. $^{*}p< 0.05$ denote significant differences between mean values measured in the indicated group compared to their vehicle control; as analyzed by one ways ANOVA/Dunnett's multiple comparison test (n=3-5).

LDH released in BAL fluid of mice after intranasal instillation with MWCNTs (50 and 500 µg/kgBW) compared to the vehicle control (1% FBS in 0.1% D-glucose) is shown in figure 7.3 below.

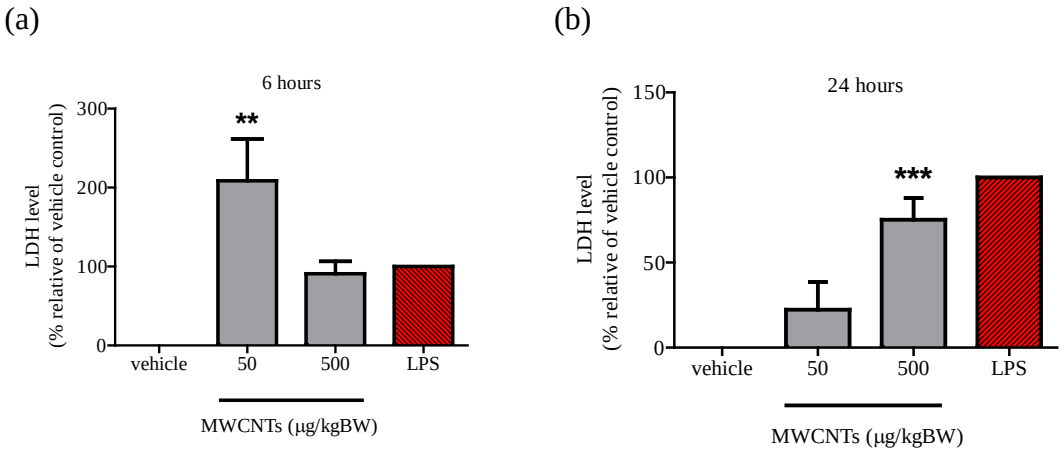

Figure 7.3 The expression of LDH activity detected in BAL of ICR mice at 6 and 24 h after intranasal instillation of the 1% FBS in 0.1% D-glucose (as a vehicle control), MWCNTs (50 and 500 µg/kgBW) and LPS (30 µg in 50 µl PBS)/mouse (as a positive control). Data represent means ± SE of at least three independent experiments. ** and *** represents statistically significant difference from a control group at $p < 0.01$ and $p < 0.001$ respectively (n=3-5).

The level of LDH released in BAL fluid after instillation with MWCNTs for 6 h increased significantly in mice treated with MWCNTs (50 and 500 µg/kgBW). However, the LDH level in mice treated with 50 µg/kgBW was higher than that of those with 500 µg/kgBW. The reason for this is unclear. At 24 h exposure, the LDH level in BAL fluid showed a significantly high level in mice treated with 500 µg/kgBW MWCNTs. These results showed a similar direction as found in mice treated with TiO_2-NPs using the same concentrations and exposure times.

7.3.3 Changes in total protein level in BAL fluid

The level of total protein in BAL fluid was measured by Bradford protocol as described in the previous section. At 6 h post TiO_2-NPs instillation, a significant increase of total protein in only the BAL fluid was found at 500 µg/kgBW TiO_2-NPs. This means that at a short exposure time, the 50 µg/kgBW TiO_2-NPs had no impact on inducing proteins. In contrast, at 24 h post TiO_2-NPs instillation, total protein level in BAL fluid slightly increased in a dose-dependent manner, but no statistical significant difference from vehicle and intact controls was observed (figure 7.4)

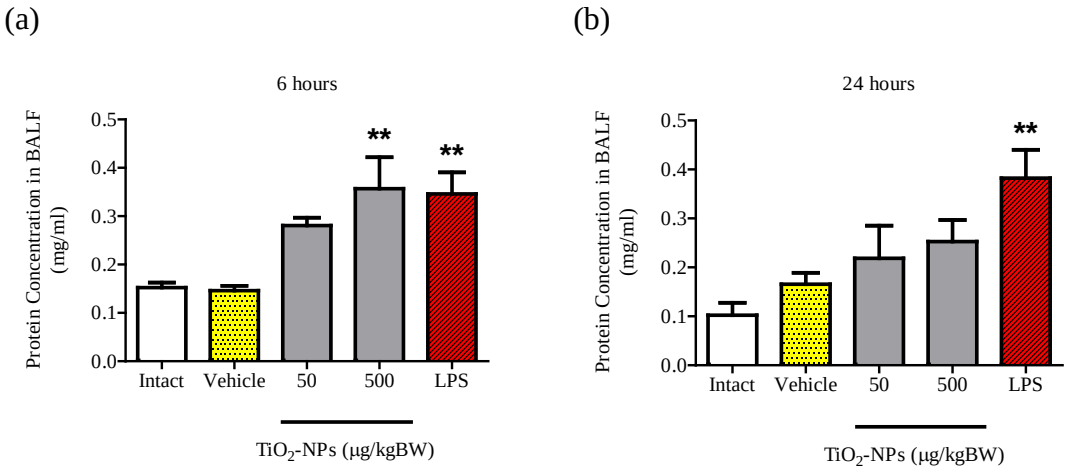

Figure 7.4 The expression of total protein contents in BALF of ICR mice at 6 and 24 h post-instillation with PBS (as a vehicle control), TiO_2-NPs (50 and 500 µg/kgBW) and LPS 30 µg/mouse (as a positive control). **Significantly different from vehicle control group at $^{**}p< 0.01$ (n=3-7).

The protein levels in BAL fluid after treatment with MWCNTs increased dose-dependently. Significant differences from the vehicle control were revealed at 500 µg/ml in both time points (figure 7.5).

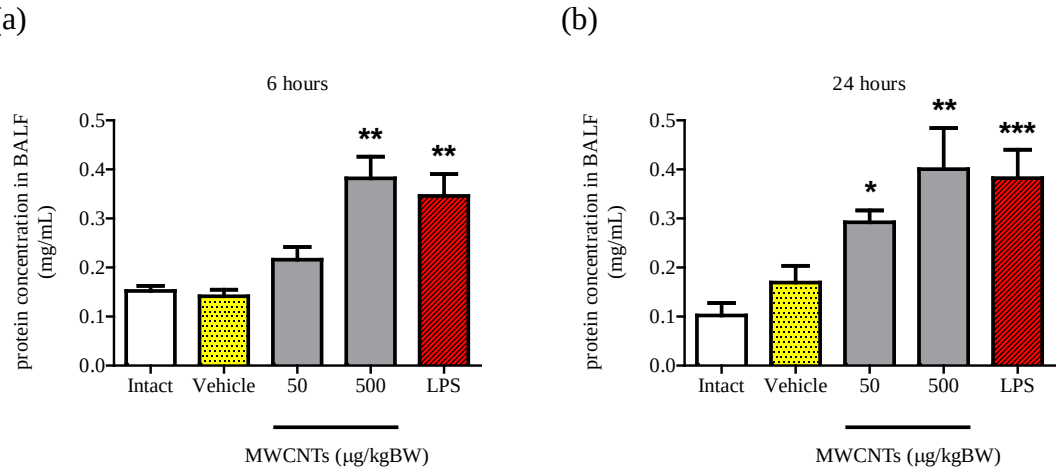

Figure 7.5 The expression of total protein contents in BALF of ICR mice at 6 and 24 h post-instillation with PBS (as a vehicle control), MWCNTs (50 and 500 µg/kgBW) and LPS 30 µg/mouse (as a positive control). *, **, *** Significantly different from vehicle control group at $^{*}p< 0.05$, $^{**}p< 0.01$ $^{***}p<0.01$ (n=3-7).

7.3.4 Pro-inflammatory cytokine released in BAL fluid

The levels of TNF-α released into BAL fluid of mice that were treated with TiO_2-NPs (50-500 µg/kgBW for 6 and 24 h) slightly increased in dose dependent manner but no significant difference from the vehicle control was observed. In contrast, the releases of IL-6 were similar in all treatments (in figure 7-6).

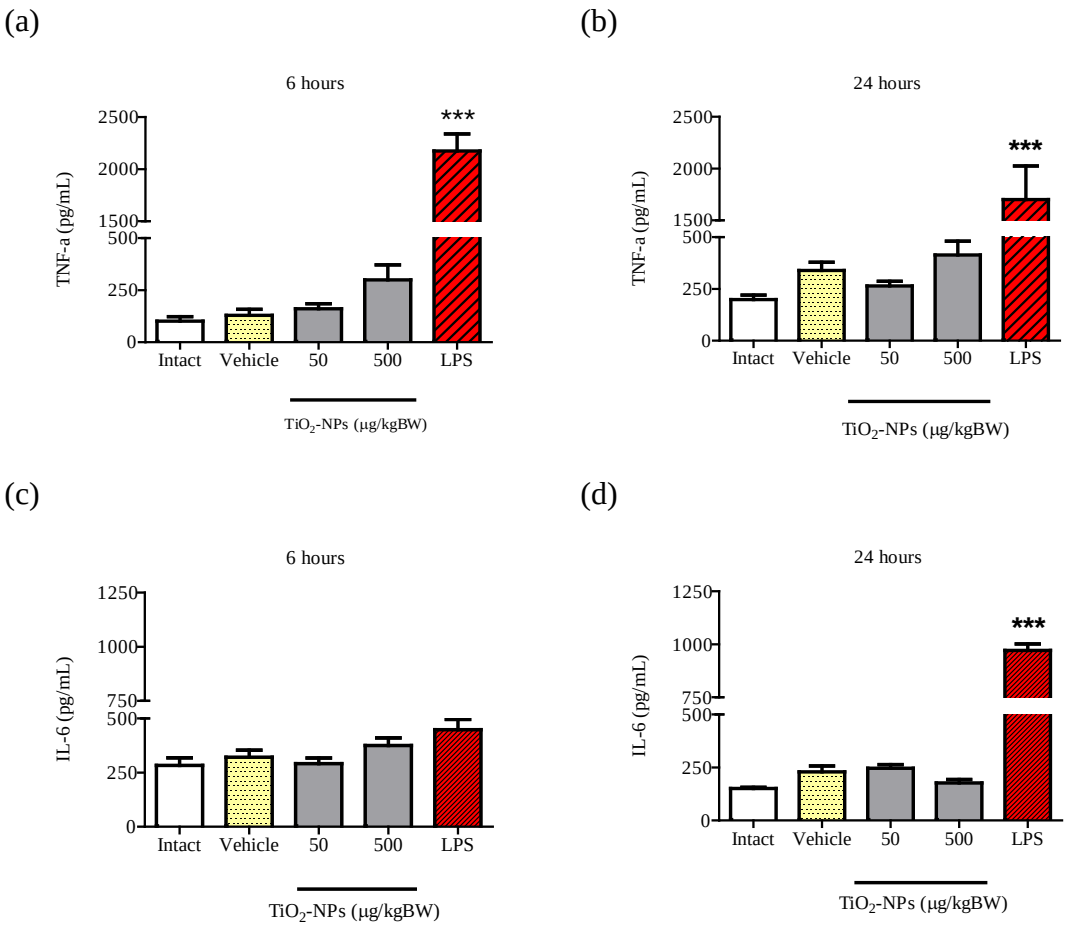

Figure 7.6 The production of TNF-α (a,b), and IL-6 (c,d) in BAL fluids of ICR mice intranasally instilled with PBS (as a vehicle control), TiO_2-NPs at concentrations 50 and 500 µg/kgBW and LPS (30 µg in 50 µl PBS)/mouse (as a positive control) for 6 and 24 h. Levels of TNF-α and IL-6 were measured in BAL fluids at 6 and 24 h post-instillation. $^{***}p< 0.001$ denoted a significant difference compared to a vehicle control group (n=3-7).

TNF-α and IL-6 released in BAL fluids after instilling mice with MWCNTs for 6 and 24 h increased in a dose-dependent manner; however, there was no significant difference of both cytokine expressions observed in mice BAL fluids excepting for the ones treated with MWCNTs at a concentration of 500 µg/kgBW MWCNTs at 6 h post-instillation (figure 7.7). At 24 h post instillation, the IL-6 levels in BAL fluids of all treatment conditions were similar to the vehicle control. The reason for this is unclear. The induction of IL-6 secretion in BAL fluid of mice after intratracheally administration with MWCNTs has been reported by Inoue *et al*. (337).

Their results showed the induction of IL-6 expression in the BAL fluid after repeating exposure with a low dose of MWCNTs (50 µg/body).

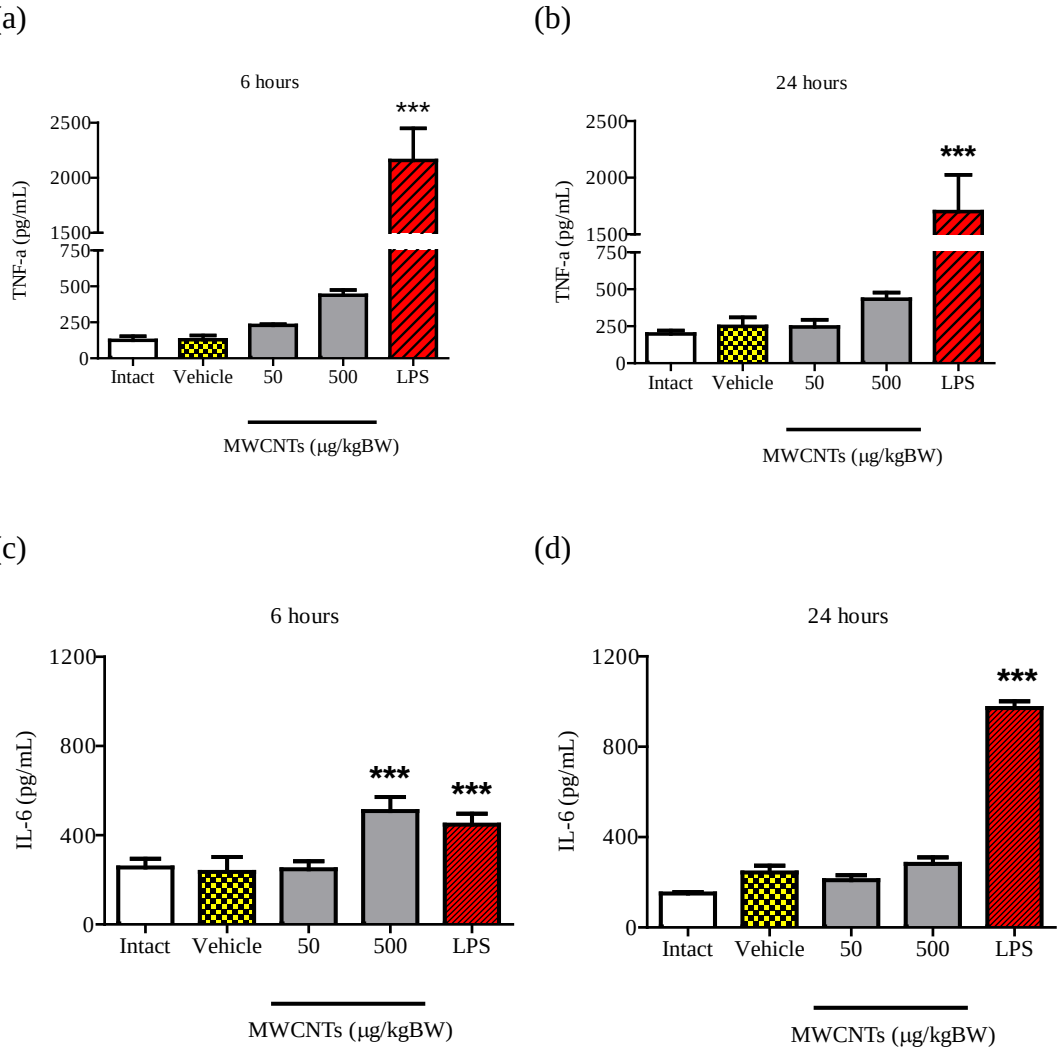

Figure 7.7 TNF-α (a,b) and IL-6 (c,d) productions in BAL fluids. ICR mice were administered through intranasal instillation with 1% FBS in 0.1% D-glucose (as a vehicle control), MWCNTs at concentrations 50 and 500 µg/kgBW and LPS 30 µg/mouse (as a positive control). Levels of TNF-α and IL-6 were measured in BAL fluids at 6 and 24 h post-instillation. *** Significantly different from a vehicle control group at $^{***}p < 0.05$ (n=4-8).

7.4 Discussion

The purpose of this chapter was to investigate the effect of two different types of nanomaterials in regard to their inflammatory responses in mice. TiO_2-NPs and MWCNTs with the same concentrations at 50 and 500 µg/kgBW were instilled in the lungs of mice via intranasal instillation; the inflammation was assessed at 6 and 24 h post exposure. The acute toxicity and inflammatory profiles of the two types of TiO_2-NPs and MWCNTs were almost similar. The expression of LDH levels was strongly induced at 6 h post-exposure. However, at 24 h post-exposure, the levels of LDH released in BAL fluids of mice treated with TiO_2-NPs and MWCNTs increased significantly only at the applied concentration of 500 µg/kgBW. The factors that induce the inflammatory response of the low solubility particles (such as TiO_2-NPs and MWCNTs) *in vivo* were explained by Roursgaard *et al*. (341). They found that the agglomeration state, the vehicle and the route of exposure were the most important factors affecting inflammation and toxicity of the NPs *in vivo*. They also suggested that the agglomerate size of NPs in vehicles might affect the clearance efficiency and deposition in the lungs. The reasons behind this phenomenon were also described: the hydrodynamic size and surface area of nanoparticles measured in solvent vehicles was different when measured in dry powder or in the aqueous state (such as dissolved in de-ionized water). When particles were suspended in vehicles, the agglomeration might have occurred from the interactions of particles and other components in the vehicle. When the concentrations of TiO_2-NPs were increased in the solvent vehicle, the agglomeration size also increased. If the sizes are in a range that is suitable for phagocytosis and de-agglomeration does not occur in the lungs, then the clearance mechanisms and the toxic responses of large particles (micro-sized particles) are different from those of small size particles (31, 341).

In this study, the effects of TiO_2-NPs and MWCNTs on inflammatory response induction *in vivo* were investigated. Inflammatory cytokines, such as IL-6 and TNF-α, that play a central role in host defense and are involved in a variety of chronic diseases when overexpressed *in vivo* (243, 244, 342) were measured. My *in vitro* study (in Chapter 5) showed that RAW 264.7 cells treated with different doses of TiO_2-NPs did not induce IL-6 production. Similarly, BAL fluids of treated mice had

no significant induction of IL-6 levels after treatment with TiO_2-NPs for 6 and 24 h. In contrast, several studies have reported that TiO_2-NPs are involved in IL-6 induction (159, 179, 343-345). The impact of NPs on mediating proinflammatory cytokine responses was discussed by Veranth *et al* (346). A high concentration of insoluble particles, especially nanosized particles, can interfere with ELISA measurements. Kobayashi *et al.* (180) studied the toxicity of TiO_2-NPs intratracheally instilled in rats. Their results indicated that the inflammatory effects of TiO_2-NPs depend on the size and agglomeration state of NPs after instillation. Similarly, with our results, at 6 and 24 h post-instillation, the signs of cytotoxicity found in BAL fluids (LDH levels) increased significantly in mice treated with 500 µg/ml TiO_2-NPs for 24 h without any effects on organ weights, and only a small increase of TNF-α was found. This implies that there is no clear relationship between the cytotoxic signals and organ weights of mice treated with TiO_2-NPs at different doses and exposure times.

The inflammatory response induced by inhaled MWCNTs is considered to have potential of lung fibrosis. In this study we have demonstrated that MWCNTs (24 h, 500 µg/kgBW) significantly induced LDH and total protein. At 6 h exposure with the same concentration, the effect is unclear. This may be due to the exposure time being too short for the particles to circulate into the lungs and the body. Han *et al*. (185) reported that an increase of inflammatory cytokines (TNF-α and IL-1β) in BAL fluids was found after 1 day of injecting 20 or 40 µg MWCNTs in 40 µl PBS into mice by oropharyngeal aspiration. Muller *et al*. (182) measured the contents of TNF-α in rat's lavage fluid after CNTs intratracheal instillation. Their results showed that TNF-α levels at 60 days after exposure decreased. It seems the exposure time is also a vital factor of inflammatory response of insoluble particles. The potential adverse health effects occurring after MWCNTs exposure were also reported by Wang *et al*. (338). Their results showed that the expressions of cytokine (IL-33), chemokine (CCL3 and CCL11) and protease production (MMP13) were high and promoted the inflammatory and fibrotic changes in the lungs.

In summary, the results of this study indicated that TiO_2-NPs and MWCNTs could induce cytotoxicity and inflammation *in vivo*. The summary of toxicity induced by TiO_2-NPs and MWCNTs in mice's lungs is shown in figure 7.8. However, their effects depend on the concentration and exposure time of these NPs.

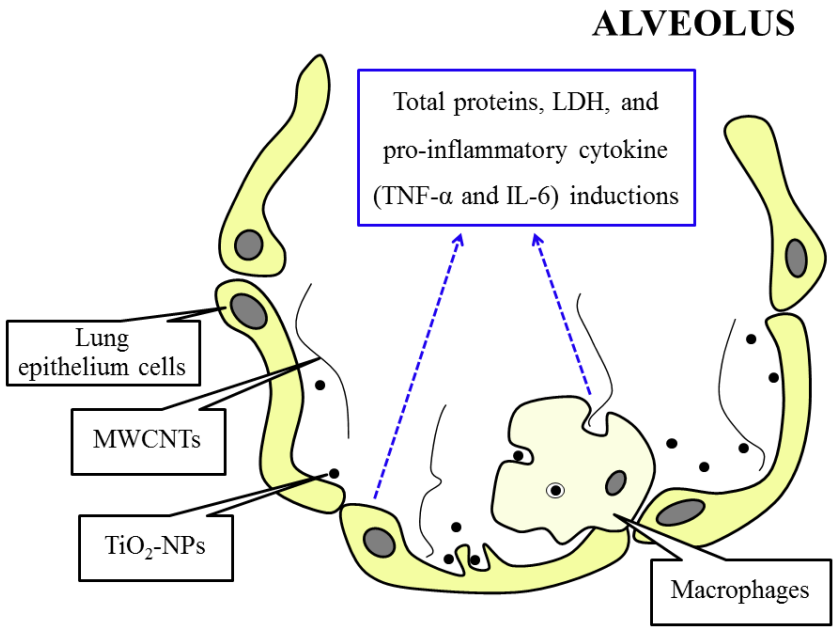

Figure 7.8 Illustration of TiO_2-NPs and MWCNTs induces inflammation and cytotoxicity in lung lining surface cells and lung macrophage cells. (Modified from Kocbach (347)).

CHAPTER VIII
CONCLUSIONS

The present study focused on the investigation of toxicity and inflammatory responses of NPs *in vitro* and *in vivo*. Two types of NPs, TiO_2-NPs and MWCNTs, were selected to have their toxicities investigated. Two different cell lines (RAW 264.7 murine macrophage cells and C6 rat glioma cells) were used in this thesis for *in vitro* study while mice were used for *in vivo* study.

After characterizations of TiO_2-NPs and MWCNTs, these particles were applied *in vitro* and *in vivo*. It was found that TiO_2-NPs at concentrations $\geq$ 25 μg/ml induced toxicity in RAW 264.7 and C6 cells. In RAW 264.7 cells, TiO_2-NPs had a potential to induce cell apoptosis as confirmed by the determination of DNA fragmentation and the measurement of phosphatidylserine (PS) translocation to the outer leaflet of the cell's plasma membrane. The mechanism of TiO_2-NP action on cytotoxicity in RAW 264.7 cells could be the oxidative stress mediated inflammatory response and subsequent cell death. The release of TNF-α found in cells might be associated with the induction of the COX-2 enzyme expression and the down-regulation of a central molecule in the Wnt signaling pathway.

In the case of C6 cells, the fragmentation of DNA was also found after cells were treated with TiO_2-NPs with the same concentrations as in RAW 264.7 cells. The results from the DNA fragmentation assay revealed that at high concentration ranges (250 to 500 μg/ml), TiO_2-NPs induced cell death. The increase of hypodiploid cells in the sub-G_0 population after staining cells with propidium iodide also supports that high concentration range of TiO_2-NPs is toxic to C6 cells. These results indicate that TiO_2-NPs at the size of 13.9 ± 1.8 nm and at the above concentrations could induce apoptosis cell death in C6 glioma cells. The down-regulation of β-catenin was also found in glioma cells treated with TiO_2-NPs. This implies that the down-regulation of β-catenin might be involved in the induction of cytotoxicity in C6 cells. With these results, there is a possibility of using TiO_2-NPs in brain cancer therapy. However,

more investigations on mechanism details and side effects of applying TiO_2-NPs in brain cancer therapy are needed in future studies.

The investigation of *in vivo* toxicity in mice showed that the intranasal instillation of TiO_2-NPs and MWCNTs negatively affected the health of mice. Generally, pulmonary edema and pulmonary cell damage can be indicated by elevation of total protein levels and LDH in mice's BAL fluid. This thesis demonstrates that mice treated with TiO_2-NPs and MWCNTs (for 24 h) at concentrations of 500 µg/kgBW could induce the release lactate dehydrogenase (LDH) in bronchoalveolar lavage fluid. The significant induction of LDH in mice treated with TiO_2-NPs and MWCNTs for 6 h at low concentrations but not at high ones might relate to the solubility of particles. Therefore, both concentration and exposure time have an impact on increasing LDH production. In the case of protein content, it seems that the concentrations of particles have a major effect on protein content induction. The induction of LDH and protein content in BAL fluid may lead to pulmonary diseases. There was no significant induction of proinflammatory cytokines (TNF-α and IL-6) in BAL fluid of mice treated with TiO_2-NPs. However, IL-6 in mice treated with MWCNTs (500 µg/kgBW) for 6 h was significantly increased. This implies that at the same concentration of particles MWCNTs can induce more adverse effects than TiO_2-NPs.

Overall, for the effects of TiO_2-NPs and MWCNTs in *in vivo* systems, the results in this thesis showed that at the same concentrations and conditions used for treating mice, MWCNTs cause more toxic effects than TiO_2-NPs do. The results can help users to consider the use of these two NPs as ingredients in daily life products. Since the NPs used in this thesis are low dispersing NPs, many researchers have tried to develop more suspended TiO_2-NPs and MWCNTs in media solution. In the future, the effect of the same type of NPs with different properties is worthy of further investigation.

REFERENCES

1. Sahoo SK, Parveen S, Panda JJ. The present and future of nanotechnology in human health care. *Nanomed-Nanotechnol*. 2007 Mar;3(1):20-31.
2. Buzea C, Blandino IIP, Robbie K. Nanomaterials and nanoparticles: sources and toxicity. *Biointerphases*. 2007;2(4):MR17 - MR172.
3. Ramesh P, Gurunathan K. Nanomaterials communication inside the living organism. *Nano communication networks 3*. [Review article]. 2012:252-6.
4. Nel A, Xia T, Madler L, Li N. Toxic potential of materials at the nanolevel. *Science*. 2006 Feb 3;311(5761):622-7.
5. Oberdörster G, Oberdörster E, Oberdörster J. Nanotoxicology: An Emerging Discipline Evolving from Studies of Ultrafine Particles. *Environmental Health Perspectives*. 2005;113(7):823-39.
6. Geiseler B, Miljevic M, ller P, Fruk L. Phototriggered Production of Reactive Oxygen Species by TIO2 Nanospheres and Rods. *Journal of Nanomaterials*. 2012;2012:9.
7. Gupta S, Tripathi M. A review of TiO2 nanoparticles. *Chin Sci Bull*. 2011 2011/06/01;56(16):1639-57.
8. Nohynek GJ, Dufour EK, Roberts MS. Nanotechnology, cosmetics and the skin: is there a health risk? *Skin Pharmacol Physiol*. [Review]. 2008;21(3):136-49.
9. Arora H, Doty C, Yuan Y, Boyle J, Petras K, Rabatic B, et al. *Nanomaterials for the Life Sciences. Weinheim*: WILEY-VCH Verlag GmbH & Co.; 2010. Available from: http://www.wiley-vch.de/books/sample/3527321683_c01.pdf.
10. Chibber S, Ansari S, Satar R. New vision to CuO, ZnO, and TiO2 nanoparticles: their outcome and effects. *Journal of Nanoparticle Research*. 2013 2013/03/26;15(4):1-13.

11. Schilling K, Bradford B, Castelli D, Dufour E, Nash JF, Pape W, et al. Human safety review of "nano" titanium dioxide and zinc oxide. *Photochem Photobiol Sci.* [Review]. 2010 Apr;9(4):495-509.
12. Firme CP, Bandaru PR. Toxicity issues in the application of carbon nanotubes to biological systems. *Nanomedicine: nanotechnology, biology, and medicine.* 2010;6(2):245-56.
13. Jain S, Singh SR, Pillai S. Toxicity Issues Related to Biomedical Applications of Carbon Nanotubes. *Nanomedicine & Nanotechnology*. [open access]. 2012;3(5).
14. Pacurari M, Castranova V, Vallyathan V. Single- and multi-wall carbon nanotubes versus asbestos: are the carbon nanotubes a new health risk to humans? *J Toxicol Environ Health A.* [Review]. 2010;73(5):378-95.
15. Borm PJ, Robbins D, Haubold S, Kuhlbusch T, Fissan H, Donaldson K, et al. The potential risks of nanomaterials: a review carried out for ECETOC. *Part Fibre Toxicol.* 2006;3:11.
16. Yang W, Peters JI, Williams RO. Inhaled nanoparticles—*A current review. International Journal of Pharmaceutics.* 2008;356:239-47.
17. Shi H, Magaye R, Castranova V, Zhao J. Titanium dioxide nanoparticles: a review of current toxicological data. *Part Fibre Toxicol*. [Research Support, Non-U.S. Gov't]. 2013;10:15.
18. Barillet S, Simon-Deckers A, Herlin-Boime N, Mayne-L'Hermite M, Reynaud C, Cassio D, et al. Toxicological consequences of TiO2, SiC nanoparticles and multi-walled carbon nanotubes exposure in several mammalian cell types: an in vitro study. *Journal of Nanoparticle Research*. 2010 2010/01/01;12(1):61-73.
19. Hussain S, Thomassen LC, Ferecatu I, Borot MC, Andreau K, Martens JA, et al. Carbon black and titanium dioxide nanoparticles elicit distinct apoptotic pathways in bronchial epithelial cells. *Part Fibre Toxicol*. [Research Support, Non-U.S. Gov't]. 2010;7:10.
20. Iavicoli I, Leso V, Fontana L, Bergamaschi A. Toxicological effects of titanium dioxide nanoparticles: a review of in vitro mammalian studies. *Eur Rev Med Pharmacol Sci.* [In Vitro Review]. 2011 May;15(5):481-508.

21. Jin C, Tang Y, Yang FG, Li XL, Xu S, Fan XY, et al. Cellular toxicity of TiO2 nanoparticles in anatase and rutile crystal phase. *Biol Trace Elem Res.* [Research Support, Non-U.S. Gov't]. 2011 Jun;141(1-3):3-15.
22. Park S, Lee YK, Jung M, Kim KH, Chung N, Ahn E-K, et al. Cellular Toxicity of Various Inhalable Metal Nanoparticles on Human Alveolar Epithelial Cells. *Inhalation Toxicology.* 2007;19(s1):59-65.
23. Migdal C, Rahal R, Rubod A, Callejon S, Colomb E, Atrux-Tallau N, et al. Internalisation of hybrid titanium dioxide/para-amino benzoic acid nanoparticles in human dendritic cells did not induce toxicity and changes in their functions. *Toxicol Lett.* 2010;199(1):34-42.
24. Stefanie W, Simon M, Peter B, Thomas S, Detlef B, Cornelia K. Cytotoxicity of titanium and silicon dioxide nanoparticles. *Journal of Physics: Conference Series.* 2009;170(1):012022.
25. Warheit DB, Hoke RA, Finlay C, Donner EM, Reed KL, Sayes CM. Development of a base set of toxicity tests using ultrafine TiO2 particles as a component of nanoparticle risk management. *Toxicol Lett.* [Research Support, Non-U.S. Gov't]. 2007 Jul 10;171(3):99-110.
26. Wilhelmi V, Fischer U, van Berlo D, Schulze-Osthoff K, Schins RP, Albrecht C. Evaluation of apoptosis induced by nanoparticles and fine particles in RAW 264.7 macrophages: facts and artefacts. *Toxicology in vitro : an international journal published in association with BIBRA.* [Research Support, Non-U.S. Gov't]. 2012 Mar;26(2):323-34.
27. Braydich-Stolle L, Schaeublin N, Murdock R, Jiang J, Biswas P, Schlager J, et al. Crystal structure mediates mode of cell death in TiO2 nanotoxicity. *Journal of Nanoparticle Research.* 2009 2009/08/01;11(6):1361-74.
28. Scherbart AM, Langer J, Bushmelev A, van Berlo D, Haberzettl P, van Schooten FJ, et al. Contrasting macrophage activation by fine and ultrafine titanium dioxide particles is associated with different uptake mechanisms. *Part Fibre Toxicol.* [Comparative Study Research Support, Non-U.S. Gov't]. 2011;8:31.
29. Singh S, Shi T, Duffin R, Albrecht C, van Berlo D, Höhr D, et al. Endocytosis, oxidative stress and IL-8 expression in human lung epithelial cells upon

treatment with fine and ultrafine TiO2: Role of the specific surface area and of surface methylation of the particles. *Toxicol Appl Pharmacol*. 2007;222(2):141-51.

30. Bhattacharya K, Davoren M, Boertz J, Schins R, Hoffmann E, Dopp E. Titanium dioxide nanoparticles induce oxidative stress and DNA-adduct formation but not DNA-breakage in human lung cells. *Part Fibre Toxicol.* 2009;6(1):17.
31. Shukla RK, Sharma V, Pandey AK, Singh S, Sultana S, Dhawan A. ROS-mediated genotoxicity induced by titanium dioxide nanoparticles in human epidermal cells. *Toxicology in vitro : an international journal published in association with BIBRA.* [Research Support, Non-U.S. Gov't]. 2011 Feb;25(1):231-41.
32. Shukla RK, Kumar A, Pandey AK, Singh SS, Dhawan A. Titanium Dioxide Nanoparticles Induce Oxidative Stress-Mediated Apoptosis in Human Keratinocyte Cells. *Journal of Biomedical Nanotechnology*. 2011;7:100-1.
33. Kang SJ, Kim BM, Lee YJ, Hong SH, Chung HW. Titanium dioxide nanoparticles induce apoptosis through the JNK/p38-caspase-8-Bid pathway in phytohemagglutinin-stimulated human lymphocytes. *Biochem Biophys Res Commun*. 2009 Sep 4;386(4):682-7.
34. Meena R, Rani M, Pal R, Rajamani P. Nano-TiO2-induced apoptosis by oxidative stress-mediated DNA damage and activation of p53 in human embryonic kidney cells. *Appl Biochem Biotechnol*. 2012 Jun;167(4):791-808.
35. Ramkumar KM, Manjula C, Gnanakumar G, Kanjwal MA, Sekar TV, Paulmurugan R, et al. Oxidative stress-mediated cytotoxicity and apoptosis induction by TiO2 nanofibers in HeLa cells. *Eur J Pharm Biopharm.* 2012 Jun;81(2):324-33.
36. Donaldson K, Murphy FA, Duffin R, Poland CA. Asbestos, carbon nanotubes and the pleural mesothelium: a review of the hypothesis regarding the role of long fibre retention in the parietal pleura, inflammation and mesothelioma. *Part Fibre Toxicol.* [Research Support, Non-U.S. Gov't Review]. 2010;7:5.

37. Shvedova AA, Pietroiusti A, Fadeel B, Kagan VE. Mechanisms of carbon nanotube-induced toxicity: focus on oxidative stress. *Toxicol Appl Pharmacol*. [Review]. 2012 Jun 1;261(2):121-33.
38. Dang PM-C, Stensballe A, Boussetta T, Raad H, Dewas C, Kroviarski Y, et al. A specific p47phox -serine phosphorylated by convergent MAPKs mediates neutrophil NADPH oxidase priming at inflammatory sites. *The Journal of Clinical Investigation*. 2006;116(7):2033-43.
39. Kampfer H, Kolb N, Manderscheid M, Wetzler C, Pfeilschifter J, Frank S. Macrophage-derived heme-oxygenase-1: expression, regulation, and possible functions in skin repair. *Mol Med.* [Research Support, Non-U.S. Gov't]. 2001 Jul;7(7):488-98.
40. Lefkowitz DL, Mills K, Castro A, Lefkowitz SS. Induction of tumor necrosis factor and macrophage-mediated cytotoxicity by horseradish peroxidase and other glycosylated proteins: the role of enzymatic activity and LPS. *Journal of leukocyte biology.* 1991 December 1, 1991;50(6):615-23.
41. McMillen TS, Heinecke JW, LeBoeuf RC. Expression of Human Myeloperoxidase by Macrophages Promotes Atherosclerosis in Mice. *Circulation.* 2005 May 31, 2005;111(21):2798-804.
42. Zhu H, Jia Z, Zhang L, Yamamoto M, Misra HP, Trush MA, et al. Antioxidants and phase 2 enzymes in macrophages: regulation by Nrf2 signaling and protection against oxidative and electrophilic stress. *Experimental biology and medicine.* [Research Support, N.I.H., Extramural Research Support, Non-U.S. Gov't]. 2008 Apr;233(4):463-74.
43. Sargent LM, Shvedova AA, Hubbs AF, Salisbury JL, Benkovic SA, Kashon ML, et al. Induction of aneuploidy by single-walled carbon nanotubes. *Environ Mol Mutagen.* [Research Support, Non-U.S. Gov't Research Support, U.S. Gov't, P.H.S.]. 2009 Oct;50(8):708-17.
44. Srivastava RK, Pant AB, Kashyap MP, Kumar V, Lohani M, Jonas L, et al. Multi-walled carbon nanotubes induce oxidative stress and apoptosis in human lung cancer cell line-A549. *Nanotoxicology.* [Research Support, Non-U.S. Gov't]. 2011 Jun;5(2):195-207.

45. Zhu L, Schrand AM, Voevodin AA, Chang DW, Dai L, Hussain SM. Assessment of Human Lung Macrophages After Exposure to Multi-Walled Carbon Nanotubes Part II. DNA Damage. *Nanoscience and Nanotechnology Letters.* 2011;3(1):94-8.
46. Lundborg M, Johard U, Lastbom L, Gerde P, Camner P. Human alveolar macrophage phagocytic function is impaired by aggregates of ultrafine carbon particles. *Environ Res.* 2001 Jul;86(3):244-53.
47. Warheit DB, Hartsky MA. Role of alveolar macrophage chemotaxis and phagocytosis in pulmonary clearance responses to inhaled particles: Comparisons among rodent species. *Microscopy Research and Technique*. 1993;26(5):412-22.
48. Warheit DB, Carakostas MC, Bamberger JR, Hartsky MA. Complement facilitates macrophage phagocytosis of inhaled iron particles but has little effect in mediating silica-induced lung inflammatory and clearance responses. *Environ Res.* [Research Support, Non-U.S. Gov't]. 1991 Dec;56(2):186-203.
49. Byrne JD, Baugh JA. *The significance of nanoparticles in particle-induced pulmonary fibrosis.* Mcgill J Med. 2008 Jan;11(1):43-50.
50. Bailey K. Physiological factors affecting drug toxicity. *Regul Toxicol Pharmacol*. 1983 Dec;3(4):389-98.
51. Khlebtsov N, Dykman L. Biodistribution and toxicity of engineered gold nanoparticles: a review of in vitro and in vivo studies. *Chem Soc Rev.* [Research Support, Non-U.S. Gov't Review]. 2011 Mar;40(3):1647-71.
52. Klaassen CD. Casarett & Doull's Toxicology: *The Basic Science of Poisons,* Seventh Edition: McGraw-Hill Education; 2007.
53. Lai JC, Lai MB, Jandhyam S, Dukhande VV, Bhushan A, Daniels CK, et al. Exposure to titanium dioxide and other metallic oxide nanoparticles induces cytotoxicity on human neural cells and fibroblasts. *International Journal of Nanomedicine*. 2008;3(4):533-45.
54. Paino IM, Marangoni VS, de Oliveira Rde C, Antunes LM, Zucolotto V. Cyto and genotoxicity of gold nanoparticles in human hepatocellular carcinoma and

peripheral blood mononuclear cells. *Toxicol Lett.* [Research Support, Non-U.S. Gov't]. 2012 Nov 30;215(2):119-25.

55. Andersson-Willman B, Gehrmann U, Cansu Z, Buerki-Thurnherr T, Krug HF, Gabrielsson S, et al. Effects of subtoxic concentrations of TiO2 and ZnO nanoparticles on human lymphocytes, dendritic cells and exosome production. *Toxicol Appl Pharmacol.* 2012;264(1):94-103.
56. Chen B, Liu Y, Song WM, Hayashi Y, Ding XC, Li WH. In vitro evaluation of cytotoxicity and oxidative stress induced by multiwalled carbon nanotubes in murine RAW 264.7 macrophages and human A549 lung cells. *Biomed Environ Sci.* [Research Support, Non-U.S. Gov't]. 2011 Dec;24(6):593-601.
57. Lewinski N, Colvin V, Drezek R. Cytotoxicity of nanoparticles. *Small.* [Research Support, Non-U.S. Gov't Research Support, U.S. Gov't, Non-P.H.S. Review]. 2008 Jan;4(1):26-49.
58. Bourdeau P. *Short-term toxicity tests for non-genotoxic effects.* Wiley; 1990.
59. Ganong WF. *Review of Medical Physiology:* McGraw Hill; 2001.
60. Abbott NJ, Patabendige AAK, Dolman DEM, Yusof SR, Begley DJ. Structure and function of the blood–brain barrier. *Neurobiology of Disease.* 2010;37(1):13-25.
61. Chen Y, Liu L. Modern methods for delivery of drugs across the blood-brain barrier. *Adv Drug Deliv Rev.* [Research Support, Non-U.S. Gov't Review]. 2012 May 15;64(7):640-65.
62. Banks WA. Drug delivery to the brain in Alzheimer's disease: Consideration of the blood–brain barrier. *Adv Drug Deliv Rev.* 2012;64(7):629-39.
63. Buckner JC, Brown PD, O'Neill BP, Meyer FB, Wetmore CJ, Uhm JH. Central Nervous System Tumors. *Mayo Clinic Proceedings.* 2007;82(10):1271-86.
64. Wong HL, Wu XY, Bendayan R. Nanotechnological advances for the delivery of CNS therapeutics. *Adv Drug Deliv Rev.* [Review]. 2012 May 15;64(7):686-700.
65. Gabathuler R. Approaches to transport therapeutic drugs across the blood–brain barrier to treat brain diseases. *Neurobiology of Disease.* 2010;37(1):48-57.

66. Han YG, Xu J, Li ZG, Ren GG, Yang Z. In vitro toxicity of multi-walled carbon nanotubes in C6 rat glioma cells. *Neurotoxicology.* [Research Support, Non-U.S. Gov't]. 2012 Oct;33(5):1128-34.
67. Lockman PR, Koziara JM, Mumper RJ, Allen DD. Nanoparticle surface charges alter blood-brain barrier integrity and permeability. *J Drug Target.* 2004 Oct-Dec;12(9-10):635-41.
68. Ma LL, Liu J, Li N, Wang J, Duan YM, Yan JY, et al. Oxidative stress in the brain of mice caused by translocated nanoparticulate TiO2 delivered to the abdominal cavity. *Biomaterials.* 2010 Jan;31(1):99-105.
69. Mistry A, Stolnik S, Illum L. Nanoparticles for direct nose-to-brain delivery of drugs. *International Journal of Pharmaceutics.* 2009 Sep 8;379(1):146-57.
70. Oberdörster G, Sharp Z, Atudorei V, Elder A, Gelein R, Kreyling W, et al. Translocation of Inhaled Ultrafine Particles to the Brain. *Inhalation Toxicology.* 2004;16(6-7):437-45.
71. Wang J, Chen C, Liu Y, Jiao F, Li W, Lao F, et al. Potential neurological lesion after nasal instillation of TiO(2) nanoparticles in the anatase and rutile crystal phases. *Toxicol Lett.* [Research Support, Non-U.S. Gov't]. 2008 Dec 15;183(1-3):72-80.
72. Hu R, Zheng L, Zhang T, Gao G, Cui Y, Cheng Z, et al. Molecular mechanism of hippocampal apoptosis of mice following exposure to titanium dioxide nanoparticles. *J Hazard Mater.* 2011;191(1–3):32-40.
73. Ze Y, Zheng L, Zhao X, Gui S, Sang X, Su J, et al. Molecular mechanism of titanium dioxide nanoparticles-induced oxidative injury in the brain of mice. *Chemosphere.* [Research Support, Non-U.S. Gov't]. 2013 Aug;92(9):1183-9.
74. Wu J, Wang C, Sun J, Xue Y. Neurotoxicity of Silica Nanoparticles: Brain Localization and Dopaminergic Neurons Damage Pathways. *ACS Nano.* 2011 2011/06/28;5(6):4476-89.
75. Shilo M, Motiei M, Hana P, Popovtzer R. Transport of nanoparticles through the blood-brain barrier for imaging and therapeutic applications. *Nanoscale.* [10.1039/C3NR04878K]. 2014;6(4):2146-52.

76. Facchino S, Abdouh M, Bernier G. Brain cancer stem cells: current status on glioblastoma multiforme. *Cancers (Basel).* 2011;3(2):1777-97.
77. Barth RF, Kaur B. Rat brain tumor models in experimental neuro-oncology: the C6, 9L, T9, RG2, F98, BT4C, RT-2 and CNS-1 gliomas. *J Neurooncol.* [Review]. 2009 Sep;94(3):299-312.
78. Doblas S, Saunders D, Kshirsagar P, Pye Q, Oblander J, Gordon B, et al. Phenyl-tert-butylnitrone induces tumor regression and decreases angiogenesis in a C6 rat glioma model. *Free Radical Biology and Medicine.* 2008;44(1):63-72.
79. Solly F, Fish R, Simard B, Bolle N, Kruithof E, Polack B, et al. Tissue-type plasminogen activator has antiangiogenic properties without effect on tumor growth in a rat C6 glioma model. *Cancer Gene Ther.* 2008;15(10):685-92.
80. Ahmed AE, Jacob S, Nagy AA, Abdel-Naim AB. Dibromoacetonitrile-induced protein oxidation and inhibition of proteasomal activity in rat glioma cells. *Toxicol Lett.* 2008;179(1):29-33.
81. Sheehan J, Ionescu A, Pouratian N, Hamilton DK, Schlesinger D, Oskouian RJ, et al. Use of trans sodium crocetinate for sensitizing glioblastoma multiforme to radiation. *J Neurosurg.* 2008;108(5):972-8.
82. Tanriover N, Ulu MO, Sanus GZ, Bilir A, Canbeyli R, Oz B, et al. The effects of systemic and intratumoral interleukin-12 treatment in C6 rat glioma model. *Neurological Research.* 2008;30(5):511-7.
83. López T, Recillas S, Guevara P, Sotelo J, Alvarez M, Odriozola JA. Pt/TiO2 brain biocompatible nanoparticles: GBM treatment using the C6 model in Wistar rats. *Acta Biomaterialia.* 2008;4(6):2037-44.
84. Gordon S. The role of the macrophage in immune regulation. *Res Immunol.* [Review]. 1998 Sep-Oct;149(7-8):685-8.
85. Hartley JW, Evans LH, Green KY, Naghashfar Z, Macias AR, Zerfas PM, et al. Expression of infectious murine leukemia viruses by RAW264.7 cells, a potential complication for studies with a widely used mouse macrophage cell line. *Retrovirology.* [Research Support, N.I.H., Intramural]. 2008;5:1.

86. Dowling A, Clift R, Grobert N, Hutton D, Oliver R, O'neill O, et al. Nanoscience and nanotechnologies: opportunities and uncertainties. *London: The Royal Society and the Royal Academy of Engineering;* 2004. Available from: http://www.nanotec.org.uk/report/Nano%20report%202004%20fin.pdf http://www.nanotec.org.uk/finalReport.htm.
87. Oberdörster G, Maynard A, Donaldson K, Castranova V, Fitzpatrick J, Ausman K, et al. Principles for characterizing the potential human health effects from exposure to nanomaterials: elements of a screening strategy. *Part Fibre Toxicol.* 2005 Oct 6;2:8.
88. Walter D. *Primary Particles – Agglomerates – Aggregates. Nanomaterials:* Wiley-VCH Verlag GmbH & Co. KGaA; 2013. p. 9-24.
89. EU. Commission Recommendation of 18 October 2011 on the definition of nanomaterial Text with EEA relevance In: Commission E, editor. Official *Journal of the European Union.* 20 October 2011 ed2011. p. 38-40.
90. Osada M, Sasaki T. Two-dimensional dielectric nanosheets: novel nanoelectronics from nanocrystal building blocks. *Advanced Materials.* [Research Support, Non-U.S. Gov't Review]. 2012 Jan 10;24(2):210-28.
91. Tiwari JN, Tiwari RN, Kim KS. Zero-dimensional, one-dimensional, two-dimensional and three-dimensional nanostructured materials for advanced electrochemical energy devices. *Progress in Materials Science.* 2012;57(4):724-803.
92. Schodek DL, Ferreira P, Ashby MF. Nanomaterials, Nanotechnologies and Design: An Introduction for Engineers and Architects: *Elsevier Science;* 2009.
93. Yilmaz C, Cetin AE, Goutzamanidis G, Huang J, Somu S, Altug H, et al. Three-dimensional crystalline and homogeneous metallic nanostructures using directed assembly of nanoparticles. *ACS Nano.* [Research Support, Non-U.S. Gov't Research Support, U.S. Gov't, Non-P.H.S.]. 2014 May 27;8(5):4547-58.
94. Nichols G, Byard S, Bloxham MJ, Botterill J, Dawson NJ, Dennis A, et al. A review of the terms agglomerate and aggregate with a recommendation for

nomenclature used in powder and particle characterization. *Journal of Pharmaceutical Sciences.* 2002;91(10):2103-9.

95. Berube D, Cummings C, Cacciatore M, Scheufele D, Kalin J. Characteristics and classification of nanoparticles: expert Delphi survey. *Nanotoxicology.* [Research Support, U.S. Gov't, Non-P.H.S.]. 2011 Jun;5(2):236-43.
96. Diebold U. The surface science of titanium dioxide. *Surface Science Reports.* 2003;48(5–8):53-229.
97. Zhao L, Chang J, Zhai W. Effect of crystallographic phases of TiO2 on hepatocyte attachment, proliferation and morphology. *J Biomater Appl.* [Comparative Study Evaluation Studies Research Support, Non-U.S. Gov't Research Support, U.S. Gov't, Non-P.H.S.]. 2005 Jan;19(3):237-52.
98. EPA US. State of the science literature review: nano titanium dioxide environmental matters. Washington, DC: U.S. Environmental Protection Agency, Division ES;2010 August 2010.
99. Rossi EM, Pylkkanen L, Koivisto AJ, Vippola M, Jensen KA, Miettinen M, et al. Airway exposure to silica-coated TiO2 nanoparticles induces pulmonary neutrophilia in mice. *Toxicol Sci.* [Research Support, Non-U.S. Gov't]. 2010 Feb;113(2):422-33.
100. Zhai HJ, Wang LS. Probing the electronic structure and band gap evolution of titanium oxide clusters (TiO2)(n)(-) (n=1-10) using photoelectron spectroscopy. *Journal of the American Chemical Society.* 2007 Mar 14;129(10):3022-6.
101. Zhang J, Zhou P, Liu J, Yu J. New understanding of the difference of photocatalytic activity among anatase, rutile and brookite TiO2. *Physical Chemistry Chemical Physics.* [10.1039/C4CP02201G]. 2014;16(38):20382-6.
102. Mantena KV. *Electrical and mechanial properties of MWCNT filled conductive adhesives on lead free surface finished PCB's*. Lexington: University of Kentucky; 2009.
103. Pal SL, Jana U, Manna PK, Mohanta GP, Manavalan R. Nanoparticle: An overview of preparation and characterization. *Journal of applied pharmaceutical science.* 2011;1(6):228-34.

104. Loeffler J, Hedderich R, Malsch I, Koskinen J, Linder M, Lojkowski W, et al. Overview on promising nanomaterials for industrial applications. In: Loeffler J, editor. Nanomaterial roadmap 20152005.

105. Lacerda L, Bianco A, Prato M, Kostarelos K. Carbon nanotubes as nanomedicines: from toxicology to pharmacology. *Adv Drug Deliv Rev*. [Research Support, Non-U.S. Gov't Review]. 2006 Dec 1;58(14):1460-70.

106. Vardharajula S, Ali SZ, Tiwari PM, Eroglu E, Vig K, Dennis VA, et al. Functionalized carbon nanotubes: biomedical applications. *International journal of nanomedicine.* [Research Support, U.S. Gov't, Non-P.H.S. Review]. 2012;7:5361-74.

107. Azeredo HMCd. Nanocomposites for food packaging applications. *Food Research International.* 2009;42(9):1240-53.

108. Dai H. Carbon nanotubes: synthesis, integration, and properties. *Acc Chem Res.* 2002 Dec;35(12):1035-44.

109. Kreupl F, Graham AP, Liebau M, Duesberg GS, Seidel R, Unger E, editors. Carbon nanotubes for interconnect applications. *Electron Devices Meeting,* 2004 IEDM Technical Digest IEEE International; 2004 13-15 Dec. 2004.

110. Dresselhaus MS, Dresselhaus G, Charlier JC, Hernandez E. Electronic, thermal and mechanical properties of carbon nanotubes. *Philos Trans A Math Phys Eng Sci*. [Research Support, Non-U.S. Gov't Research Support, U.S. Gov't, Non-P.H.S. Review]. 2004 Oct 15;362(1823):2065-98.

111. Benda P, Lightbody J, Sato G, Levine L, Sweet W. Differentiated rat glial cell strain in tissue culture. *Science.* [In Vitro]. 1968 Jul 26;161(3839):370-1.

112. Intertek. Energy Dispersive X-Ray Analysis (EDX). 2014 [cited 2014 2 April 2014]; Available from: http://www.intertek.com/analysis/microscopy/edx/.

113. Samberg M. Biological Interactions of Silver Nanoparticles. Raleigh, North Carolina: North Carolina State University; 2012.

114. Oberdorster G. Safety assessment for nanotechnology and nanomedicine: concepts of nanotoxicology. *J Intern Med.* [Research Support, N.I.H., Extramural Research Support, U.S. Gov't, Non-P.H.S.]. 2010 Jan;267(1):89-105.

115. Fischer HC, Chan WC. Nanotoxicity: the growing need for in vivo study. *Curr Opin Biotechnol.* [Research Support, Non-U.S. Gov't Review]. 2007 Dec;18(6):565-71.

116. Donaldson K, Stone V, Tran CL, Kreyling W, Borm PJ. Nanotoxicology. *Occup Environ Med.* [Editorial]. 2004 Sep;61(9):727-8.

117. Medina C, Santos-Martinez MJ, Radomski A, Corrigan OI, Radomski MW. Nanoparticles: pharmacological and toxicological significance. *British Journal of Pharmacology.* 2007;150:552-8.

118. Singh N, Manshian B, Jenkins GJ, Griffiths SM, Williams PM, Maffeis TG, et al. NanoGenotoxicology: the DNA damaging potential of engineered nanomaterials. *Biomaterials.* [Research Support, Non-U.S. Gov't Review]. 2009 Aug;30(23-24):3891-914.

119. Maynard AD, Warheit DB, Philbert MA. The new toxicology of sophisticated materials: nanotoxicology and beyond. *Toxicol Sci.* [Research Support, N.I.H., Extramural Research Support, Non-U.S. Gov't Review]. 2011 Mar;120 Suppl 1:S109-29.

120. Trouiller B, Reliene R, Westbrook A, Solaimani P, Schiestl RH. Titanium Dioxide Nanoparticles Induce DNA Damage and genetic instability in vivo in mice. *Cancer Research.* 2009 15 november 2009;69(22):8784-9.

121. Boelsterli UA. *Mechanistic Toxicology: The Molecular Basis of How Chemicals Disrupt Biological Targets:* Taylor & Francis; 2002.

122. Stahl W, Sies H. Oxidative stress. Institut für Biochemie und Molekularbiologie I, Heinrich-Heine-Universität Düsseldorf; 2010 [cited 2011 8 May]; Available from: http://www.uniklinik-duesseldorf.de/img/ejbfile/Homepage-ros-10-11-16.pdf?id=20038.

123. Thannickal VJ, Fanburg BL. Reactive oxygen species in cell signaling. Am J *Physiol Lung Cell Mol Physiol.* [Research Support, U.S. Gov't, P.H.S. Review]. 2000 Dec;279(6):L1005-28.

124. Allen RG, Tresini M. Oxidative stress and gene regulation. *Free Radic Biol Med.* 2000;28(3):463-99.

125. Voeikov VL. Reactive oxygen species (ROS) pathogens or sources of vital energy? Part 1. ROS in normal and pathologic physiology of living systems. *J Altern Complement Med.* [Review]. 2006 Mar;12(2):111-8.

126. Ray PD, Huang BW, Tsuji Y. Reactive oxygen species (ROS) homeostasis and redox regulation in cellular signaling. *Cell Signal.* [Research Support, N.I.H., Extramural Review]. 2012 May;24(5):981-90.

127. Voeikov VL. Reactive oxygen species (ROS): pathogens or sources of vital energy? Part 2. Bioenergetic and bioinformational functions of ROS. *J Altern Complement Med.* [Review]. 2006 Apr;12(3):265-70.

128. Porter DW, Leonard SS, Castranova V. Particles and Cellular Oxidative and Nitrosative stress. In: Donaldson K, Borm P, editors. *Particle Toxicology:* CRC Press; 2006. p. 119-38.

129. Orient A, Donko A, Szabo A, Leto TL, Geiszt M. Novel sources of reactive oxygen species in the human body. *Nephrol Dial Transplant.* [Editorial Research Support, Non-U.S. Gov't Review]. 2007 May;22(5):1281-8.

130. Porter DW, Leonard SS, Castranova V. Particles and cellular oxidative and nitrosative stress. In: Donaldson K, Borm P, editors. *Particle toxicology.* Boca Raton: CRC Press/Taylor & Francis Group; 2007. p. 434.

131. Heck DE, Vetrano AM, Mariano TM, Laskin JD. UVB Light Stimulates Production of Reactive Oxygen Species: UNEXPECTED ROLE FOR CATALASE. *Journal of Biological Chemistry.* 2003 June 20, 2003;278(25):22432-6.

132. Castello PR, Drechsel DA, Patel M. Mitochondria Are a Major Source of Paraquat-induced Reactive Oxygen Species Production in the Brain. *Journal of Biological Chemistry.* 2007 May 11, 2007;282(19):14186-93.

133. Ali S, Jain SK, Abdulla M, Athar M. Paraquat induced DNA damage by reactive oxygen species. *Biochem Mol Biol Int.* [Research Support, Non-U.S. Gov't]. 1996 May;39(1):63-7.

134. Chung MY, Lazaro RA, Lim D, Jackson J, Lyon J, Rendulic D, et al. Aerosol-Borne Quinones and Reactive Oxygen Species Generation by Particulate Matter Extracts. *Environmental Science & Technology.* 2006 2006/08/01;40(16):4880-6.

135. Shen HM, Zhang Z, Zhang QF, Ong CN. Reactive oxygen species and caspase activation mediate silica-induced apoptosis in alveolar macrophages. *Am J Physiol Lung Cell Mol Physiol.* [Research Support, Non-U.S. Gov't]. 2001 Jan;280(1):L10-7.

136. Lin W, Huang YW, Zhou XD, Ma Y. In vitro toxicity of silica nanoparticles in human lung cancer cells. *Toxicol Appl Pharmacol.* 2006 Dec 15;217(3):252-9.

137. Donaldson K, Borm P. *Particle Toxicology:* Taylor & Francis; 2006.

138. Geiser M, Kreyling W. Deposition and biokinetics of inhaled nanoparticles. *Part Fibre Toxicol.* 2010;7(1):2.

139. Maynard AD, Aitken RJ. Assessing exposure to airborne nanomaterials: Current abilities and future requirements. *Nanotoxicology.* 2007;1(1):26-41.

140. Bystrzejewska-Piotrowska G, Golimowski J, Urban PL. Nanoparticles: their potential toxicity, waste and environmental management. *Waste Manag.* [Research Support, Non-U.S. Gov't Review]. 2009 Sep;29(9):2587-95.

141. Hoet P, Boczkowski J. What's new in Nanotoxicology? Brief review of the 2007 literature. *Nanotoxicology.* 2008;2(3):171-82.

142. Long TC, Tajuba J, Sama P, Saleh N, Swartz C, Parker J, et al. Nanosize titanium dioxide stimulates reactive oxygen species in brain microglia and damages neurons in vitro. *Environmental Health Perspectives.* 2007 Nov;115(11):1631-7.

143. Yamakoshi Y, Umezawa N, Ryu A, Arakane K, Miyata N, Goda Y, et al. Active oxygen species generated from photoexcited fullerene (C60) as potential medicines: O_2^{-}* versus $^1O_2$. *Journal of the American Chemical Society.* 2003 Oct 22, 2003;125(42):12803-9.

144. Suh WH, Suslick KS, Stucky GD, Suh YH. Nanotechnology, nanotoxicology, and neuroscience. *Prog Neurobiol.* [Research Support, N.I.H., Extramural Research Support, Non-U.S. Gov't Research Support, U.S. Gov't, Non-P.H.S. Review]. 2009 Feb;87(3):133-70.

145. Manke A, Wang L, Rojanasakul Y. Mechanisms of nanoparticle-induced oxidative stress and toxicity. *Biomed Res Int.* [Research Support, N.I.H.,

Extramural Research Support, U.S. Gov't, Non-P.H.S.]. 2013;2013:942916.

146. Aydın A, Sipahi H, Charehsaz M. Nanoparticles Toxicity and Their Routes of Exposures2012.

147. Pujalte I, Passagne I, Brouillaud B, Treguer M, Durand E, Ohayon-Courtes C, et al. Cytotoxicity and oxidative stress induced by different metallic nanoparticles on human kidney cells. *Part Fibre Toxicol.* [Research Support, Non-U.S. Gov't]. 2011;8:10.

148. Yang H, Liu C, Yang D, Zhang H, Xi Z. Comparative study of cytotoxicity, oxidative stress and genotoxicity induced by four typical nanomaterials: the role of particle size, shape and composition. *J Appl Toxicol.* [Comparative Study Research Support, Non-U.S. Gov't]. 2009 Jan;29(1):69-78.

149. De Berardis B, Civitelli G, Condello M, Lista P, Pozzi R, Arancia G, et al. Exposure to ZnO nanoparticles induces oxidative stress and cytotoxicity in human colon carcinoma cells. *Toxicol Appl Pharmacol.* 2010 Apr 29.

150. Yah CS, Simate GS, Iyuke SE. Nanoparticles toxicity and their routes of exposures. *Pak J Pharm Sci.* 2012;25(2):477-91.

151. Li JJe, Muralikrishnan S, Ng C-T, Yung L-YL, Bay B-H. Nanoparticle-induced pulmonary toxicity. *Experimental Biology and Medicine.* 2010 September 1, 2010;235(9):1025-33.

152. Park EJ, Park K. Oxidative stress and pro-inflammatory responses induced by silica nanoparticles in vivo and in vitro. *Toxicol Lett.* [In Vitro]. 2009 Jan 10;184(1):18-25.

153. Park EJ, Yi J, Chung KH, Ryu DY, Choi J, Park K. Oxidative stress and apoptosis induced by titanium dioxide nanoparticles in cultured BEAS-2B cells. *Toxicol Lett.* [Research Support, Non-U.S. Gov't]. 2008 Aug 28;180(3):222-9.

154. Shukla RK, Kumar A, Gurbani D, Pandey AK, Singh S, Dhawan A. TiO2 nanoparticles induce oxidative DNA damage and apoptosis in human liver cells. *Nanotoxicology.* 2013;7(1):48-60.

155. Sheng L, Ze Y, Wang L, Yu X, Hong J, Zhao X, et al. Mechanisms of TiO2 nanoparticle-induced neuronal apoptosis in rat primary cultured hippocampal neurons. *Journal of Biomedical Materials Research Part A.* 2014:n/a-n/a.

156. Liu K, Lin X, Zhao J. Toxic effects of the interaction of titanium dioxide nanoparticles with chemicals or physical factors. *International Journal of Nanomedicine.* [Research Support, Non-U.S. Gov't Review]. 2013;8:2509-20.

157. Xiong S, Tang Y, Ng HS, Zhao X, Jiang Z, Chen Z, et al. Specific surface area of titanium dioxide (TiO2) particles influences cyto- and photo-toxicity. *Toxicology.* [Comparative Study Research Support, Non-U.S. Gov't]. 2013 Feb 8;304:132-40.

158. Jin C-Y, Zhu B-S, Wang X-F, Lu Q-H. Cytotoxicity of Titanium Dioxide Nanoparticles in Mouse Fibroblast Cells. *Chemical research in toxicology.* 2008 2008/09/15;21(9):1871-7.

159. Nishanth R, Jyotsna R, Schlager J, Hussain S, P. R. Inflammatory responses of RAW 264.7 macrophages upon exposure to nanoparticles: Role of ROS-NFκB signaling pathway. *Nanotoxicology.* 2011 2011 Mar 21.

160. Stone V, Barlow P, GR. H, DM. B. Proinflammatory effects of particles on macrophages and epithelial cells. In: Donaldson K, Borm P, editors. *Particle toxicology.* Boca Raton: CRC press; 2007. p. 183-96.

161. Roursgaard M. *Inflammatory effects of nanoparticles in lungs of mice. Copenhagen:* University of Copenhagen; 2009.

162. Gilmour MI, Steven T, Saxena RK. Effect of particles on the immune system. In: Donaldson K, Borm P, editors. *Particle toxicology.* Boca Raton: CRC Press; 2007. p. 245-57.

163. Cui Y, Liu H, Zhou M, Duan Y, Li N, Gong X, et al. Signaling pathway of inflammatory responses in the mouse liver caused by TiO2 nanoparticles. *J Biomed Mater Res A.* [Research Support, Non-U.S. Gov't]. 2011 Jan;96(1):221-9.

164. Stevenson R, Hueber AJ, Hutton A, McInnes IB, Graham D. Nanoparticles and inflammation. *ScientificWorldJournal.* [Review]. 2011;11:1300-12.

165. Park MV, Neigh AM, Vermeulen JP, de la Fonteyne LJ, Verharen HW, Briede JJ, et al. The effect of particle size on the cytotoxicity, inflammation, developmental toxicity and genotoxicity of silver nanoparticles. *Biomaterials.* 2011 Dec;32(36):9810-7.

166. Choi J, Zhang Q, Reipa V, Wang NS, Stratmeyer ME, Hitchins VM, et al. Comparison of cytotoxic and inflammatory responses of photoluminescent silicon nanoparticles with silicon micron-sized particles in RAW 264.7 macrophages. *Journal of Applied Toxicology.* 2009;29(1):52-60.

167. Kim SB, Tao H. Nanoscale Titanium Dioxide Particles Modulate Signaling Cascades for Tumor Necrosis Factor-α Release from Macrophages. *Journal of Health Science.* 2011;57(2):177-83.

168. Ricciotti E, FitzGerald GA. Prostaglandins and inflammation. *Arterioscler Thromb Vasc Biol.* [Research Support, N.I.H., Extramural Review]. 2011 May;31(5):986-1000.

169. Grosch S, Maier TJ, Schiffmann S, Geisslinger G. Cyclooxygenase-2 (COX-2)-independent anticarcinogenic effects of selective COX-2 inhibitors. *J Natl Cancer Inst.* [Research Support, Non-U.S. Gov't Review]. 2006 Jun 7;98(11):736-47.

170. Li M, Deng H, Zhao J, Dai D, Tan X. PPARg pathway activation results in apoptosis and COX-2 inhibition in HepG2 cells. *World Journal of Gastroenterology.* 2003;9(6):1220-6.

171. Bartels AL, Leendersand KL. Cyclooxygenase and neuroinflammation in Parkinson's disease neurodegeneration. *Current Neuropharmacology.* 2010;8:62-8.

172. Tsatsanis C, Androulidaki A, Venihaki M, Margioris AN. Signalling networks regulating cyclooxygenase-2. *Int J Biochem Cell Biol.* [Review]. 2006;38(10):1654-61.

173. Telliez A, Furman C, Pommery N, Hénichart J. Mechanisms Leading to COX-2 Expression and COX-2 Induced Tumorigenesis: Topical Therapeutic Strategies Targeting COX-2 Expression and Activity. *Anti-Cancer Agents in Medicinal Chemistry.* 2006;6:187-208.

174. Xu A, Chai Y, Nohmi T, Hei TK. Genotoxic responses to titanium dioxide nanoparticles and fullerene in gpt delta transgenic MEF cells. *Part Fibre Toxicol.* 2009;6:3.

175. Sayers BC. *The Role of COX-2 in the Inflammatory and Fibrotic Response in the Lung Following Exposure to Multi-Walled Carbon Nanotubes* [Ph.D.]. Ann Arbor: North Carolina State University; 2013.

176. Inoue K, Takano H, Yanagisawa R, Sakurai M, Ichinose T, Sadakane K, et al. Effects of nano particles on antigen-related airway inflammation in mice. *Respir Res.* 2005;6:106.

177. Bermudez E, Mangum JB, Asgharian B, Wong BA, Reverdy EE, Janszen DB, et al. Long-term pulmonary responses of three laboratory rodent species to subchronic inhalation of pigmentary titanium dioxide particles. *Toxicol Sci.* [Comparative Study Research Support, Non-U.S. Gov't]. 2002 Nov;70(1):86-97.

178. Sager TM, Kommineni C, Castranova V. Pulmonary response to intratracheal instillation of ultrafine versus fine titanium dioxide: role of particle surface area. *Part Fibre Toxicol.* 2008;5:17.

179. Park EJ, Yoon J, Choi K, Yi J, Park K. Induction of chronic inflammation in mice treated with titanium dioxide nanoparticles by intratracheal instillation. *Toxicology.* [Research Support, Non-U.S. Gov't]. 2009 Jun 16;260(1-3):37-46.

180. Kobayashi N, Naya M, Endoh S, Maru J, Yamamoto K, Nakanishi J. Comparative pulmonary toxicity study of nano-TiO(2) particles of different sizes and agglomerations in rats: different short- and long-term post-instillation results. *Toxicology.* [Comparative Study Research Support, U.S. Gov't, Non-P.H.S.]. 2009 Oct 1;264(1-2):110-8.

181. van Ravenzwaay B, Landsiedel R, Fabian E, Burkhardt S, Strauss V, Ma-Hock L. Comparing fate and effects of three particles of different surface properties: nano-TiO(2), pigmentary TiO(2) and quartz. *Toxicol Lett.* [Comparative Study]. 2009 May 8;186(3):152-9.

182. Muller J, Huaux Fo, Moreau N, Misson P, Heilier J-Fo, Delos M, et al. Respiratory toxicity of multi-wall carbon nanotubes. *Toxicol Appl Pharmacol.* 2005;207:221– 31.

183. Chou CC, Hsiao HY, Hong QS, Chen CH, Peng YW, Chen HW, et al. Single-walled carbon nanotubes can induce pulmonary injury in mouse model. *Nano Lett.* 2008 Feb;8(2):437-45.

184. Hsieh WY, Chou CC, Ho CC, Yu SL, Chen HY, Chou HY, et al. Single-walled carbon nanotubes induce airway hyperreactivity and parenchymal injury in mice. *Am J Respir Cell Mol Biol.* [Research Support, Non-U.S. Gov't]. 2012 Feb;46(2):257-67.

185. Han SG, Andrews R, Gairola CG. Acute pulmonary response of mice to multi-wall carbon nanotubes. *Inhalation Toxicology.* 2010 Mar;22(4):340-7.

186. Strober W. Trypan blue exclusion test of cell viability. *Curr Protoc Immunol.* 2001 May;Appendix 3:Appendix 3B.

187. Riss TL, Moravec RA, Niles AL, Benink HA, Worzella TJ, Minor L. Cell Viability Assays. In: Sittampalam GS, Gal-Edd N, Arkin M, Auld D, Austin C, Bejcek B, et al., editors. Assay Guidance Manual. Bethesda (MD): Eli Lilly & Company and the National Center for Advancing Translational Sciences; 2004-. 2013.

188. Promega. *CellTiter-Glo^{r} Luminesent Cell Viability Assay.* Promega Corporation; 2012.

189. LeBel CP, Ischiropoulos H, Bondy SC. Evaluation of the Probe 2‘,7‘-Dichiorofluorescin as an Indicator of reactive oxygen species formation and oxidative stress. *Chemical research in toxicology.* 1992;2(5):227-31.

190. Subramaniam SR, Ellis EM. Esculetin-induced protection of human hepatoma HepG2 cells against hydrogen peroxide is associated with the Nrf2-dependent induction of the NAD(P)H: Quinone oxidoreductase 1 gene. *Toxicol Appl Pharmacol.* 2011 Jan 15;250(2):130-6.

191. Sgonc R, Gruber J. Apoptosis detection: an overview. *Exp Gerontol.* [Research Support, Non-U.S. Gov't Review]. 1998 Sep;33(6):525-33.

192. Ioannou YA, Chen FW. Quantitation of DNA fragmentation in apoptosis. *Nucleic Acids Res*. [Research Support, U.S. Gov't, P.H.S.]. 1996 Mar 1;24(5):992-3.

193. Fink SL, Cookson BT. Apoptosis, pyroptosis, and necrosis: mechanistic description of dead and dying eukaryotic cells. *Infection and Immunity.* [Research Support, Non-U.S. Gov't Research Support, U.S. Gov't, P.H.S. Review]. 2005 Apr;73(4):1907-16.

194. Kotamraju S, Konorev EA, Joseph J, Kalyanaraman B. Doxorubicin-induced apoptosis in endothelial cells and cardiomyocytes is ameliorated by nitrone spin traps and ebselen. Role of reactive oxygen and nitrogen species. *J Biol Chem.* [Research Support, U.S. Gov't, P.H.S.]. 2000 Oct 27;275(43):33585-92.

195. Watjen W, Beyersmann D. Cadmium-induced apoptosis in C6 glioma cells: influence of oxidative stress. *Biometals.* [Research Support, Non-U.S. Gov't]. 2004 Feb;17(1):65-78.

196. Darzynkiewicz Z, Bedner E, Smolewski P. Analysis of Apoptosis by Laser-Scanning Cytometry. In: Davis MA, editor. *Apoptosis Methods in Pharmacology and Toxicology.* Totowa, NJ: Humana Press; 2002. p. 37-58.

197. Akbari B, Tavandashti MP, Zandrahimi M. Particle size characterization of nanopartiles - A practical approach. *Iranian Journal of Materials Science & Engineering.* 2011;8(2):48-56.

198. Baer DR, Engelhard MH, Johnson GE, Laskin J, Lai J, Mueller K, et al. Surface characterization of nanomaterials and nanoparticles: Important needs andchallenging opportunities. *Journal of Vacuum Science & Technology A.* 2013;31(5):-.

199. Anumolu R, Pease LF. Rapid Nanoparticle Characterization. In: Hashim DAA, editor. The Delivery of Nanoparticles: *InTech;* 2012. p. 540.

200. Skoglund S, Lowe TA, Hedberg J, Blomberg E, Wallinder IO, Wold S, et al. Effect of Laundry Surfactants on Surface Charge and Colloidal Stability of Silver Nanoparticles. *Langmuir.* 2013 Jul 16;29(28):8882-91.

201. Xu R. Light Scattering. In: Scarlett B, editor. *Particle Characterization: Light Scattering Methods:* Springer Netherlands; 2002. p. 56-110.

202. *Guidelines for Dynamic Light Scattering Measurement and Analysis* [database on the Internet]. nanocomposix.com. 2012.

203. *Zeta potential analysis of nanoparticles* [database on the Internet]. nanocomposix.com. 2012.

204. Clogston J, Patri A. Zeta Potential Measurement. In: McNeil SE, editor. *Characterization of Nanoparticles Intended for Drug Delivery*: Humana Press; 2011. p. 63-70.

205. Júnior JAA, Baldo JB. The Behavior of Zeta Potential of Silica Suspensions. New *Journal of Glass and Ceramics.* 2014;4:29-37.

206. Bootz A, Vogel V, Schubert D, Kreuter J. Comparison of scanning electron microscopy, dynamic light scattering and analytical ultracentrifugation for the sizing of poly(butyl cyanoacrylate) nanoparticles. *European Journal of Pharmaceutics and Biopharmaceutics.* 2004;57(2):369-75.

207. Wei Z. *An investigation of toxicity and immune effects of common metal oxide nanoparticles.* New york: Rensselaer Polytechnic Institute; 2010.

208. Galindo-Rodriguez S, Allemann E, Fessi H, Doelker E. Physicochemical parameters associated with nanoparticle formation in the salting-out, emulsification-diffusion, and nanoprecipitation methods. *Pharm Res.* [Comparative Study, Research Support, Non-U.S. Gov't]. 2004 Aug;21(8):1428-39.

209. Xie Y, Heo S, Yoo S, Ali G, Cho S. Synthesis and Photocatalytic Activity of Anatase TiO2 Nanoparticles-coated Carbon Nanotubes. *Nanoscale Research Letters.* 2010 2010/03/01;5(3):603-7.

210. Shao D, Ren X, Hu J, Chen Y, Wang X. Preconcentration of Pb2+ from aqueous solution using poly(acrylamide) and poly(N,N-dimethylacrylamide) grafted multiwalled carbon nanotubes. Colloids and Surfaces A: *Physicochemical and Engineering Aspects.* 2010;360(1–3):74-84.

211. Afolabi AS, Abdulkareem AS, Iyuke SE. Synthesis of carbon nanotubes and nanoballs by swirled floating catalyst chemical vapour deposition method. *Journal of Experimental Nanoscience.* 2007 2007/12/01;2(4):269-77.

212. Becker S, Mundandhara S, Devlin RB, Madden M. Regulation of cytokine production in human alveolar macrophages and airway epithelial cells in response to ambient air pollution particles: further mechanistic studies. *Toxicol Appl Pharmacol.* [Review]. 2005 Sep 1;207(2 Suppl):269-75.

213. Goldstein E, Bartlema HC. Role of the alveolar macrophage in pulmonary bacterial defense. *Bull Eur Physiopathol Respir.* [Review]. 1977 Jan-Feb;13(1):57-67.

214. Brain JD. Macrophage damage in relation to the pathogenesis of lung diseases. *Environmental Health Perspectives.* [Research Support, U.S. Gov't, Non-P.H.S. Research Support, U.S. Gov't, P.H.S. Review]. 1980 Apr;35:21-8.

215. Bowden DH. The pulmonary macrophage. *Environmental Health Perspectives.* [Review]. 1976 Aug;16:55-60.

216. Scull CM, Hays WD, Fischer TH. Macrophage pro-inflammatory cytokine secretion is enhanced following interaction with autologous platelets. *J Inflamm (Lond).* 2010;7:53.

217. Thomassen MJ, Divis LT, Fisher CJ. Regulation of human alveolar macrophage inflammatory cytokine production by interleukin-10. *Clin Immunol Immunopathol.* 1996 Sep;80(3 Pt 1):321-4.

218. Soromou LW, Zhang Z, Li R, Chen N, Guo W, Huo M, et al. Regulation of inflammatory cytokines in lipopolysaccharide-stimulated RAW 264.7 murine macrophage by 7-O-methyl-naringenin. *Molecules.* [Research Support, Non-U.S. Gov't]. 2012;17(3):3574-85.

219. Hiraiwa K, van Eeden SF. Contribution of lung macrophages to the inflammatory responses induced by exposure to air pollutants. *Mediators of Inflammation*. [Review]. 2013;2013:619523.

220. Park EJ, Zahari NE, Kang MS, Lee S, Lee K, Lee BS, et al. Toxic response of HIPCO single-walled carbon nanotubes in mice and RAW264.7 macrophage cells. *Toxicol Lett.* [Research Support, Non-U.S. Gov't]. 2014 Aug 17;229(1):167-77.

221. Oberdorster G. Pulmonary effects of inhaled ultrafine particles. *Int Arch Occup Environ Health*. [Research Support, U.S. Gov't, P.H.S. Review]. 2001 Jan;74(1):1-8.

222. Dorger M, Krombach F. Response of alveolar macrophages to inhaled particulates. *Eur Surg Res.* [Review]. 2002 Jan-Apr;34(1-2):47-52.

223. Bowden DH. The alveolar macrophage. *Environmental Health Perspectives.* [Research Support, Non-U.S. Gov't Review]. 1984 Apr;55:327-41.

224. Sandberg WJ, Lag M, Holme JA, Friede B, Gualtieri M, Kruszewski M, et al. Comparison of non-crystalline silica nanoparticles in IL-1beta release from macrophages. *Part Fibre Toxicol.* [Comparative Study Research Support, Non-U.S. Gov't]. 2012;9:32.

225. Jones CF, Grainger DW. In vitro assessments of nanomaterial toxicity. *Adv Drug Deliv Rev.* [Research Support, N.I.H., Extramural Review]. 2009 Jun 21;61(6):438-56.

226. Zhang T, Tang M, Kong L, Li H, Zhang S, Xue Y, et al. Comparison of cytotoxic and inflammatory responses of pristine and functionalized multi-walled carbon nanotubes in RAW 264.7 mouse macrophages. *J Hazard Mater.* [Comparative Study Research Support, Non-U.S. Gov't]. 2012 Jun 15;219-220:203-12.

227. Morimoto Y, Izumi H, Kuroda E. Significance of persistent inflammation in respiratory disorders induced by nanoparticles. *J Immunol Res.* [Research Support, Non-U.S. Gov't]. 2014;2014:962871.

228. Peters T, Henry PJ. Protease-activated receptors and prostaglandins in inflammatory lung disease. *British Journal of Pharmacology.* [Research Support, Non-U.S. Gov't Review]. 2009 Oct;158(4):1017-33.

229. Lee JK, Sayers BC, Chun KS, Lao HC, Shipley-Phillips JK, Bonner JC, et al. Multi-walled carbon nanotubes induce COX-2 and iNOS expression via MAP kinase-dependent and -independent mechanisms in mouse RAW264.7 macrophages. *Part Fibre Toxicol.* [Research Support, N.I.H., Extramural Research Support, N.I.H., Intramural Research Support, Non-U.S. Gov't]. 2012;9:14.

230. Claria J. Cyclooxygenase-2 biology. *Curr Pharm Des.* [Review]. 2003;9(27):2177-90.

231. Araki Y, Okamura S, Hussain SP, Nagashima M, He P, Shiseki M, et al. Regulation of cyclooxygenase-2 expression by the Wnt and ras pathways. *Cancer Research.* 2003 Feb 1;63(3):728-34.

232. Camilli TC, Weeraratna AT. Striking the target in Wnt-y conditions: intervening in Wnt signaling during cancer progression. *Biochem Pharmacol.* [Research Support, N.I.H., Intramural Review]. 2010 Sep 1;80(5):702-11.

233. Park GY, Christman JW. Involvement of cyclooxygenase-2 and prostaglandins in the molecular pathogenesis of inflammatory lung diseases. *Am J Physiol Lung Cell Mol Physiol.* [Research Support, N.I.H., Extramural Research Support, U.S. Gov't, Non-P.H.S. Review]. 2006 May;290(5):L797-805.

234. Nunez F, Bravo S, Cruzat F, Montecino M, De Ferrari GV. Wnt/beta-catenin signaling enhances cyclooxygenase-2 (COX2) transcriptional activity in gastric cancer cells. *PLoS One.* [Research Support, Non-U.S. Gov't]. 2011;6(4):e18562.

235. Kannan K, Jain SK. Oxidative stress and apoptosis. *Pathophysiology.* 2000;7(3):153-63.

236. Matés JM, Sánchez-Jiménez FM. Role of reactive oxygen species in apoptosis: implications for cancer therapy. *Int J Biochem Cell Biol.* 2000;32(2):157-70.

237. Bradley JR. TNF-mediated inflammatory disease. *J Pathol.* [Research Support, Non-U.S. Gov't Review]. 2008 Jan;214(2):149-60.

238. Popa C, Netea MG, van Riel PLCM, van der Meer JWM, Stalenhoef AFH. The role of TNF-α in chronic inflammatory conditions, intermediary metabolism, and cardiovascular risk. *Journal of Lipid Research.* 2007 April 1, 2007;48(4):751-62.

239. Khan HA, Abdelhalim MA, Alhomida AS, Al Ayed MS. Transient increase in IL-1beta, IL-6 and TNF-alpha gene expression in rat liver exposed to gold nanoparticles. *Genet Mol Res.* [Research Support, Non-U.S. Gov't]. 2013;12(4):5851-7.

240. Murphy FA, Schinwald A, Poland CA, Donaldson K. The mechanism of pleural inflammation by long carbon nanotubes: interaction of long fibres with macrophages stimulates them to amplify pro-inflammatory responses in

mesothelial cells. *Part Fibre Toxicol.* [Research Support, Non-U.S. Gov't]. 2012;9:8.

241. Akira S, Kishimoto T. IL-6 and NF-IL6 in acute-phase response and viral infection. *Immunol Rev.* [Review]. 1992 Jun;127:25-50.

242. Heinrich PC, Castell JV, Andus T. Interleukin-6 and the acute phase response. *The Biochemical Journal.* [Review]. 1990 Feb 1;265(3):621-36.

243. Bauer J, Herrmann F. Interleukin-6 in clinical medicine. *Ann Hematol.* [Review]. 1991 Jun;62(6):203-10.

244. Simpson RJ, Hammacher A, Smith DK, Matthews JM, Ward LD. Interleukin-6: structure-function relationships. *Protein Sci.* [Research Support, Non-U.S. Gov't Review]. 1997 May;6(5):929-55.

245. Pissuwan D, Kumagai Y, Smith NI. Effect of Surface-Modified Gold Nanorods on the Inflammatory Cytokine Response in Macrophage Cells. *Particle & Particle Systems Characterization.* 2013;30(5):427-33.

246. Schmalz G, Schuster U, Schweikl H. Influence of metals on IL-6 release in vitro. *Biomaterials.* 1998 Sep;19(18):1689-94.

247. Clarke BM. *In vitro toxicity and inflammatory response induced by copper nanoparticles in rat alveolar macrophages*. Ohio: Air force institute of technology; 2008.

248. Shapiro L. beta-catenin and its multiple partners: promiscuity explained. *Nat Struct Biol.* 2001 Jun;8(6):484-7.

249. George SJ. Wnt pathway: a new role in regulation of inflammation. *Arterioscler Thromb Vasc Biol.* [Comment Editorial Review]. 2008 Mar;28(3):400-2.

250. Palomaki J, Karisola P, Pylkkanen L, Savolainen K, Alenius H. Engineered nanomaterials cause cytotoxicity and activation on mouse antigen presenting cells. *Toxicology.* [Research Support, Non-U.S. Gov't]. 2010 Jan 12;267(1-3):125-31.

251. Fisichella M, Berenguer F, Steinmetz G, Auffan M, Rose J, Prat O. Intestinal toxicity evaluation of TiO2 degraded surface-treated nanoparticles: a combined physico-chemical and toxicogenomics approach in caco-2 cells. *Part Fibre Toxicol.* [Research Support, Non-U.S. Gov't]. 2012;9:18.

252.Zhang Y, Fong CC, Wong MS, Tzang CH, Lai WP, Fong WF, et al. Molecular mechanisms of survival and apoptosis in RAW 264.7 macrophages under oxidative stress. *Apoptosis : an international journal on programmed cell death.* [Research Support, Non-U.S. Gov't]. 2005 May;10(3):545-56.

253.Roy R, Kumar S, Tripathi A, Das M, Dwivedi PD. Interactive threats of nanoparticles to the biological system. *Immunol Lett.* [Research Support, Non-U.S. Gov't]. 2014 Mar-Apr;158(1-2):79-87.

254.Moller W, Hofer T, Ziesenis A, Karg E, Heyder J. Ultrafine particles cause cytoskeletal dysfunctions in macrophages. *Toxicol Appl Pharmacol.* [Research Support, Non-U.S. Gov't]. 2002 Aug 1;182(3):197-207.

255.Vamanu CI, Cimpan MR, Hol PJ, Sornes S, Lie SA, Gjerdet NR. Induction of cell death by TiO2 nanoparticles: studies on a human monoblastoid cell line. *Toxicology in vitro : an international journal published in association with BIBRA.* [Research Support, Non-U.S. Gov't]. 2008 Oct;22(7):1689-96.

256.Goncalves DM, Chiasson S, Girard D. Activation of human neutrophils by titanium dioxide (TiO2) nanoparticles. *Toxicology in vitro : an international journal published in association with BIBRA.* [In Vitro Research Support, Non-U.S. Gov't]. 2010 Apr;24(3):1002-8.

257.Liu SC, Xu LJ, Zhang T, Ren GG, Yang Z. Oxidative stress and apoptosis induced by nanosized titanium dioxide in PC12 cells. *Toxicology.* 2010 Jan 12;267(1-3):172-7.

258.Wu J, Sun J, Xue Y. Involvement of JNK and P53 activation in G2/M cell cycle arrest and apoptosis induced by titanium dioxide nanoparticles in neuron cells. *Toxicol Lett.* [Research Support, Non-U.S. Gov't]. 2010 Dec 15;199(3):269-76.

259.Wan R, Mo Y, Zhang X, Chien S, Tollerud DJ, Zhang Q. Matrix metalloproteinase-2 and -9 are induced differently by metal nanoparticles in human monocytes: The role of oxidative stress and protein tyrosine kinase activation. *Toxicol Appl Pharmacol.* 2008 Dec 1;233(2):276-85.

260.Kang SJ, Kim BM, Lee YJ, Chung HW. Titanium dioxide nanoparticles trigger p53-mediated damage response in peripheral blood lymphocytes. Environ *Mol Mutagen.* 2008 Jun;49(5):399-405.

261. Sayes CM, Wahi R, Kurian PA, Liu Y, West JL, Ausman KD, et al. Correlating nanoscale titania structure with toxicity: a cytotoxicity and inflammatory response study with human dermal fibroblasts and human lung epithelial cells. *Toxicol Sci.* [Research Support, Non-U.S. Gov't]. 2006 Jul;92(1):174-85.

262. Geiser M, Rothen-Rutishauser B, Kapp N, Schurch S, Kreyling W, Schulz H, et al. Ultrafine particles cross cellular membranes by nonphagocytic mechanisms in lungs and in cultured cells. *Environmental health perspectives.* [Research Support, Non-U.S. Gov't]. 2005 Nov;113(11):1555-60.

263. Simon HU, Haj-Yehia A, Levi-Schaffer F. Role of reactive oxygen species (ROS) in apoptosis induction. *Apoptosis.* 2000 Nov;5(5):415-8.

264. Wang C, Youle RJ. The role of mitochondria in apoptosis*. *Annu Rev Genet.* [Comparative Study Research Support, N.I.H., Intramural Review]. 2009;43:95-118.

265. Kroemer G, Galluzzi L, Brenner C. Mitochondrial Membrane Permeabilization in Cell Death2007.

266. Sinha K, Das J, Pal P, Sil P. Oxidative stress: the mitochondria-dependent and mitochondria-independent pathways of apoptosis. *Arch Toxicol.* 2013 2013/07/01;87(7):1157-80.

267. Suen DF, Norris KL, Youle RJ. Mitochondrial dynamics and apoptosis. *Genes Dev*. [Review]. 2008 Jun 15;22(12):1577-90.

268. Tzifi F, Economopoulou C, Gourgiotis D, Ardavanis A, Papageorgiou S, Scorilas A. The Role of BCL2 Family of Apoptosis Regulator Proteins in Acute and Chronic Leukemias. *Adv Hematol.* 2012;2012:524308.

269. Czabotar PE, Lessene G, Strasser A, Adams JM. Control of apoptosis by the BCL-2 protein family: implications for physiology and therapy. *Nat Rev Mol Cell Biol.* [Research Support, Non-U.S. Gov't Review]. 2014 Jan;15(1):49-63.

270. Brunelle JK, Letai A. Control of mitochondrial apoptosis by the Bcl-2 family. Journal of Cell Science. 2009 February 15, 2009;122(4):437-41.

271.Kasai H, Yamamoto K, Koseki T, Yokota M, Nishihara T. Involvement of caspase activation through release of cytochrome c from mitochondria in apoptotic cell death of macrophages infected with Actinobacillus actinomycetemcomitans. *FEMS Microbiology Letters.* 2004;233(1):29-35.

272.Feghali CA, Wright TM. Cytokines in acute and chronic inflammation. *Front Biosci*. [Review]. 1997 Jan 1;2:d12-26.

273.Morishige T, Yoshioka Y, Tanabe A, Yao XL, Tsunoda S, Tsutsumi Y, et al. Titanium dioxide induces different levels of IL-1 beta production dependent on its particle characteristics through caspase-1 activation mediated by reactive oxygen species and cathepsin B. *Biochem Biophys Res Commun.* 2010 Feb 5;392(2):160-5.

274.Kocbach A, Todandsdal AI, Lag M, Refsnes A, Schwarze PE. Differential binding of cytokines to environmentally relevant particles: A possible source for misinterpretation of in vitro results? *Toxicol Lett*. 2008 Jan 30;176(2):131-7.

275.Muller L, Riediker M, Wick P, Mohr M, Gehr P, Rothen-Rutishauser B. Oxidative stress and inflammation response after nanoparticle exposure: differences between human lung cell monocultures and an advanced three-dimensional model of the human epithelial airways. *J R Soc Interface.* [Research Support, Non-U.S. Gov't]. 2010 Feb 6;7 Suppl 1:S27-40.

276.Dekali S, Divetain A, Kortulewski T, Vanbaelinghem J, Gamez C, Rogerieux F, et al. Cell cooperation and role of the P2X(7) receptor in pulmonary inflammation induced by nanoparticles. *Nanotoxicology.* [Research Support, Non-U.S. Gov't]. 2013 Dec;7(8):1302-14.

277.Federico A, Morgillo F, Tuccillo C, Ciardiello F, Loguercio C. Chronic inflammation and oxidative stress in human carcinogenesis. *Int J Cancer*. [Review]. 2007 Dec 1;121(11):2381-6.

278.Lee J, Kosaras B, Aleyasin H, Han JA, Park DS, Ratan RR, et al. Role of cyclooxygenase-2 induction by transcription factor Sp1 and Sp3 in neuronal oxidative and DNA damage response. *FASEB journal : official publication of the Federation of American Societies for Experimental Biology.* [Research Support, N.I.H., Extramural Research Support, Non-

U.S. Gov't Research Support, U.S. Gov't, Non-P.H.S.]. 2006 Nov;20(13):2375-7.

279. Greenhough A, Smartt HJ, Moore AE, Roberts HR, Williams AC, Paraskeva C, et al. The COX-2/PGE2 pathway: key roles in the hallmarks of cancer and adaptation to the tumour microenvironment. *Carcinogenesis.* [Research Support, Non-U.S. Gov't Review]. 2009 Mar;30(3):377-86.

280. Badie B, Schartner JM, Hagar AR, Prabakaran S, Peebles TR, Bartley B, et al. Microglia cyclooxygenase-2 activity in experimental gliomas: possible role in cerebral edema formation. *Clin Cancer Res.* [Research Support, Non-U.S. Gov't]. 2003 Feb;9(2):872-7.

281. Sang X, Li B, Ze Y, Hong J, Ze X, Gui S, et al. Toxicological Mechanisms of Nanosized Titanium Dioxide-Induced Spleen Injury in Mice after Repeated Peroral Application. *Journal of Agricultural and Food Chemistry.* 2013 2013/06/12;61(23):5590-9.

282. Wang X, Meng X, Sun X, Liu M, Gao S, Zhao J, et al. Wnt/beta-catenin signaling pathway may regulate cell cycle and expression of cyclin A and cyclin E protein in hepatocellular carcinoma cells. *Cell Cycle.* 2009 May 15;8(10):1567-70.

283. Olmeda D, Castel S, Vilaro S, Cano A. Beta-catenin regulation during the cell cycle: implications in G2/M and apoptosis. *Mol Biol Cell.* [Research Support, Non-U.S. Gov't]. 2003 Jul;14(7):2844-60.

284. Cortes-Vieyra R, Bravo-Patino A, Valdez-Alarcon JJ, Juarez MC, Finlay BB, Baizabal-Aguirre VM. Role of glycogen synthase kinase-3 beta in the inflammatory response caused by bacterial pathogens. *J Inflamm (Lond).* 2012;9(1):23.

285. Thanendrarajan S, Kim Y, Schmidt-Wolf IG. Understanding and Targeting the Wnt/beta-Catenin Signaling Pathway in Chronic Leukemia. *Leuk Res Treatment.* 2011;2011:329572.

286. Jiang G, Xiao X, Zeng Y, Nagabhushanam K, Majeed M, Xiao D. Targeting beta-Catenin signaling to induce apoptosis in human breast cancer cells by z-Guggulsterone and Gugulipid extract of Ayurvedic medicine plant

Commiphora mukul. *BMC Complementary and Alternative Medicine*. 2013;13(1):203.

287. Pecina-Slaus N. Wnt signal transduction pathway and apoptosis: a review. *Cancer Cell Int.* 2010;10:22.

288. Nejak-Bowen KN. *beta-catenin in liver: A matter of life and death* [Ph.D.]. Ann Arbor: University of Pittsburgh; 2010.

289. Thompson MD, Monga SP. WNT/beta-catenin signaling in liver health and disease. *Hepatology.* [Research Support, N.I.H., Extramural Research Support, Non-U.S. Gov't Review]. 2007 May;45(5):1298-305.

290. Tan X, Behari J, Cieply B, Michalopoulos GK, Monga SP. Conditional deletion of beta-catenin reveals its role in liver growth and regeneration. *Gastroenterology.* [Research Support, N.I.H., Extramural Research Support, Non-U.S. Gov't]. 2006 Nov;131(5):1561-72.

291. Torres M, Forman HJ. Redox signaling and the MAP kinase pathways. *Biofactors.* [Review]. 2003;17(1-4):287-96.

292. Wu Y, Zhou BP. TNF-[alpha]/NF-[kappa]B/Snail pathway in cancer cell migration and invasion. *Br J Cancer.* 2010;102(4):639-44.

293. Zhao Y, Usatyuk PV, Gorshkova IA, He D, Wang T, Moreno-Vinasco L, et al. Regulation of COX-2 expression and IL-6 release by particulate matter in airway epithelial cells. *Am J Respir Cell Mol Biol.* [Research Support, Non-U.S. Gov't Research Support, U.S. Gov't, Non-P.H.S.]. 2009 Jan;40(1):19-30.

294. Thompson EA, Sayers BC, Glista-Baker EE, Shipkowski KA, Taylor AJ, Bonner JC. Innate immune responses to nanoparticle exposure in the lung. *J Environ Immunol Toxicol.* 2013;1(3):150-6.

295. Urner M, Schlicker A, Z'Graggen B R, Stepuk A, Booy C, Buehler KP, et al. Inflammatory response of lung macrophages and epithelial cells after exposure to redox active nanoparticles: effect of solubility and antioxidant treatment. *Environmental Science & Technology.* [Research Support, Non-U.S. Gov't]. 2014 Dec 2;48(23):13960-8.

296. Bianchi MG, Allegri M, Costa AL, Blosi M, Gardini D, Del Pivo C, et al. Titanium dioxide nanoparticles enhance macrophage activation by LPS

through a TLR4-dependent intracellular pathway. *Toxicology Research.* [10.1039/C4TX00193A]. 2015.

297. Sakai N, Wada T, Furuichi K, Iwata Y, Yoshimoto K, Kitagawa K, et al. p38 MAPK phosphorylation and NF-kappa B activation in human crescentic glomerulonephritis. *Nephrol Dial Transplant*. [Research Support, Non-U.S. Gov't]. 2002 Jun;17(6):998-1004.

298. Idriss HT, Naismith JH. TNFα and the TNF receptor superfamily: Structure-function relationship(s). *Microscopy Research and Technique.* 2000;50(3):184-95.

299. Son Y, Cheong Y-K, Kim N-H, Chung H-T, Kang DG, Pae H-O. Mitogen-Activated Protein Kinases and Reactive Oxygen Species: How Can ROS Activate MAPK Pathways? *J Signal Transduct.* 2011;2011:792639.

300. Sohaebuddin SK. *Mechanism of nanoparticle and nanotube-induced cell death* [M.S.]. Ann Arbor: The University of Texas at Arlington; 2008.

301. Jaeger A, Weiss DG, Jonas L, Kriehuber R. Oxidative stress-induced cytotoxic and genotoxic effects of nano-sized titanium dioxide particles in human HaCaT keratinocytes. *Toxicology.* 2012;296(1–3):27-36.

302. Wilhelmi V, Fischer U, Weighardt H, Schulze-Osthoff K, Nickel C, Stahlmecke B, et al. Zinc oxide nanoparticles induce necrosis and apoptosis in macrophages in a p47phox- and Nrf2-independent manner. *PLoS One.* [Research Support, Non-U.S. Gov't]. 2013;8(6):e65704.

303. Lovisolo D, Gilardino A, Ruffinatti F. When Neurons Encounter Nanoobjects: Spotlight on Calcium Signalling. *Int J Environ Res Public Health.* 2014;11(9):9621-37.

304. Simon M, Barberet P, Delville M-H, Moretto P, Seznec H. Titanium dioxide nanoparticles induced intracellular calcium homeostasis modification in primary human keratinocytes. Towards an in vitro explanation of titanium dioxide nanoparticles toxicity. *Nanotoxicology.* 2011;5(2):125-39.

305. Wu Q, Guo D, Du Y, Liu D, Wang D, Bi H. UVB irradiation enhances TiO2 nanoparticle-induced disruption of calcium homeostasis in human lens epithelial cells. *Photochem Photobiol.* [Research Support, Non-U.S. Gov't]. 2014 Nov-Dec;90(6):1324-31.

306.Forman HJ, Torres M. Reactive oxygen species and cell signaling: respiratory burst in macrophage signaling. *American journal of respiratory and critical care medicine.* [Research Support, U.S. Gov't, P.H.S. Review]. 2002 Dec 15;166(12 Pt 2):S4-8.

307.McIlwain DR, Berger T, Mak TW. Caspase Functions in Cell Death and Disease. Cold Spring Harbor Perspectives in Biology. 2013 April 1, 2013;5(4).

308.Hernandez-Pedro NY, Rangel-Lopez E, Magana-Maldonado R, de la Cruz VP, del Angel AS, Pineda B, et al. Application of nanoparticles on diagnosis and therapy in gliomas. *Biomed Res Int.* [Review]. 2013;2013:351031.

309.Fang Z, Kulldorff M, Gregorio DI. Brain cancer mortality in the United States, 1986 to 1995: a geographic analysis. *Neuro Oncol.* [Comparative Study Research Support, U.S. Gov't, P.H.S.]. 2004 Jul;6(3):179-87.

310.Sathornsumetee S. Neuro-Oncology: An Emerging Neurologic Subspecialty in Thailand. *Siriraj Medical Journal.* 2010;63:174-6.

311.Masserini M. Nanoparticles for Brain Drug Delivery. ISRN Biochemistry. 2013;2013:18.

312.Bouzier-Sore AK, Ribot E, Bouchaud V, Miraux S, Duguet E, Mornet S, et al. Nanoparticle phagocytosis and cellular stress: involvement in cellular imaging and in gene therapy against glioma. *NMR Biomed.* [Evaluation Studies Research Support, Non-U.S. Gov't]. 2010 Jan;23(1):88-96.

313.Jain KK. Nanobiotechnology-based strategies for crossing the blood-brain barrier. *Nanomedicine.* [Review]. 2012 Aug;7(8):1225-33.

314.van Rooy I, Cakir-Tascioglu S, Hennink WE, Storm G, Schiffelers RM, Mastrobattista E. In vivo methods to study uptake of nanoparticles into the brain. *Pharm Res.* [Comparative Study Research Support, Non-U.S. Gov't Review]. 2011 Mar;28(3):456-71.

315.Hanada S, Fujioka K, Inoue Y, Kanaya F, Manome Y, Yamamoto K. Cell-based in vitro blood-brain barrier model can rapidly evaluate nanoparticles' brain permeability in association with particle size and surface modification. *Int J Mol Sci.* [Research Support, Non-U.S. Gov't]. 2014;15(2):1812-25.

316.Wang J, Liu Y, Jiao F, Lao F, Li W, Gu Y, et al. Time-dependent translocation and potential impairment on central nervous system by intranasally

instilled TiO(2) nanoparticles. *Toxicology.* [Research Support, Non-U.S. Gov't]. 2008 Dec 5;254(1-2):82-90.

317. Bedner E, Li X, Gorczyca W, Melamed MR, Darzynkiewicz Z. Analysis of apoptosis by laser scanning cytometry. *Cytometry.* 1999;35(3):181-95.

318. Wang F, Gao F, Lan M, Yuan H, Huang Y, Liu J. Oxidative stress contributes to silica nanoparticle-induced cytotoxicity in human embryonic kidney cells. *Toxicology in vitro : an international journal published in association with BIBRA.* 2009 Aug;23(5):808-15.

319. Salcedo-Tello P, Ortiz-Matamoros A, Arias C. GSK3 Function in the Brain during Development, Neuronal Plasticity, and Neurodegeneration. *Int J Alzheimers Dis.* 2011;2011:189728.

320. Willert K, Nusse R. Beta-catenin: a key mediator of Wnt signaling. *Curr Opin Genet Dev*. 1998 Feb;8(1):95-102.

321. Clevers H. Wnt/β-Catenin Signaling in Development and Disease. *Cell.* 2006;127(3):469-80.

322. Kazem A, Sayed KE, Kerm YE. Prognostic significance of COX-2 and β-catenin in colorectal carcinoma. *Alexandria Journal of Medicine.* 2014;50(3):211-20.

323. Greenspan EJ, Madigan JP, Boardman LA, Rosenberg DW. Ibuprofen Inhibits Activation of Nuclear beta-Catenin in Human Colon Adenomas and Induces the Phosphorylation of GSK-3 beta. *Cancer Prev Res.* 2011 Jan;4(1):161-71.

324. Maier TJ, Janssen A, Schmidt R, Geisslinger G, Grosch S. Targeting the beta-catenin/APC pathway: a novel mechanism to explain the cyclooxygenase-2-independent anticarcinogenic effects of celecoxib in human colon carcinoma cells. *FASEB journal : official publication of the Federation of American Societies for Experimental Biology*. [Research Support, Non-U.S. Gov't]. 2005 Aug;19(10):1353-5.

325. Huerta-García E, Pérez-Arizti JA, Márquez-Ramírez SG, Delgado-Buenrostro NL, Chirino YI, Iglesias GG, et al. Titanium dioxide nanoparticles induce strong oxidative stress and mitochondrial damage in glial cells. *Free Radical Biology and Medicine.* 2014;73(0):84-94.

326. Peters A, Veronesi B, Calderon-Garciduenas L, Gehr P, Chen LC, Geiser M, et al. Translocation and potential neurological effects of fine and ultrafine particles a critical update. *Part Fibre Toxicol.* 2006;3:13.

327. Long TC, Saleh N, Tilton RD, Lowry GV, Veronesi B. Titanium Dioxide (P25) Produces Reactive Oxygen Species in Immortalized Brain Microglia (BV2): Implications for Nanoparticle Neurotoxicity†. *Environmental Science & Technology.* 2006;40(14):4346-52.

328. Kitz K. *Transcriptional Regulation of Cox-2 Expression in human Osteosarcoma Cells.* Graz: Medical University of Graz; 2011.

329. Geiser M, Quaile O, Wenk A, Wigge C, Eigeldinger-Berthou S, Hirn S, et al. Cellular uptake and localization of inhaled gold nanoparticles in lungs of mice with chronic obstructive pulmonary disease. *Part Fibre Toxicol.* [Research Support, Non-U.S. Gov't]. 2013;10:19.

330. Srinivas A, Rao PJ, Selvam G, Goparaju A, Murthy PB, Reddy PN. Oxidative stress and inflammatory responses of rat following acute inhalation exposure to iron oxide nanoparticles. *Hum Exp Toxicol.* [Research Support, Non-U.S. Gov't]. 2012 Nov;31(11):1113-31.

331. Shinde SK, Grampurohit ND, Gaikwad DD, Jadhav SL, Gadhave MV, Shelke PK. Toxicity induced by nanoparticles. *Asian Pacific Journal of Tropical Disease.* 2012;2(4):331-4.

332. Han SG, Lee JS, Ahn K, Kim YS, Kim JK, Lee JH, et al. Size-dependent clearance of gold nanoparticles from lungs of Sprague-Dawley rats after short-term inhalation exposure. *Arch Toxicol.* 2014 Jun 17.

333. Libby P. Inflammatory Mechanisms: The Molecular Basis of Inflammation and Disease. *Nutrition Reviews.* 2007;65:S140-S6.

334. Kidd BL, Urban LA. Mechanisms of inflammatory pain. *British Journal of Anaesthesia.* 2001 July 1, 2001;87(1):3-11.

335. Li Y, Zhang Y, Yan B. Nanotoxicity overview: nano-threat to susceptible populations. *Int J Mol Sci.* [Research Support, Non-U.S. Gov't]. 2014;15(3):3671-97.

336. Popov VN. Carbon nanotubes: properties and application. *Mat Sci Eng R.* 2004 Jan 15;43(3):61-102.

337. Inoue K-i, Koike E, Yanagisawa R, Hirano S, Nishikawa M, Takano H. Effects of multi-walled carbon nanotubes on a murine allergic airway inflammation model. *Toxicol Appl Pharmacol.* 2009;237(3):306-16.

338. Wang X, Katwa P, Podila R, Chen P, Ke PC, Rao AM, et al. Multi-walled carbon nanotube instillation impairs pulmonary function in C57BL/6 mice. *Part Fibre Toxicol.* [Research Support, N.I.H., Extramural Research Support, Non-U.S. Gov't]. 2011;8:24.

339. Park E-J, Cho W-S, Jeong J, Yi J, Choi K, Park K. Pro-inflammatory and potential allergic responses resulting from B cell activation in mice treated with multi-walled carbon nanotubes by intratracheal instillation. *Toxicology.* 2009;259(3):113-21.

340. Bradford MM. A rapid and sensitive method for the quantitation of microgram quantities of protein utilizing the principle of protein-dye binding. *Analytical Biochemistry.* 1976;72(1–2):248-54.

341. Roursgaard M, Jensen KA, Poulsen SS, Jensen NEV, Poulsen LK, Hammer M, et al. Acute and Subchronic Airway Inflammation after Intratracheal Instillation of Quartz and Titanium Dioxide Agglomerates in Mice. *ScientificWorldJournal.* 2011;11:801-25.

342. Kaplanski G, Marin V, Montero-Julian F, Mantovani A, Farnarier C. IL-6: a regulator of the transition from neutrophil to monocyte recruitment during inflammation. *Trends Immunol.* 2003 Jan;24(1):25-9.

343. Ma L, Zhao J, Wang J, Liu J, Duan Y, Liu H, et al. The Acute Liver Injury in Mice Caused by Nano-Anatase TiO2. *Nanoscale Research Letters.* 2009;4(11):1275-85.

344. Yazdi AS, Guarda G, Riteau N, Drexler SK, Tardivel A, Couillin I, et al. Nanoparticles activate the NLR pyrin domain containing 3 (Nlrp3) inflammasome and cause pulmonary inflammation through release of IL-1alpha and IL-1beta. *Proc Natl Acad Sci U S A.* [Research Support, Non-U.S. Gov't]. 2010 Nov 9;107(45):19449-54.

345. Sun Q, Tan D, Ze Y, Sang X, Liu X, Gui S, et al. Pulmotoxicological effects caused by long-term titanium dioxide nanoparticles exposure in mice. *J*

Hazard Mater. [Research Support, Non-U.S. Gov't]. 2012 Oct 15;235-236:47-53.

346. Veranth JM, Kaser EG, Veranth MM, Koch M, Yost GS. Cytokine responses of human lung cells (BEAS-2B) treated with micron-sized and nanoparticles of metal oxides compared to soil dusts. *Part Fibre Toxicol.* 2007;4:2.

347. Kocbach A. *Pro-inflammatory potential of particles from residential wood smoke and traffic : importance of physicochemical characteristic:* University of Oslo; 2008.

APPENDIX

DOCUMENTARY PROOF OF ETHICAL CLEARANCE

Protocol No. MUSC54-033-243

Documentary Proof of Ethical Clearance
Faculty of Science, Mahidol University

Protocol Title:	Oxidative stress and pro-inflammatory responses induced by metal-based nanoparticles *in vivo*
Principal Investigator:	Associate Professor Krongtong Yoovathaworn
Address:	Department of Pharmacology, Faculty of Science, Mahidol University
E-mail:	skyo@mahidol.ac.th.com

Approved by the Faculty of Science, Mahidol University Animal Care and Care and Use Committee
SCMU-ACUC Review

☐ Disapproved ☑ Approval Recommended

Signature of Chairman:

(Assoc.Prof.Sukumal Chongthammakun)

Date of Approval: February 9, 2012

Expiry Date : February 28, 2013

BIOGRAPHY

NAME	Patinya Sukwong
DATE OF BIRTH	16 March 1976
PLACE OF BIRTH	Songkhla, Thailand
INSTITUTIONS ATTENDED	Kasetsart University, 1993-1997 Bachelor of Science (General Science) Mahidol University, 1997-2002 Master of Science (Environmental Technology and Management) Mahidol University, 2007-2014 Doctor of Philosophy (Toxicology)
RESEARCH GRANTS	Center of Excellence on Environmental Health and Toxicology, Postgraduate Education and Research Development Office (PERDO), Ministry of Education.
HOME ADDRESS	5/344 soi 20 Samakee Rd. Bangtarad Parkret, Nonthaburi Province, Thailand
EMPLOYMENT ADDRESS	Faculty of Science and Technology, Suan Dusit Rajabhat University 228-228/1-3 Sirinthorn Rd., Bangplad, Bangkok, 10700